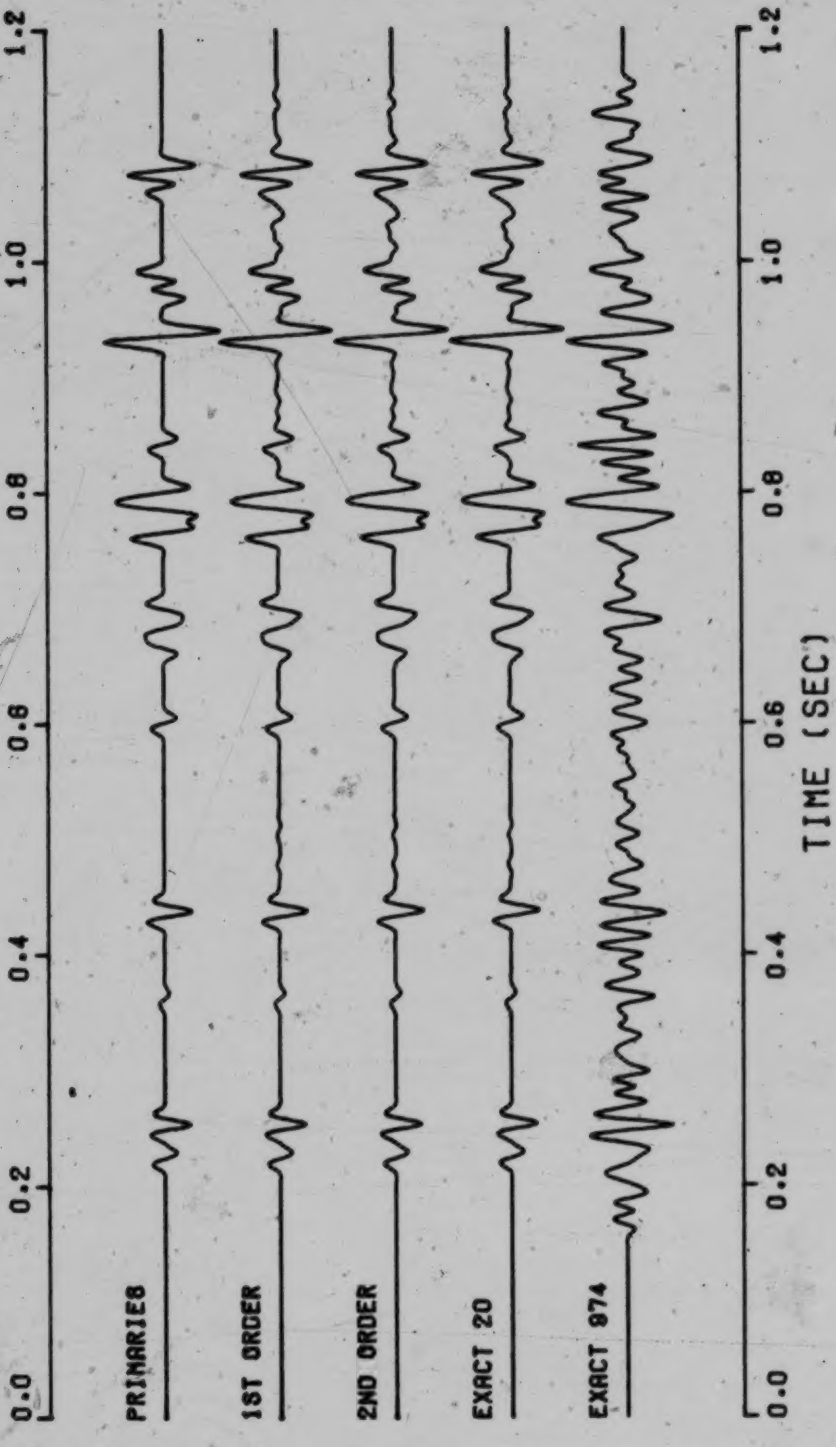

Figure 2.9 Comparison of synthetic seismograms for 20 layer model.

and 974 layer models. This points out the second problem in the generation of synthetic seismograms, namely matching the model to the real earth. It is felt that the 974 layer model is a more realistic model of what the true earth might be like.

The wavelet used in constructing the synthetic seismograms in figure 2.9 is shown in figure 2.10. This wavelet is an exponentially damped sine wave. The equation of this wavelet is

$$S(t) = \sin(wt)\exp(-w^2t^2/b^2) \qquad (2.58)$$

with w equal two pi times the dominant frequency (35 Hz) and the damping constant b=2. This wavelet is defined for the absolute value of t less than 45 msec and is zero elsewhere. The spectrum peaks at 35 Hz and is 6 db down at 12 and 65 Hz. Table 2.3 compares the CPU times and number of phases for the synthetic traces made from the 20 layer model. The CPU times are for an Amdahl 470-V6 computer.

Figure 2.11 compares primaries only synthetic seismograms without geometric spreading for 20, 54, 97, 174 and 974 layer models with the exact solution for the 974 layer model. All of these models were made from the same well log used before with the only difference being the percentage change in velocity required before a new layer was recognized when the log was blocked. The wavelet shown in figure 2.10 was also used for these seismograms. From

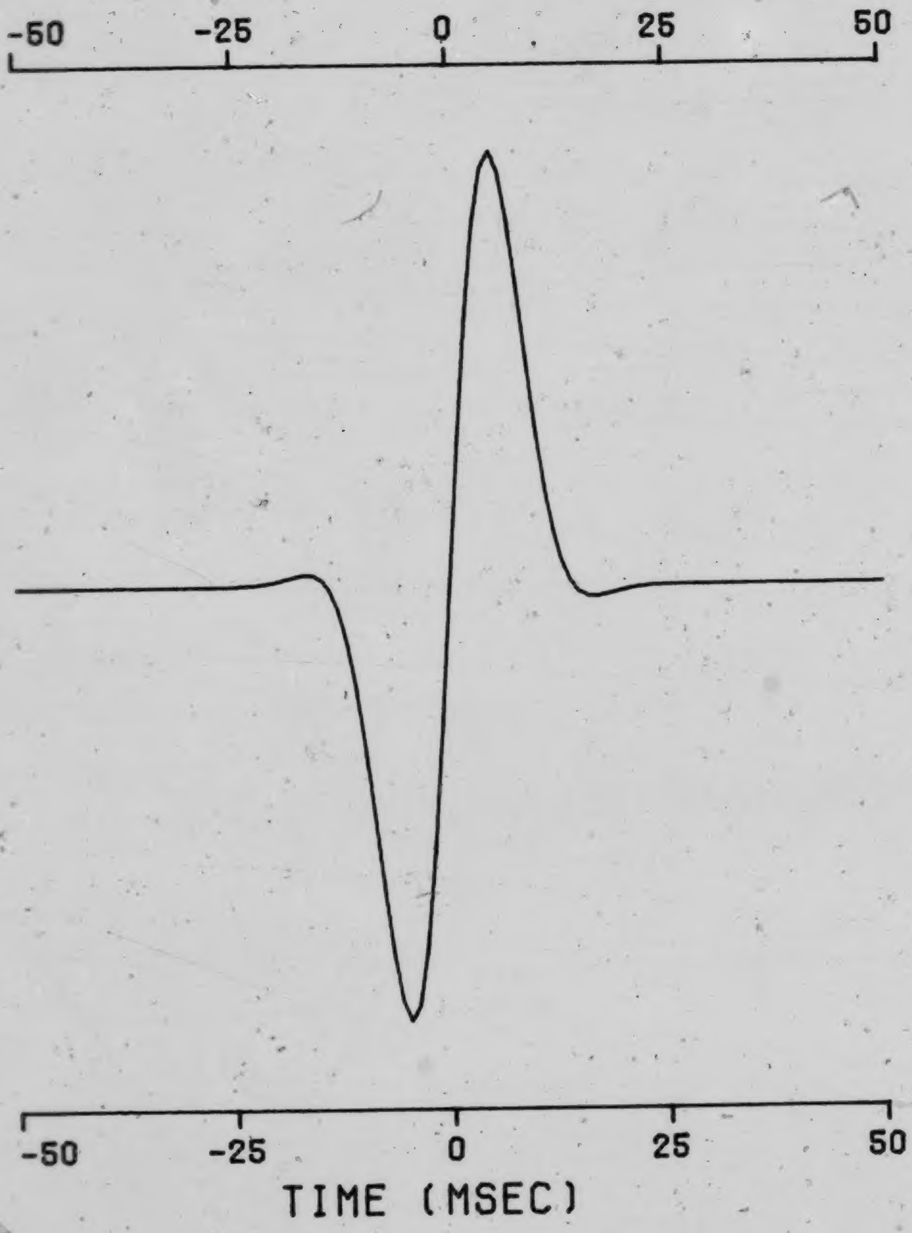

Figure 2.10 35 Hz damped sine wave wavelet.

Method	MNHS	Number of phases	CPU time (sec)
Primaries	20	20	
1st order	20	1079	5.63
	22	1150	13.83
2nd order	20	26521	42.59
	24	30207	436.12

Table 2.3 Comparison of CPU times and number of phases for 20 layer model.

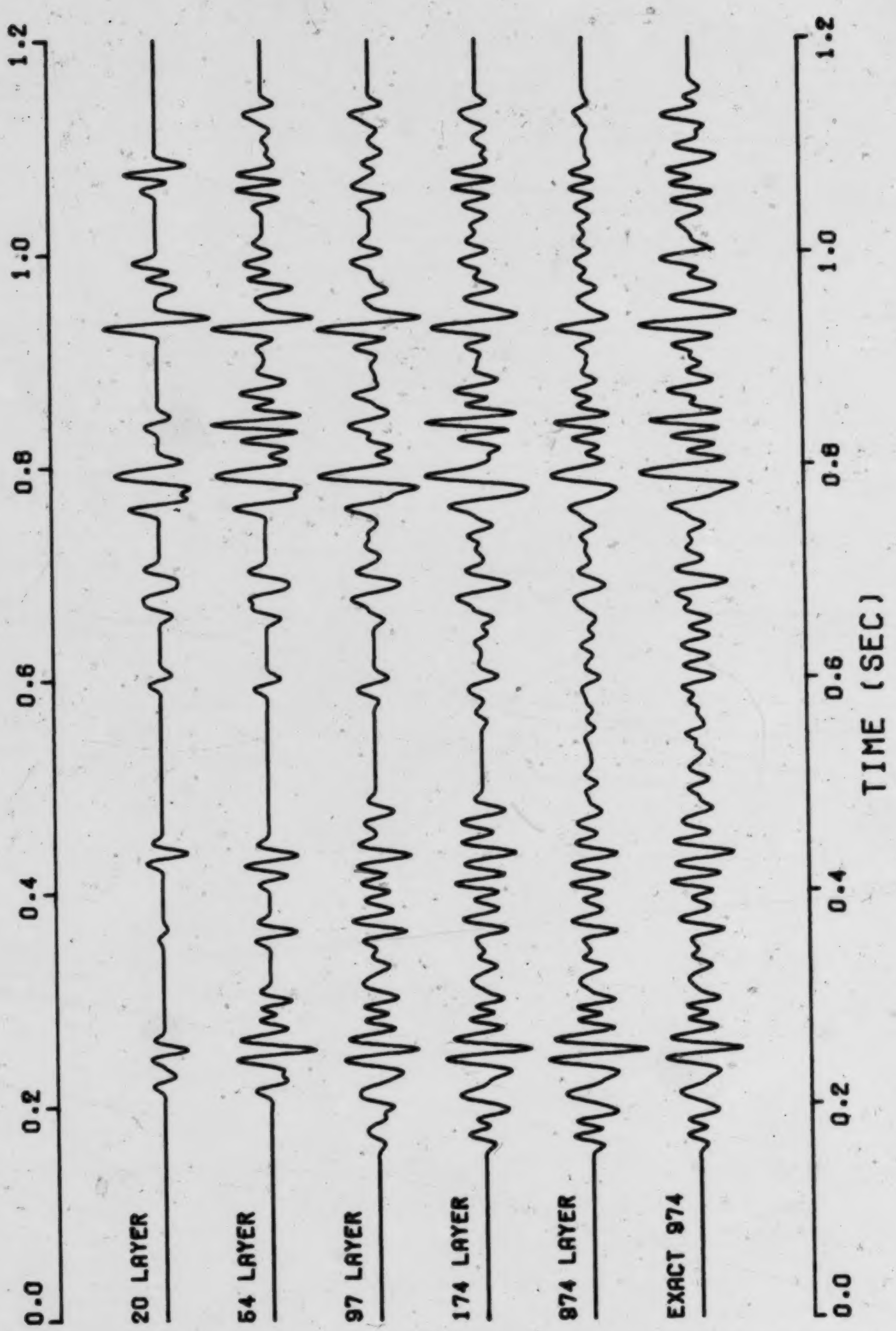

Figure 2.11 Primaries only synthetics for the model near Edmonton, Alberta.

this figure it is apparent that the models with 54 or more layers are good approximations to the 974 layer exact solution and that the comparison improves as the number of layers is increased.

Figure 2.12 compares synthetics for the same models used in figure 2.11; however, in the cases of the 20 to 974 layer ray tracing synthetic traces, all first order surface multiples have been included in addition to all primaries. The wavelet shown in figure 2.10 was used for this figure as well. Again models of 54 or more layers show good agreement. The inclusion of surface multiples has not improved the comparison very much and certainly not enough to justify the large increase in the number of rays required for models with more than 54 layers.

2.3 Synthetic Seismograms With Absorption by Ray Methods

In this section the problem of constructing non-vertical incidence synthetic seismograms which include the effects of absorption and dispersion by ray methods will be briefly examined. As was done for the vertical incidence seismograms, the absorption will be handled mathematically by allowing the wave number, velocity and elastic modulus to be complex functions of frequency. The displacement will be written as

$$U = U(0)\exp[i(wt-\underline{K}\bullet\underline{r})] \qquad (2.59)$$

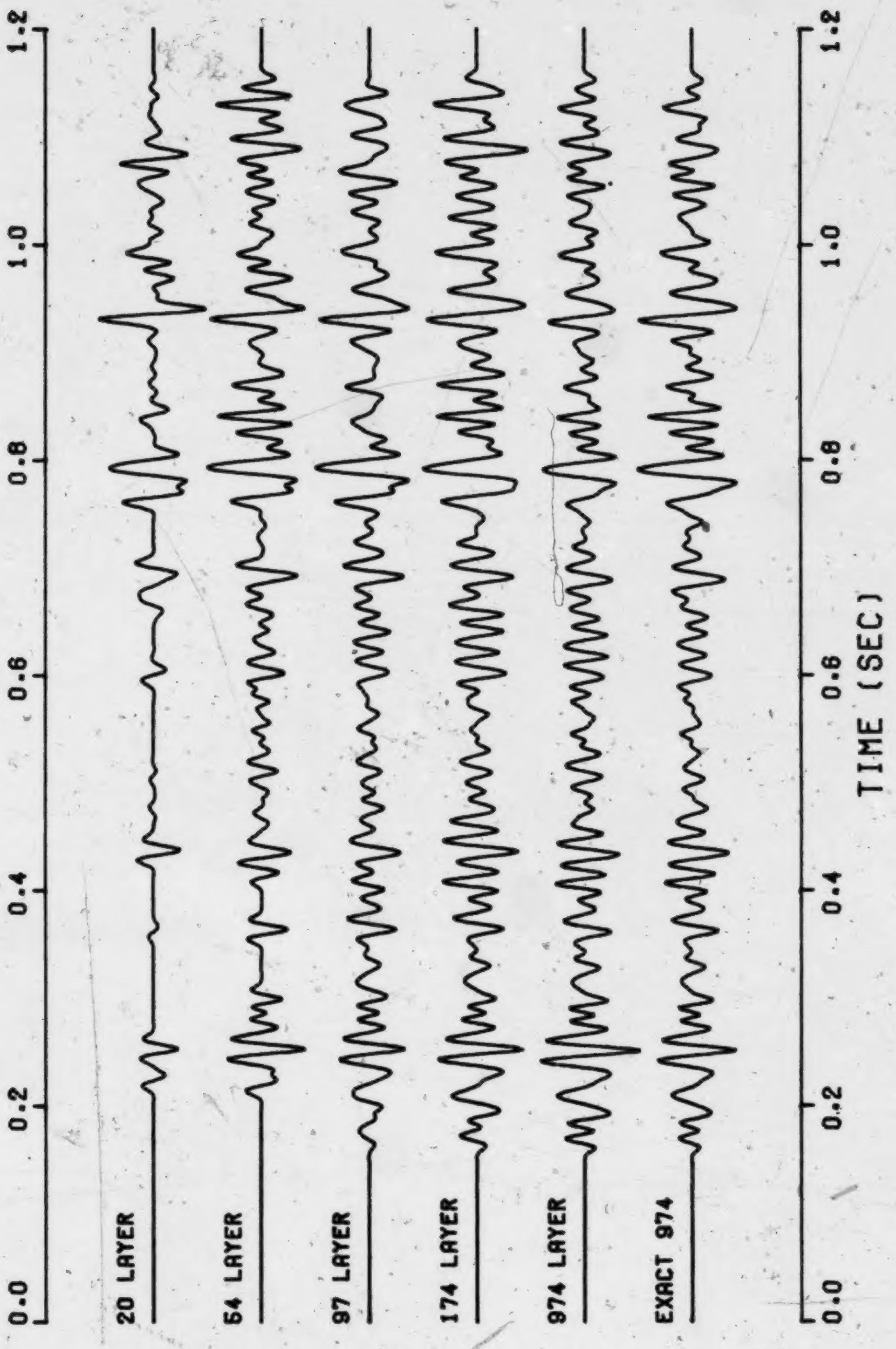

Figure 2.12 Primaries plus surface multiples synthetics for the model near Edmonton, Alberta.

where $\underline{r}$ is the position vector and $\underline{K}$ is the complex propagation constant which will be written as

$$\underline{K} = \underline{P} - i\underline{A} \tag{2.60}$$

where $\underline{P}$ is the phase vector and $\underline{A}$ is the attenuation vector. For plane waves the geometric interpretation of the direction of these vectors is that $\underline{P}$ is perpendicular to planes of constant phase (wave fronts) and $\underline{A}$ is perpendicular to planes of constant amplitude (Borchert, 1973). In general $\underline{P}$ and $\underline{A}$ do not need to be in the same direction.

In the elastic case, where no absorption is present, the formulas used for the reflection and transmission coefficients in the zero'th approximation of asymptotic ray theory are just those of plane waves (Cerveny and Ravindra, 1971). In the anelastic case, where absorption is present, the problem of calculating the reflection and transmission coefficients for plane waves at a plane interface has been examined by Lockett (1962). He showed how to set up a 4 by 4 matrix equation which must be solved for the appropriate coefficients; however, he did not provide an analytic expression for the actual solutions. His equations are in terms of displacements. Cooper and Reiss (1966) and Cooper (1967) have solved the same problem in terms of potentials. The problem has been further discussed for SH waves by Borchert (1977). The solution is obtained in the same manner as for the elastic case except that the velocity, wave number and elastic modulus are replaced by their complex equivalents. As a result, the reflection and transmission coefficients become complex functions of frequency. At an interface the solution is still further complicated by the fact that the angle between the phase vector and the attenuation vector must be calculated.

As a result of the introduction of the complex wave vector equation 1.23 now becomes

$$M/\rho = w^2/\underline{K}\bullet\underline{K}. \qquad (2.61)$$

Substituting equation 1.29 into equation 2.61 and equating real and imaginary parts leads to

$$\mathrm{Re}[\underline{K}\bullet\underline{K}] = |P|^2-|A|^2 = \frac{\rho w^2}{m(1+1/Q^2)} \qquad (2.62)$$

and

$$\mathrm{Im}[\underline{K}\bullet\underline{K}] = -2\underline{A}\bullet\underline{P} = -2|A||P|\cos(g) = \frac{-\rho w^2}{m(Q+1/Q)} \qquad (2.63)$$

where Re and Im indicate the real and imaginary parts of the terms in brackets and g is the angle between $\underline{A}$ and $\underline{P}$. Equations 2.62 and 2.63 can be solved for $|A|$ and $|P|$ to yield

$$|P| = w(\rho/m)^{1/2}(F+G)^{1/2} \qquad (2.64)$$

and

$$|A| = w(\rho/m)^{1/2}(F-G)^{1/2} \qquad (2.65)$$

where

$$G = Q^2/2(Q^2+1) \tag{2.66}$$

and

$$F = G\ (1 + 1/Q^2\cos^2 g)^{1/2}. \tag{2.67}$$

Since the phase velocity, c, is equal to w/|P| then

$$c = (m/\rho)^{1/2}(F+G)^{-1/2}. \tag{2.68}$$

Equation 2.68 points out some of the complications which result from the angle g between A and P. The phase velocity is now slightly dependent on this angle, as is the absorption which is given by exp(-A•r). This will make ray tracing more complicated since it is no longer possible simply to apply Snell's law directly when going from one medium to the next. This angle is a result of the boundary conditions at the interface. Since A is perpendicular to the planes of constant amplitude, then a uniform plane wave source in an infinite medium will produce waves where A and P are parallel. Such waves are referred to as homogeneous waves. Presence of an interface can lead to a transmitted wave in which A and P are no longer parallel. Such a wave is referred to as an inhomogeneous wave (Borcherdt, 1973).

Consider a plane P wave striking an interface and producing reflected and transmitted P and S waves as shown in figure 2.13. For simplicity the transmitted and reflected S waves are not shown in figure 2.13. The angle

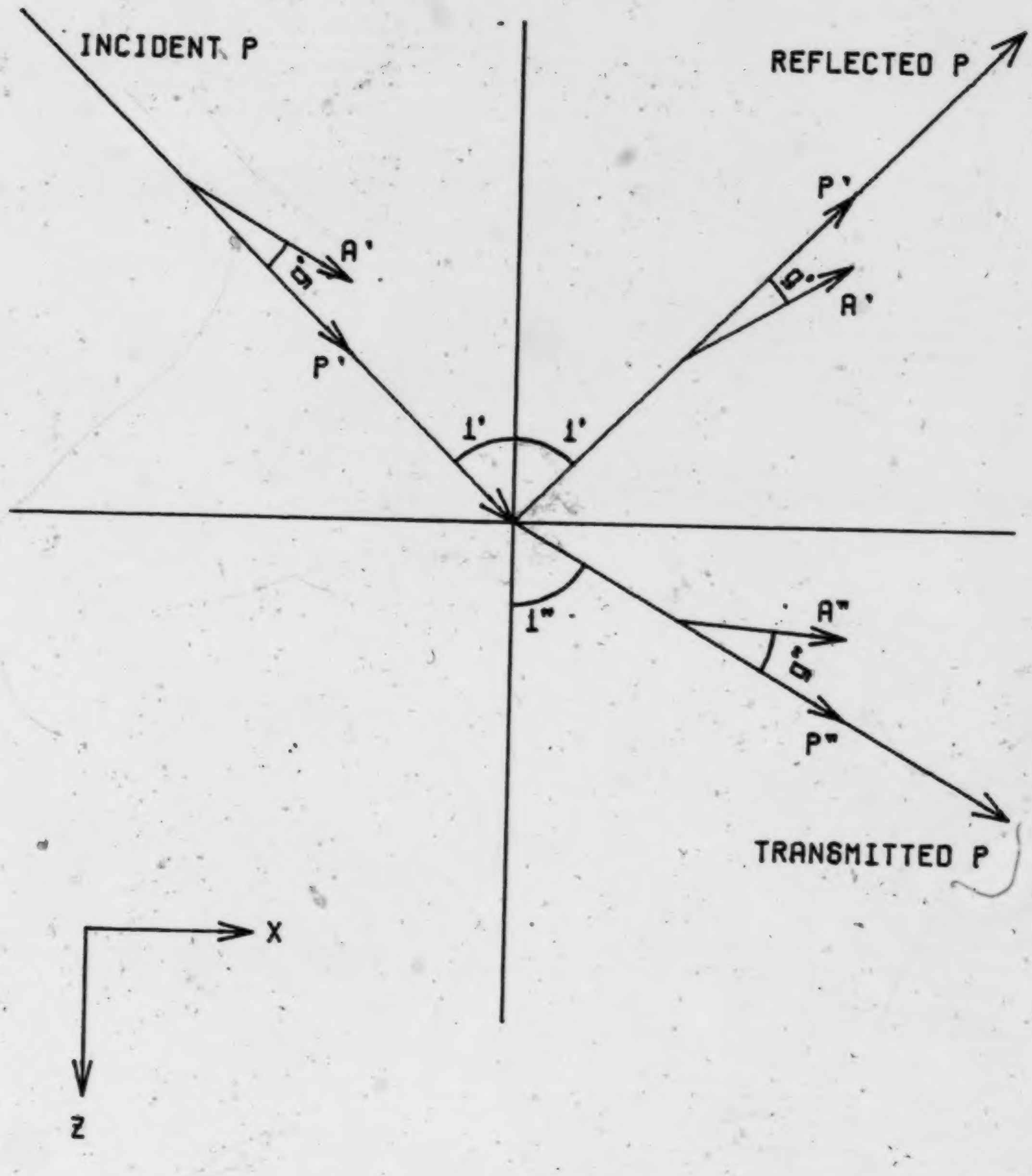
INCIDENT P
REFLECTED P
P'
A'
a
P'
a
A'
i'
i'
i"
A"
a
P"
TRANSMITTED P
X
Z

Figure 2.13 Non-vertical reflection and transmission of P waves.

between the incident ray and the normal to the interface is i' and the angle between the transmitted ray and the normal is i''. In medium 1 the angle between $\underline{A}'$ and $\underline{P}'$ is g' and in medium 2 the angle between $\underline{A}''$ and $\underline{P}''$ is g''. These angles are drawn in the sense that will be used for measuring positive angles in this thesis. Lockett (1962) has shown that the x component of the complex wave vector $\underline{K}$ as denoted by Kx must be constant. This leads to

$$Px' = Px'' \qquad (2.69)$$

and

$$Ax' = Ax''. \qquad (2.70)$$

Equation 2.69 is just Snell's law and equation 2.70 is a complex addition to Snell's law. This same law applies to the reflected and transmitted S waves. Equations 2.69 and 2.70 are a direct result of the boundary conditions which require the continuity of displacement and normal stress across a boundary.

The procedure used in this thesis to describe an absorptive medium is to specify the density, homogeneous phase velocity, and Q value at a particular frequency for the medium. The real part of the complex modulus is then calculated from the homogeneous phase velocity using equations 2.66 to 2.68 with $g=0$. Futterman's model is used to give the frequency dependence of the homogeneous phase velocity and Q. Alternatively, m could be specified instead of the homogeneous phase velocity and a relation for the frequency dependence of m could be easily calculated. At an interface these parameters, which characterize the medium, are known on both sides of the interface and i' and g' are known on one side of the boundary. Using equations 2.64 to 2.67 and simple geometry the x components, Px' and Ax', and the z components, Pz' and Az', can be calculated. Equations 2.69 and 2.70 then allow calculation of Px" and Ax". Equations 2.62 and 2.63 can then be applied to the second medium. They represent two equations in two unknowns (namely Pz" and Az") and can be solved to give

$$Kz''^2 = \mathrm{Re}[\underline{K}''\bullet\underline{K}''] - Px''^2 + Ax''^2 + i(\mathrm{Im}[\underline{K}''\bullet\underline{K}''] + 2Ax''Px'') \quad (2.71)$$

where the real and imaginary parts of $\underline{K}''\bullet\underline{K}''$ are calculated from equations 2.62 and 2.63 and Px" and Ax" are calculated from equations 2.69 and 2.70. From equations 2.60 and 2.71

$$Pz'' = \pm\mathrm{Re}[Kz''^2]^{1/2} \quad (2.72)$$

and

$$-Az'' = \pm\mathrm{Im}[Kz''^2]^{1/2}. \quad (2.73)$$

The square root in equations 2.72 and 2.73 is the principal value of the square root. For angles less than the critical angle the top sign is used in equations 2.72 and 2.73. Then from simple geometry

$$i'' = \tan^{-1}(Px''/Pz'') \quad (2.74)$$

and

$$g'' = 90^\circ - \tan^{-1}(Az''/Ax'') - i''. \qquad (2.75)$$

Once g" has been calculated using equation 2.75 it is possible to calculate the phase velocity in the second medium using equations 2.66 to 2.68.

Equations 2.69 to 2.75 along with equations 2.62 and 2.63 are used in tracing a ray from one medium to the next. When tracing a ray (solving for the ray parameter for a given offset distance) it is necessary to use these equations along the ray path. This makes the calculation more complicated than in the elastic case where Snell's law is used directly in going from one layer to the next.

Another point that must now be considered is the frequency dependence of the absorption. The absorption will depend on $|A|\cos(g)$ and thus from equation 2.65 it is apparent that, if the absorption is to be an exactly linear function of frequency, then the quantity $\cos^2 g\,(F-G)/m$ must be a constant. Eliminating m from this expression by using equation 2.68 gives the equation

$$c[(Q^2+1/\cos^2 g)^{1/2}+Q] = \text{constant}. \qquad (2.76)$$

For homogeneous waves this equation is always true because of equations 2.41 and 2.42. For inhomogeneous waves this equation would only be true if Q also had some dependence on g. However, since it is necessary to know Q in order to calculate g when passing through an interface, it was decided not to allow Q to depend on g. This approximation means that the absorption is only an exactly linear function of frequency for homogeneous waves. For inhomogeneous waves the absorption is not an exactly linear function of frequency. If $|A(g)|$ is the magnitude of $\underline{A}$ for a specific value of g then from equation 2.65 it is obvious that

$$\frac{|A(g)|\cos(g)}{|A(0)|} = \left[\frac{(Q^2+1/\cos^2 g)^{1/2}-Q}{(Q^2+1)^{1/2}-Q}\right]^{1/2}\cos(g). \qquad (2.77)$$

Table 2.4 lists values of $|A(g)|\cos(g)$ divided by $|A(0)|$ at various frequencies for various values of g and values of Q of 25 and 50. The variation of the homogeneous phase velocity and Q as a function of frequency is given by Futterman's model. From the table it is obvious that the deviation of the absorption from an exactly linear function of frequency is very small if Q is not allowed to depend on g. Not allowing this dependence means that it is necessary only to iterate on i and not on i and g when tracing a ray. This will simplify things a great deal.

Lockett (1962) describes the method for setting up the equations which must be solved for the reflection and transmission coefficients in the anelastic problem. The boundary conditions are the same as for the elastic problem and the only change is that elastic modulus, phase velocity, and wave number are complex functions of frequency. This means that the reflection and transmission coefficients are

		frequency		
		10 Hz	50 Hz	250 Hz
$g=15°$	$Q=25$	.999986	.999986	.999986
	$Q=50$	.999996	.999996	.999996
$g=30°$	$Q=25$	.999936	.999933	.999931
	$Q=50$	.999984	.999983	.999983
$g=45°$	$Q=25$	.999808	.999800	.999792
	$Q=50$	.999951	.999950	.999949
$g=60°$	$Q=25$	.999426	.999402	.999377
	$Q=50$	.999853	.999850	.999847
$g=75°$	$Q=25$	.997353	.997244	.997129
	$Q=50$	.999319	.999305	.999291

Table 2.4 Values of $|A(g)|\cos(g)/|A(0)|$.

complex functions of frequency indicating that there is a change of phase on reflection or transmission. Let the general form for an incident wave be given for P waves by

$$\underline{U}(p) = [L(p), N(p)] \exp[-i\underline{K}(p) \cdot \underline{r}] \qquad (2.78a)$$

and for S waves by

$$\underline{U}(s) = [N(s), -L(s)] \exp[-i\underline{K}(s) \cdot \underline{r}] \qquad (2.78b)$$

where the p or s in parentheses indicates that the quantity applies to P or S waves respectively. $\underline{K}$ is given by equation 2.60 and [L, N] and [N, -L] are complex unit vectors in the x-z plane. L and N are complex and obey the equation

$$L^2+N^2=1. \qquad (2.79)$$

The equations for L and N are

$$L = Kx/(\underline{K} \cdot \underline{K})^{1/2} \qquad (2.80a)$$

and

$$N = Kz/(\underline{K} \cdot \underline{K})^{1/2} \qquad (2.80b)$$

where $\underline{K}$ is the complex wave vector associated with the given wave (P or S). For homogeneous waves L and N equal the sine and cosine of the incidence angle respectively. For inhomogeneous waves L and N are complex implying that the x and z components of the displacement have different phases. This means that the particle motion at the given frequency is elliptical. This elliptical motion will occur for all inhomogeneous waves and again is a result of the boundary conditions at the interface. The general form of a reflected P wave is

$$\underline{U}(p) = [L(p), -N(p)]\ R(p)\ \exp[-i\underline{K}(p)\bullet\underline{r}]$$

and of a reflected S wave is

$$\underline{U}(s) = [N(s), L(s)]\ R(s)\ \exp[-i\underline{K}(s)\bullet\underline{r}].$$

Likewise the general form of a transmitted P wave is

$$\underline{U}(p) = [L(p), N(p)]\ T(p)\ \exp[-i\underline{K}(p)\bullet\underline{r}]$$

and of a transmitted S wave is

$$\underline{U}(s) = [N(s), -L(s)]\ T(s)\ \exp[-i\underline{K}(s)\bullet\underline{r}]$$

where R and T denote the appropriate complex reflection and transmission coefficients.

Following a procedure similar to that used by Cerveny and Ravindra (1971) the boundary conditions at an interface lead to a set of 4 by 4 matrix equations which can be solved for the 16 possible reflection and transmission coefficients at an interface. These equations are written as

$$A(4\text{x}4)\ R(4\text{x}4) = B(4\text{x}4) \qquad (2.81)$$

where A, R and B are 4 x 4 matrices. If A(i,j), R(i,j) and B(i,j) denote the element in the i'th row and j'th column of the matrices A, R and B respectively, then

$$B(i,j) = (-1)^{i} \; A(i,j). \tag{2.82}$$

B(i,j) represents the reflection or transmission coefficient for a reflected or transmitted wave of the type indicated by by the index i when the incident wave is of the type indicated by the index j. i or j take on the values 1 to 4 to indicate respectively, a P wave in medium 1, an S wave in medium 1, a P wave in medium 2, and an S wave in medium 2. The components of the matrix A are written as

$$A(1,1) = L'(p) \tag{2.83a}$$

$$A(1,2) = N'(s) \tag{2.83b}$$

$$A(1,3) = -L''(p) \tag{2.83c}$$

$$A(1,4) = -N''(s) \tag{2.83d}$$

$$A(2,1) = -N'(p) \tag{2.83e}$$

$$A(2,2) = L'(s) \tag{2.83f}$$

$$A(2,3) = -N''(p) \tag{2.83g}$$

$$A(2,4) = L''(s) \tag{2.83h}$$

$$A(3,1) = M'(p)\{Kx'L'(p)+Kz'(p)N'(p)\} - 2M'(s)\{Kx'L'(p)\} \tag{2.83i}$$

$$A(3,2) = -\,2M'(s)\,\{Kx'N'(s)\} \tag{2.83j}$$

$$A(3,3) = -M''(p)\{Kx''L''(p)+Kz''(p)N''(p)\} - 2M''(s)\{Kx''L''(p)\} \tag{2.83k}$$

$$A(3,4) = 2M''(s)\{Kx''N''(s)\} \qquad (2.83l)$$

$$A(4,1) = -M'(s)\{Kx'N'(p)+Kz'(p)L'(p)\} \qquad (2.83m)$$

$$A(4,2) = M'(s)\{Kx'L'(s)-Kz'(s)N'(s)\} \qquad (2.83n)$$

$$A(4,3) = -M''(s)\{Kx''N''(p)+Kz''(p)L''(p)\} \qquad (2.83o)$$

$$A(4,4) = M''(s)\{Kx''L''(s)-Kz''(s)N''(s)\} \qquad (2.83p)$$

where the prime refers to medium 1 and the double prime to medium 2.

The problem of calculating the geometric spreading for elastic waves is described in detail in Cerveny and Ravindra (1971). The derivations of the formulas for the geometric spreading for waves in absorptive media will be derived in exactly the same manner. The only difference is that the phase velocity is now a function of g, and g depends the initial value of i at the source. This will make the formula for the spreading slightly more complicated. For a P wave which travels from the surface down through a series of homogeneous layers, is reflected, and returns to the surface, the spreading function (equation 2.142 of Cerveny and Ravindra, 1971) contains a multiplying factor inside the summation. This factor I is given by

$$I(j) = \cos^2\{i(j)\} + \sin^2\{i(j)\}[\mathrm{Re}\{K^2(1)Pz(j)/P^2(1)Kz(j)\}]$$

where the j in parentheses indicates that the parameter applies to layer j.

Thus a synthetic seismogram which includes the effects of absorption and dispersion can be calculated by making the modifications described above to the elastic ray theory. The tracing of rays is more complicated because of the angle g, and the ray parameter and spreading are functions of frequency. Also, the reflection and transmission coefficients are complex functions of frequency. For rays in inhomogeneous layers the amplitude computation in the elastic theory contains a factor involving the square root of the product of density and velocity. This factor would also have to be rederived for the case of inhomogeneous absorping layers. For a series of homogeneous layers this factor is one. The synthetic seismogram including absorption must be computed in the frequency domain and transformed to the time domain. This means that the computation for each ray must be done at all desired frequencies. Performing these computations at each frequency makes this procedure extremely expensive and time consuming on a digital computer. Even if the computations are performed at as few as 100 frequencies, there is an increase of two orders of magnitude in the number of computations required for the anelastic seismogram in comparison to the elastic seismogram. In addition, the anelastic computations are more complicated and require more computer time. Therefore, it is necessary to find approximations that allow computation of the anelastic seismogram without tracing rays at each frequency.

The first approximation would be to ignore the frequency dependence of certain quantities. Using this approximation these quantities would be evaluated at a dominant frequency, f', and would be assumed to have this value at all frequencies. The quantities whose frequency dependence will be ignored are the geometric spreading, ray parameter and the reflection and transmission coefficients.

In order to examine the frequency dependence of the reflection and transmission coefficients, several calculations were made for a simple model. Figures 2.14 to 2.18 show the results of some of these calculations. The velocity, density and Q value for medium 1 were 4 km/sec, 2.0 gm/cc and 30. For medium 2 these parameters had the values 6, 2.5 and 60 respectively. The velocities are the homogeneous phase velocities and along with the Q values apply at a frequency of 40 Hz. The frequency dependence of these quantities is given by Futterman's model. Values of the angles i' and g' for the P wave in medium 1 were specified and apply at 40 Hz also. Values of i" and g" refer to the reflected or transmitted wave and thus apply to the same medium as i' and g' for reflections and to the other medium for transmissions. Solid curves are the amplitude curves and dashed curves are the phase curves. Figure 2.14 is the P wave reflection coefficient for an incident P wave in medium 1. Figure 2.15 is the P reflection coefficient for a P wave incident in medium 2. Figure 2.16 is the reflection coefficient for an S wave when

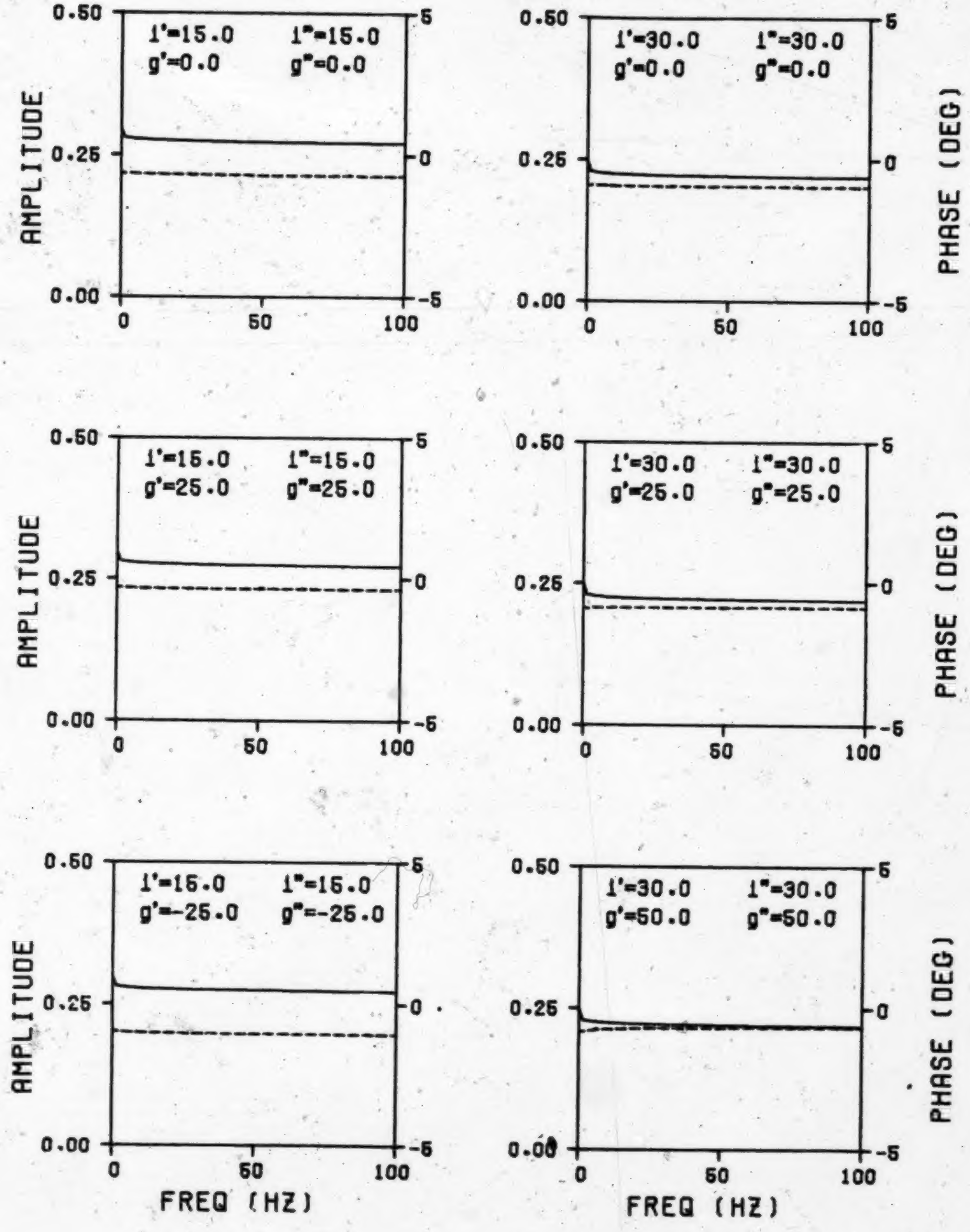

Figure 2.14 Reflection coefficient P1P1. The solid line is the amplitude and the dashed line is the phase.

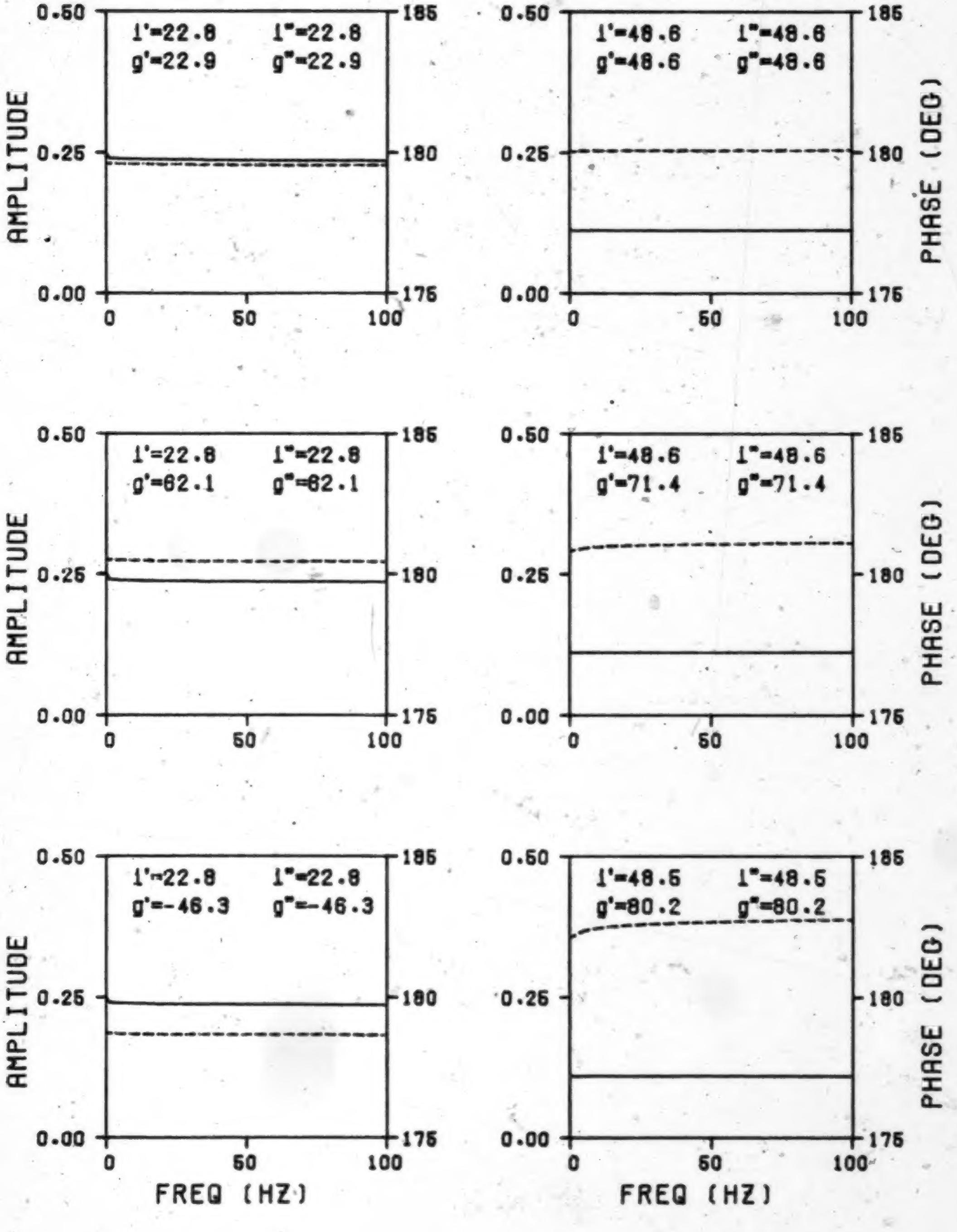

Figure 2.15 Reflection coefficient P2P2. The solid line is the amplitude and the dashed line is the phase.

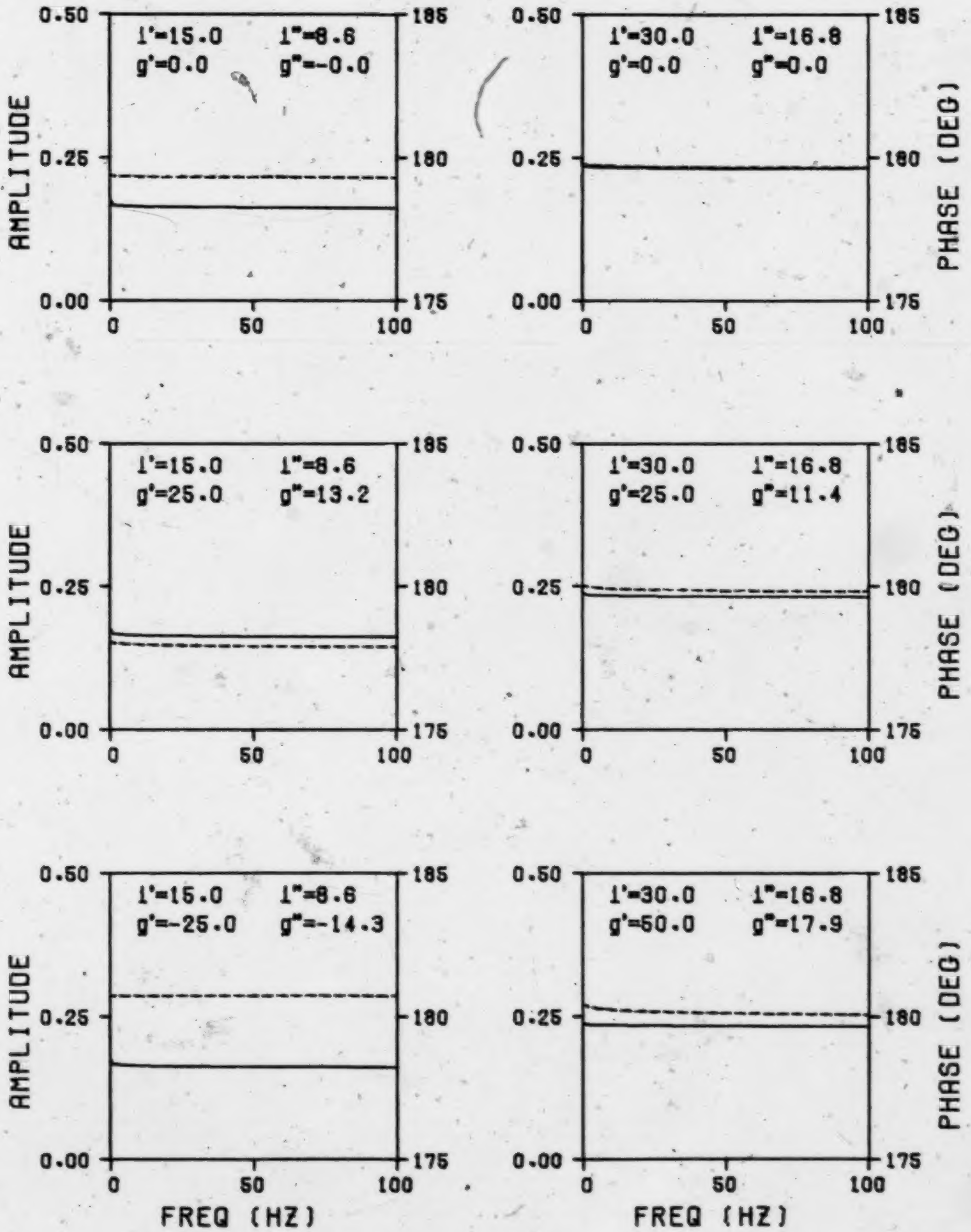

Figure 2.16 Reflection coefficient P1S1. The solid line is the amplitude and the dashed line is the phase.

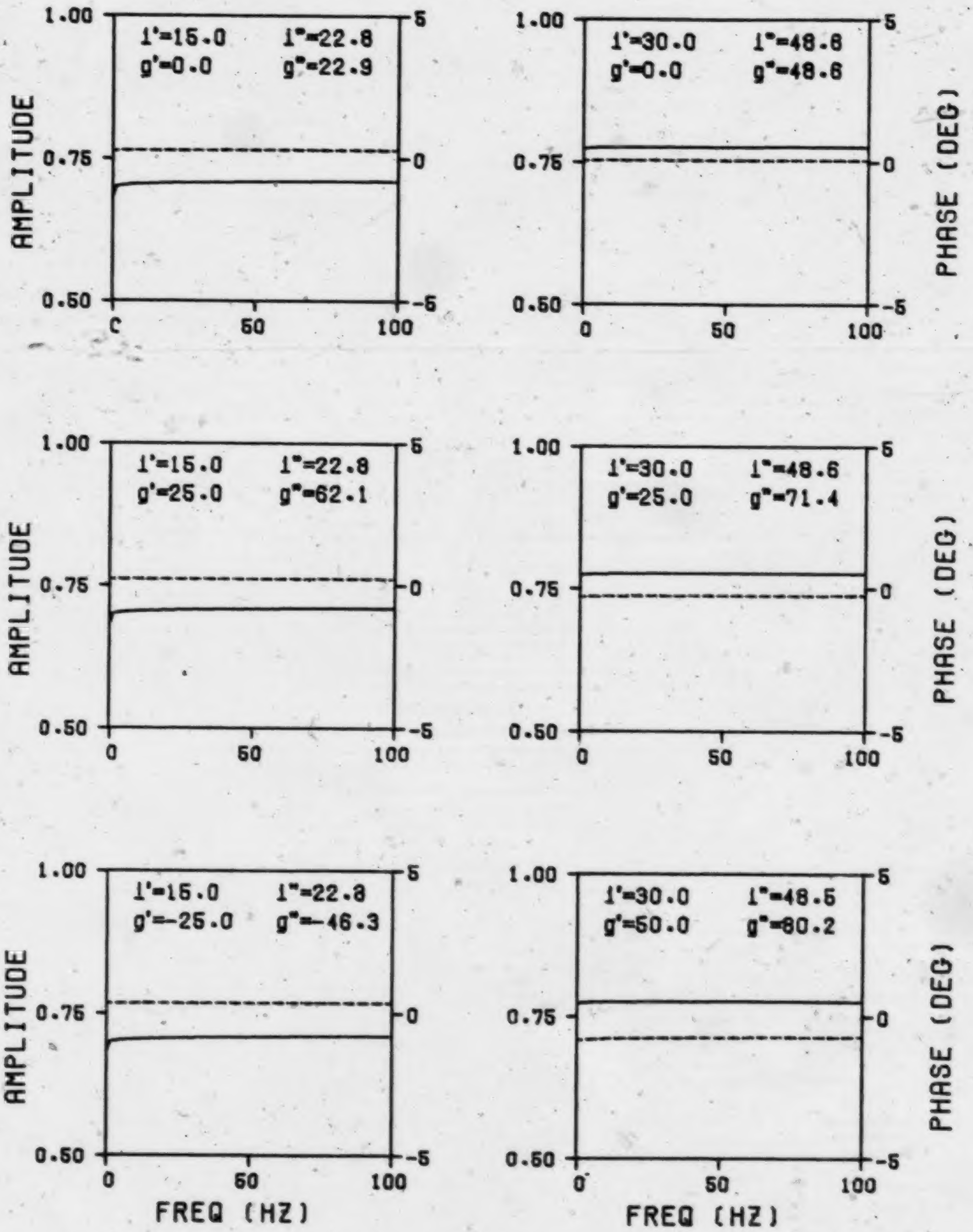

Figure 2.17 Transmission coefficient P|P2. The solid line is the amplitude and the dashed line is the phase.

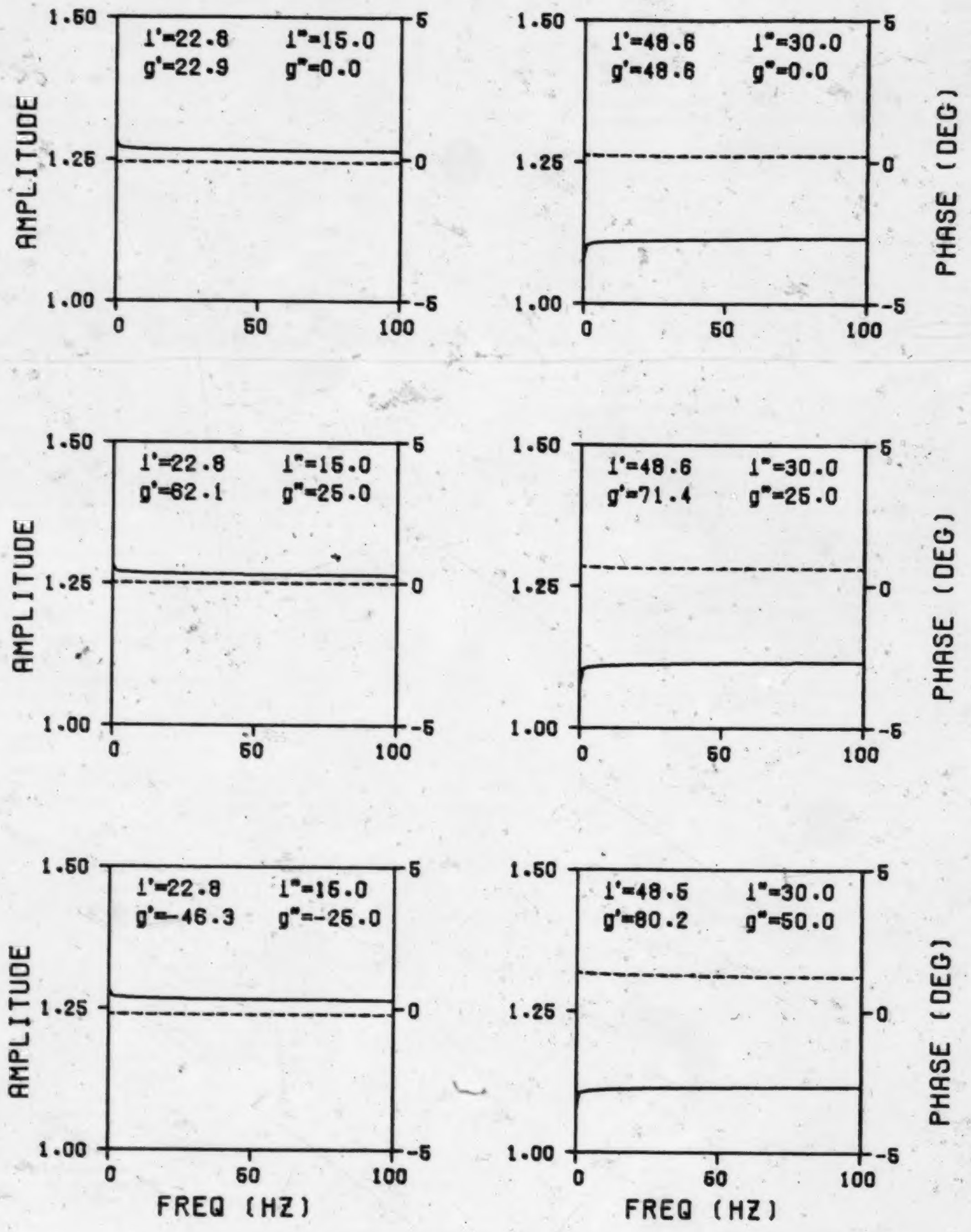

Figure 2.18 Transmission coefficient P2P1. The solid line is the amplitude and the dashed line is the phase.

a P wave is incident in medium 1. Figure 2.17 is the transmission coefficient for a P wave when a P wave is incident in medium 1. Figure 2.18 is the P transmission coefficient when a P wave is incident in medium 2. These figures illustrate only a few of many examples studied. The result of these studies is that the reflection and transmission coefficients are not very sensitive functions of frequency. They are also not very sensitive to small changes in i and are quite insensitive to small changes in g.

The dispersion is very important to the shape of the reflected pulse and can not be ignored. If the absorption coefficient is a linear function of frequency, then the dispersion along the ray can be calculated using Futterman's model if the absorption is known at only one frequency. The absorption at the dominant frequency f' along a ray can be written as $\exp(-w't'/2q')$ where w' is the dominant angular frequency, t' is the arrival time at the receiver for the frequency f' and 1/2q' is an averaged value of $(Q^2+1)^{1/2}-Q$ along the ray. The amplitude due to the absorption at any angular frequency w can be approximated by

$$A(w) = \exp(-wt'/2q'). \tag{2.84}$$

Using equations 1.15 and 2.42 and assuming the rays all travel the same distance from the source to the receiver means that the phase factor as a function of frequency is

$$B(w) = \exp[-iwt'(1-\ln(f/f')/\pi q')]. \qquad (2.85)$$

All rays do not travel exactly the same distance since the angle i is a function of frequency. However, this angle does not change very much over 2 or 3 octaves and thus the assumption is quite good. This makes it possible to calculate the amplitude and phase at all frequencies by doing the calculation of absorption at the dominant frequency f' only. This procedure accounts for the dispersion as well. The synthetic seismogram in the frequency domain is given by

$$X(w) = Y(w')A(w)B(w) \qquad (2.86)$$

where Y(w') includes the product of the reflection and transmission coefficients and the geometric spreading. A(w) and B(w) are given by equations 2.84 and 2.85.

In order to examine the variation with frequency of the ray parameter and the spreading correction another model experiment was done. A 17 layer model was constructed by blocking sonic and density logs obtained at a well near Fox Creek, Alberta. The Q structure of the model was made up. Table 2.5 lists the layer thicknesses, velocities, densities and Q values for this model. The ray considered was a P wave which travelled down through the model from the surface, was reflected from the half space and returned to the surface. Table 2.6 gives the variation with frequency of the ray parameter and geometric spreading factor of this

Thickness (m)	Velocity (m/sec)	Density (gm/cc)	Q value
947.6	2709	2.26	40
669.3	3471	2.41	55
7.9	2629	2.19	45
96.6	3852	2.44	55
9.1	2839	1.94	45
8.8	4251	2.57	60
6.4	3347	2.24	50
25.3	4002	2.43	60
6.4	2983	1.85	50
115.8	4137	2.51	60
58.5	3365	2.18	50
367.9	5.357	2.65	75
6.4	4328	2.50	60
378.9	5976	2.48	80
251.5	4535	2.58	65
19.5	5367	2.69	75
9.1	4306	2.61	60
half space	6151	2.68	80

Table 2.5 17 layer model near Fox Creek, Alberta.

Frequency (Hz)	Normalized Ray Parameter	Normalized Spreading	Phase Error (degrees)
Offset = 469 meters			
10	1.0077	1.0034	0.0034
20	1.0038	1.0017	0.0069
40	1.0	1.0	0.0
80	0.9962	0.9983	0.0275
160	0.9923	0.9966	0.0000
Offset = 1073 meters			
10	1.0076	1.0035	0.0069
20	1.0038	1.0018	0.0206
40	1.0	1.0	0.0
80	0.9962	0.9982	0.0549
160	0.9924	0.9965	0.0549
Offset = 1676 meters			
10	1.0075	1.0038	0.0000
20	1.0038	1.0019	0.0137
40	1.0	1.0	0.0
80	0.9962	0.9981	-.0275
160	0.9925	0.9962	-.0549

Table 2.6 Frequency dependence of ray parameter, spreading and dispersion approximation.

ray for 3 offset distances. The ray parameter and spreading are normalized to the values at 40 Hz. Also shown in the table is the difference between the phase calculated as the argument in equation 2.85 and the true phase calculated by tracing the ray at the indicated frequency. It is clear from this table that the ray parameter and geometric spreading function are not very sensitive to changes in frequency. The approximation used to account for the dispersion is very good.

As a final test on the accuracy of the approximations, the amplitude and phase of the reflected P wave considered for table 2.6 were calculated. Table 2.7 lists the ratio of the approximate amplitude to the true amplitude and the difference between the approximate and the true phase. The true amplitude and phase are obtained by tracing the ray and evaluating the amplitude at the exact frequency. The approximate amplitude and phase are obtained by using the approximation given by equation 2.86. Geometric spreading was included in the calculation.

From table 2.7 it can be concluded that the single frequency approximation given by equation 2.86 is quite accurate over a frequency range of 4 octaves. Since each ray is traced at only one frequency and the amplitude is calculated based on a calculation done at only one frequency, then this approximation does not require significantly more computations than a synthetic seismogram

Frequency (Hz)	Amplitude Ratio (approx to true)	Phase Error (deg) (approx-true)
Offset = 469 meters		
10	1.0047	0.0017
20	1.0030	0.0044
30	1.0007	0.0140
40	1.0	0.0
50	.9977	0.0000
60	1.0000	0.0000
80	1.0001	0.0140
100	.9968	0.0140
120	.9946	-.0280
140	.9935	-.0280
160	.9940	-.0420
Offset = 1073 meters		
10	1.0051	0.0061
20	1.0032	0.0157
30	1.0008	0.0420
40	1.0	0.0
50	.9977	0.0140
60	1.0000	0.0140
80	1.0000	0.0420
100	.9966	0.0560
120	.9943	0.0000
140	.9933	-.0140
160	.9937	0.0280
Offset = 1676 meters		
10	1.0057	0.0009
20	1.0036	0.0105
30	1.0009	0.0140
40	1.0	0.0
50	.9975	0.0000
60	.9998	-.0140
80	.9997	-.0420
100	.9963	0.0000
120	.9940	-.0699
140	.9929	-.0979
160	.9934	-.0699

Table 2.7 Accuracy of single frequency approximation.

without absorption or dispersion. If greater accuracy is required, it can be obtained by tracing a ray at two frequencies and calculating the spreading and the reflection and transmission contribution to the amplitude at both frequencies. The equation for the seismogram in this case is written as

$$X(w) = Y(w)A(w)B(w) \tag{2.87}$$

where $A(w)$ and $B(w)$ are given by equations 2.84 and 2.85. $Y(w)$ is the complex function of frequency which includes the effects of spreading and reflections and transmissions. $Y(w)$ is given by the formula

$$Y(w) = Y(w') \; [1 + b \ln(w/w')] \tag{2.88}$$

where w' is the dominant angular frequency and the constant b is obtained by evaluating $Y(w)$ at w' and at a second frequency. The logarithmic frequency dependence is used since this is the form of the frequency dependence of the velocity, and it is mainly this dependence which causes $Y(w)$ to vary. Examination of table 2.6 and figures 2.14 to 2.18 indicates that this is the proper form of frequency dependence to use. Since the ray is now traced and the amplitude is evaluated at two frequencies, the computation time with this approximation would be twice that of the single frequency approximation. Table 2.8 lists the ratio of the approximate amplitude to the true amplitude and the difference between the approximate and the true phase using

Frequency (Hz)	Amplitude Ratio (approx to true)	Phase Error (deg) (approx-true)
Offset = 469 meters		
10	.9999	0.0017
20	1.0007	0.0044
30	.9997	0.0140
40	1.0	0.0
50	.9985	0.0000
60	1.0014	0.0000
80	1.0025	0.0140
100	.9999	0.0140
120	.9983	-.0280
140	.9978	-.0280
160	.9986	-.0420
Offset = 1073 meters		
10	.9999	0.0061
20	1.0006	0.0157
30	.9997	0.0420
40	1.0	0.0
50	.9985	0.0140
60	1.0015	0.0140
80	1.0026	0.0420
100	1.0000	0.0560
120	.9984	0.0000
140	.9979	-.0140
160	.9988	0.0280
Offset = 1676 meters		
10	.9999	0.0009
20	1.0006	0.0105
30	.9997	0.0140
40	1.0	0.0
50	.9985	0.0000
60	1.0015	-.0140
80	1.0026	-.0420
100	1.0002	0.0000
120	.9986	-.0699
140	.9981	-.0979
160	.9992	-.0699

Table 2.8 Accuracy of two frequency approximation.

this two frequency approximation. The ray used in calculating table 2.8 is the same as that for table 2.7. It is quite apparent that this approximation gives excellent accuracy.

As a final comparison, a P wave, primaries only synthetic seismogram was calculated for the model listed in table 2.5. The calculation was done at offset distances of 469 and 1676 meters. The calculation was done using the single frequency approximation of equation 2.86, the two frequency approximation of equation 2.87, and exactly. Figure 2.19 shows the comparisons of the three methods. Geometric spreading was not included in the calculaticn and a 20 to 80 Hz zero phase Butterworth band pass filter was applied tc all traces. The dominant frequency used was 40 Hz and for the two frequency method the second frequency was 80 Hz. The exact synthetic was calculated at all frequencies between 10 and 160 Hz. All seismograms consisted cf 1024 points with a sample interval of 2 msec. The CPU times required to calculate each trace were measured on an Amdahl 470 V7 computer at the University of Alberta and were .54 sec for the single frequency method, .67 sec for the two frequency method and 41.0 sec for the exact method. It is apparent that there is hardly any detectable difference between the three methods. As a final comparison figure 2.20 compares the exact traces from figure 2.19 to synthetic traces calculated at the same offsets with no absorpticn or dispersion. The same 20 to 80 Hz bandpass

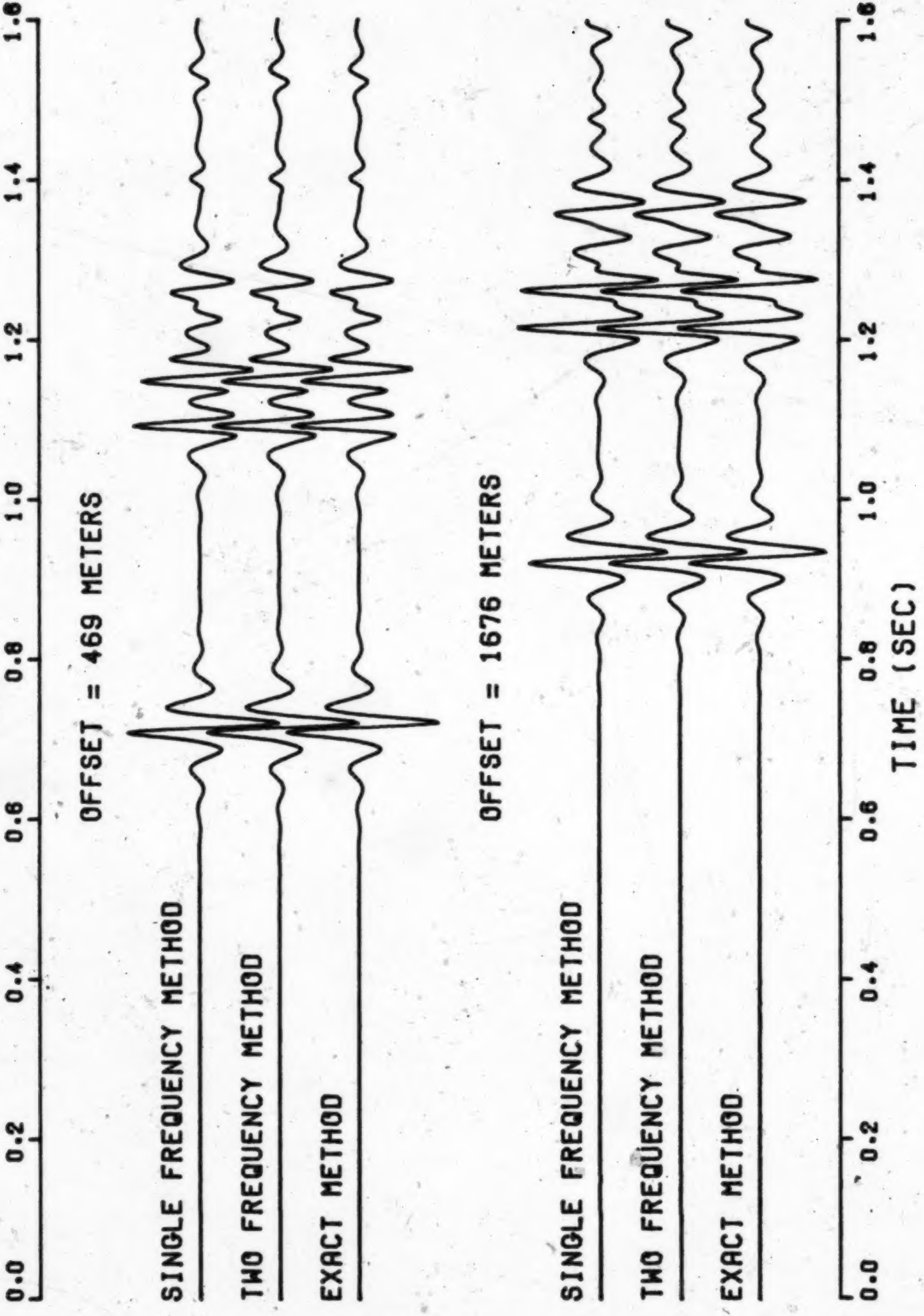

Figure 2.19 Comparison of 3 ray methods for including absorption in synthetic seismograms.

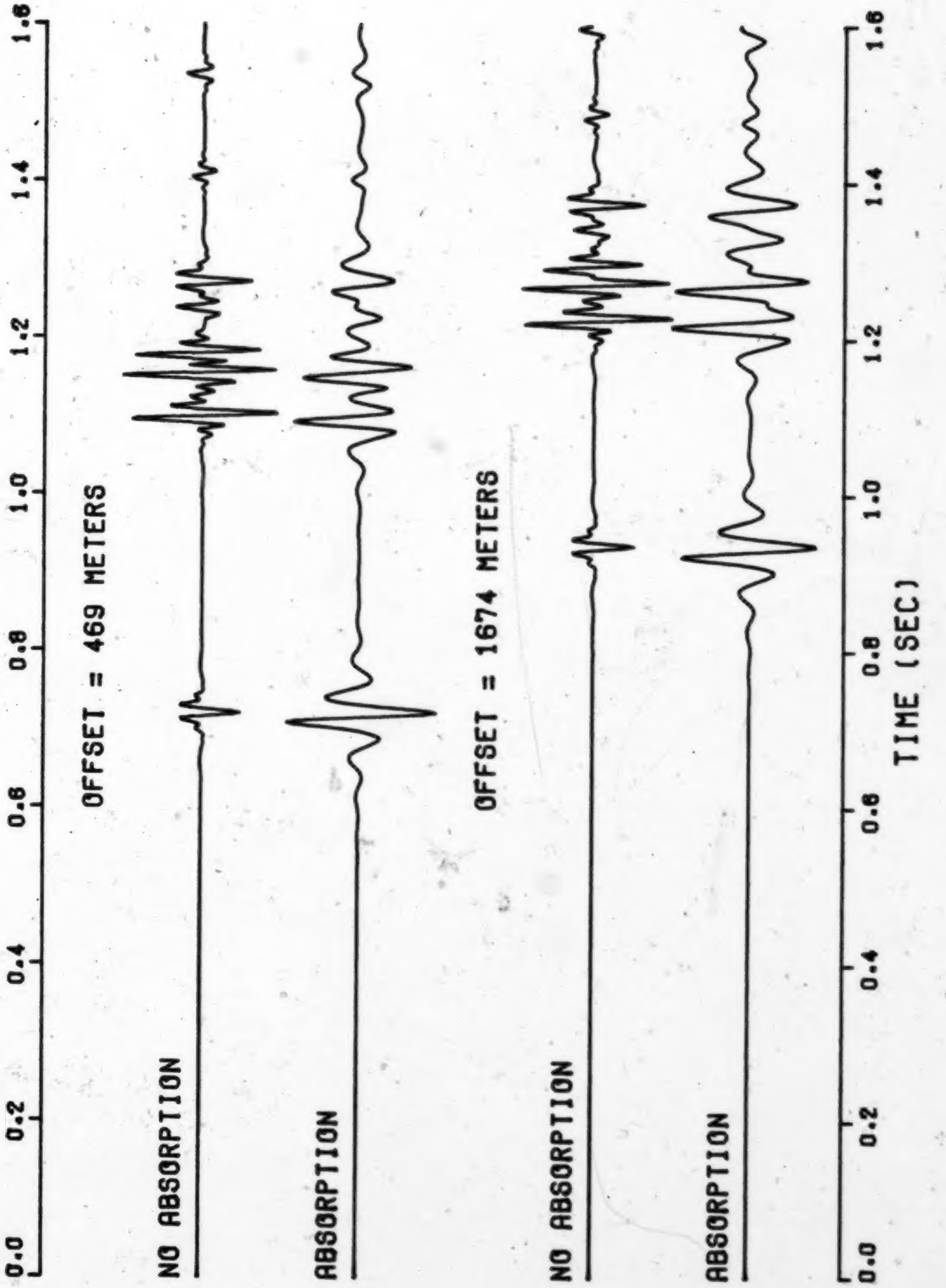

Figure 2.20 Comparison of synthetic seismograms with and without absorption.

filter was used and spreading was not included in the calculation of these traces.

In conclusion it can be said that the calculation of ray synthetic seismograms which include the effects of absorption and dispersion can be done very accurately without greatly increasing the cost due to the inclusion of the absorption and dispersion. This conclusion has only been demonstrated for seismograms including reflections and refractions at less than the critical angle and not for calculations involving head waves. However, it seems apparent that the theory for head waves could be modified following the same procedure as for the case of reflections and refractions.

3. THE SPECTRAL RATIO METHOD

3.1 Introduction

In this thesis absorption will be measured using the spectral ratio method. If $F'(w)$ is the complex Fourier spectrum of a pulse which has travelled a distance z' from the source and $F''(w)$ is the complex Fourier spectrum of a pulse which has travelled a distance z'' in the same medium, then from equation 2.3

$$F''(w) = F'(w) \exp[-iK(z''-z')] \qquad (3.1)$$

where K is the complex wave number given by equation 1.22. From equations 3.1 and 1.22

$$\ln [\,|F''(w)|/|F'(w)|\,] = -a(z''-z') \qquad (3.2)$$

where "a" is the absorption coefficient which is given by equation 2.8. Also from equations 3.1 and 1.22

$$c(w) = \frac{-w(z''-z')}{\mathrm{Arg}\{F''(w)\}-\mathrm{Arg}\{F'(w)\}} \qquad (3.3)$$

where Arg indicates the argument (phase) of the complex quantity in the brackets.

Equations 3.2 and 3.3 define the spectral ratio method. Equation 3.2 indicates that a plot of the natural logarithm of the ratio of the amplitude spectra from two distances against frequency can be used to determine the nature of the frequency dependence of the absorption coefficient. If the absorption coefficient is a linear function of frequency then this plot will be a straight line with slope m. In this case from equations 3.2 and 2.9

$$Q \doteq -\pi(z''-z')/cm. \tag{3.4}$$

Note that equation 3.4 is approximate and would only be exact if Q was replaced by Q' of equation 2.41. For large Q, Q' and Q are approximately equal. Equation 3.3 indicates that the dispersion curve can be calculated from the difference of the phase spectra at the two distances.

Strictly speaking, the spectral ratio method as defined by equations 3.2 and 3.3 is only exact for a wave travelling in an infinite medium. The presence of layering, which causes reflection and transmission effects, affects the validity of these equations. This is a topic which is discussed in a later section of this chapter. Also, in a three dimensional medium $\underline{K}$ is a vector given by equation 2.60 and "a" in equation 3.2 is replaced by $|A|\cos(g)$ where $|A|$ is given by equation 2.65. In this case equation 3.4 is only exact if Q is replaced by Q" where

$$Q'' = [(Q^2+1/\cos^2 g)^{1/2} + Q] / 2. \tag{3.5}$$

Again for large Q, Q" is approximately equal to Q.

In order to apply the spectral ratio method it is necessary to obtain a spectral estimate from the data. The problem of spectral estimation is a classical one which has been discussed in detail by many authors (see for instance chapter 9 of Kanasewich, 1975). The method of spectral estimation used in this thesis is based on a smoothed Fourier estimate. The choice of this spectral estimate over several other estimation techniques was based on a series of model studies which will be described briefly in this chapter.

Spectral analysis methods can be divided into three broad classes, each of which assumes a different model for the data. These models are the moving average or MA model, the autoregressive or AR model, and the mixed autoregressive moving average or ARMA model. A fourth type of model which would fall into the third class of models is the autoregressive integrated moving average model or ARIMA model. These models are discussed in detail in Box and Jenkins (1970).

3.2 MA Spectral Estimation

The MA model of a process is given in terms of z transforms as

$$X(z) = A(z,q)Z(z) \tag{3.6}$$

where $X(z)$ is the z transform of the MA time series, $Z(z)$ is the input process, and $A(z,q)$ is the z transform of a polynomial of order q given by

$$A(z,q) = 1 + a(1)z + a(2)z^2 + \dots + a(q)z^q. \qquad (3.7)$$

The order of the MA process given by equation 3.6 is q. This process is the familiar convolutional model.

A seismogram may be visualized as a series of spikes (reflection coefficients) convolved with a wavelet. In terms of the MA model the z transform of the spikes is Z(z) and the z transform of the wavelet is A(z,q). X(z) is the z transform of the seismogram. Of course A(z,q) changes with time because of the absorption. If a seismogram has been recorded at some point that signal is just A(z,q) (neglecting for now the effect of interfering reflections which will be discussed in a later section). The spectral estimate of that signal is obtained by evaluating A(z,q) on the unit circle given by z=exp(-iw) where w is the angular frequency. This evaluation on the unit circle is nothing more than a Fourier transform and so it can be concluded that a Fourier spectral estimate is the correct estimate to use in the spectral ratio method of measuring Q

There are many Fourier spectral estimation techniques available. Several of these classical estimates are discussed by Blackman and Tukey, 1959. Rather than use the transform of a weighted version of an estimate of the autocovariance function, it is computationally easier to transform the recorded pulse directly to obtain the periodogram. The procedure which is used in this thesis is to taper the ends of the data with a cosine bell (page 98 of Kanasewich, 1975) and then to apply an FFT (fast fourier transform) to the tapered series. The complex transform is then smoothed by averaging over several adjoining frequencies centred about the desired frequency. This smoothing is identical to the procedure described by Kanasewich, 1975 for a Daniell spectral estimate, except that for the Daniell estimate it is the power that is averaged.

In order to test this method a simple model consisting of two traces was considered. The first synthetic trace was at a distance of 200 meters from the source and the second was at a distance of 400 meters in the same medium. The medium had a velocity of 4 km/sec, a density of 2.5 gm/cc and a Q of 25. The velocity and Q values apply at 100 Hz and the sample interval was 1 msec. To further test this method, random noise was added to the data. Figure 3.1 shows this data. The top two traces are the data with no noise and the bottom two traces are the same data with 25% random noise added.

The complex spectra for the two distances were calculated using the method outlined above. The window length was 50 msec and 3 data points at each end of the window were weighted with the cosine bell taper. Zeroes were then added to bring the window length for the FFT to

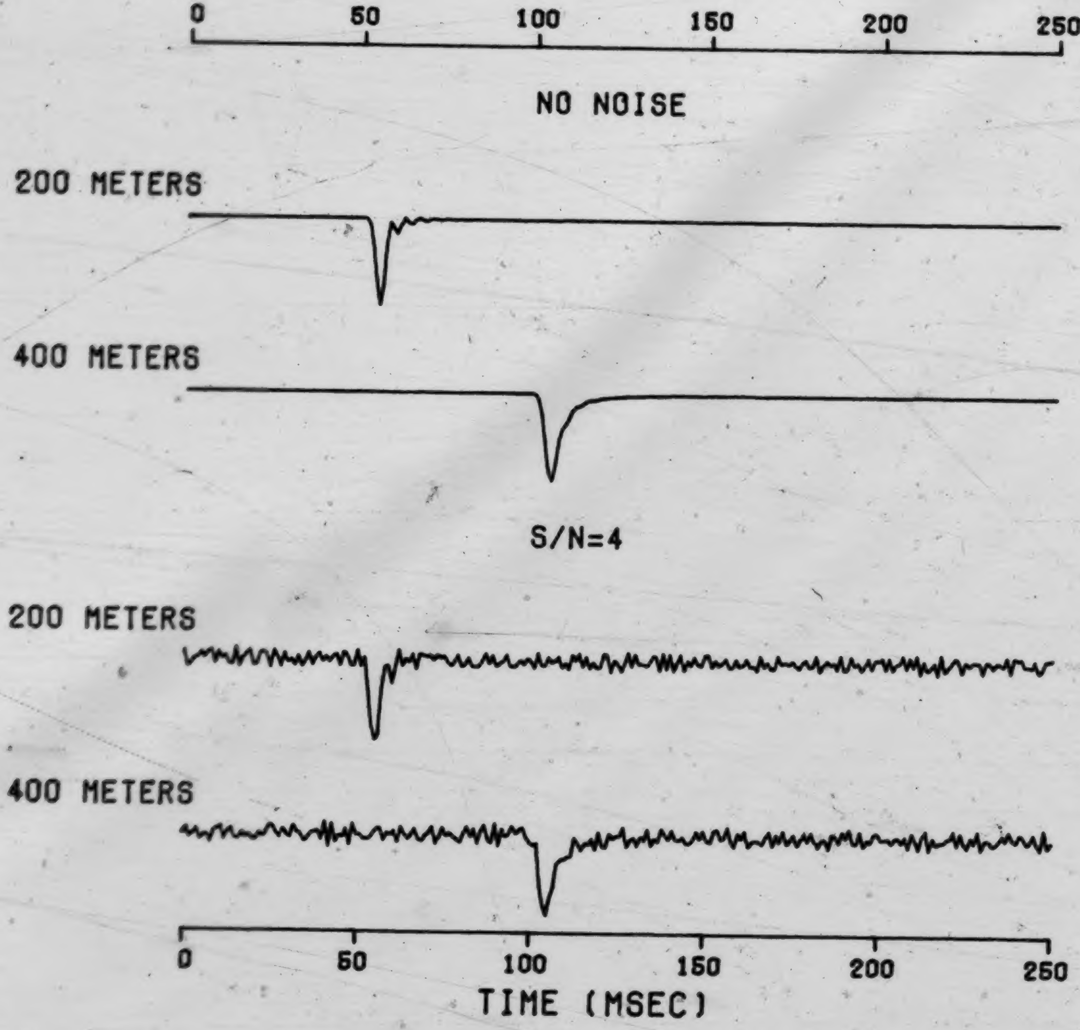

Figure 3.1 Traces used in testing spectral ratio method.

1024 points. This leads to better frequency resolution and does not cause any significant errors since the data is essentially zero outside the analysis window. After the FFT, the smoothing was done over a window which was 10 Hz wide. The natural logarithm of the ratio of the amplitude spectra was calculated and plotted against frequency. The phase velocity was calculated using equation 3.3 and plotted against frequency. Note that in using equation 3.3 it is necessary to "unwrap" the phase curve. This is done by first removing a linear trend, which represents a static time shift of one of the analysis windows, from the phase curve and then by detecting large jumps in the curve (for example -170° to 170°) and correcting these (changing 170° to -190°). The linear trend which was removed is then added back to the phase curve. In addition, a further linear trend representing a static time difference equal to the time between the start of the two analysis windows is added to the phase curve. This ensures that the phase for both windows is calculated relative to the same point in time.

Figure 3.2 shows the plots of the natural logarithm of the amplitude spectral ratio versus frequency and of the phase velocity versus frequency using this method of spectral estimation for the noise-free traces from figure 3.1. The x's are the calculated values and the solid lines are the theoretically correct values. For clarity, only every fourth point is plotted. Note that the effect of the cosine taper causes a slight error in the slope of the

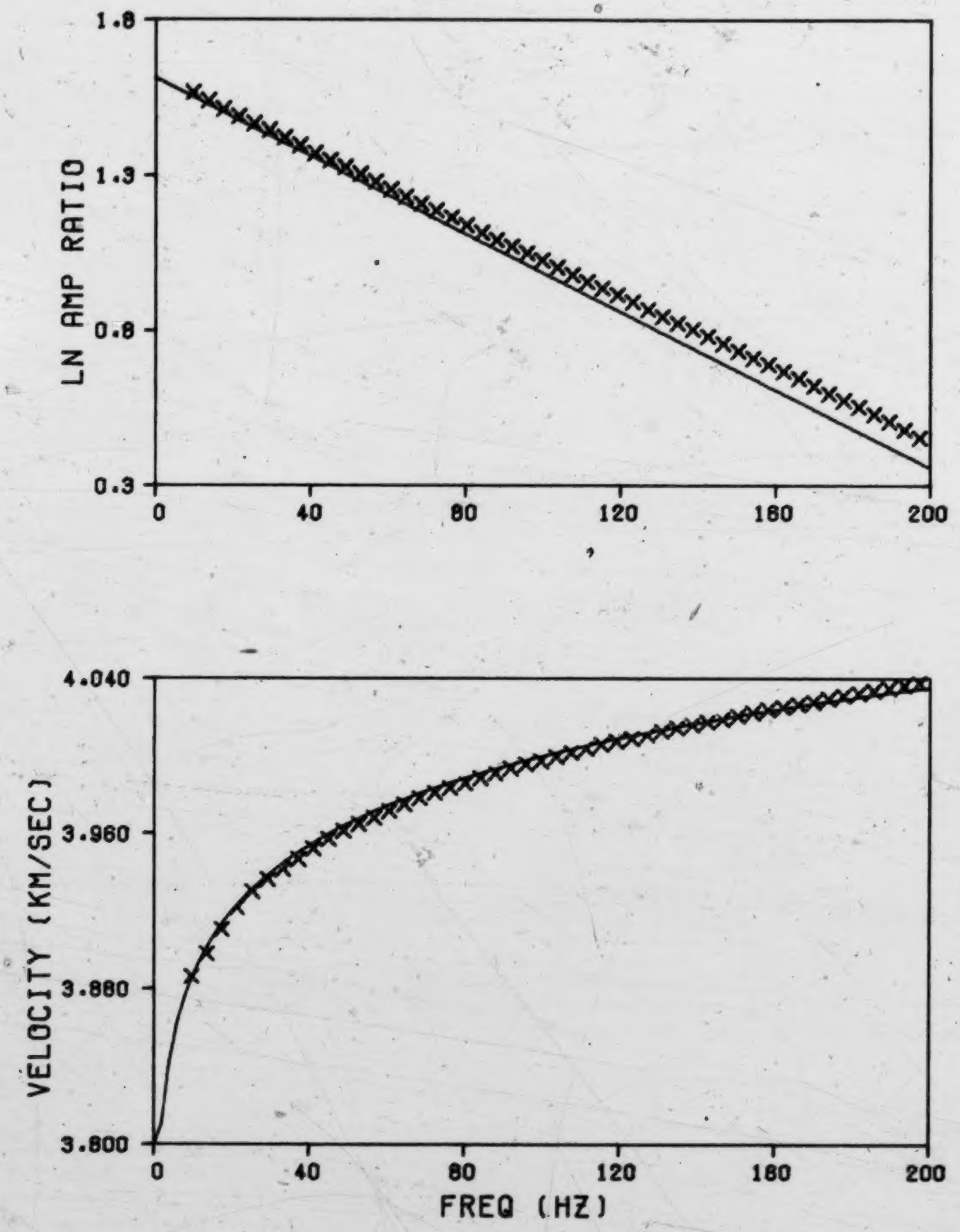

Figure 3.2 Smoothed Fourier spectral ratio plot and dispersion curve for noise-free test example.

spectral ratio plot. The cosine taper is applied to avoid sharp discontinuites at the ends of the data; however, for this simple example there is no such discontinuity and so the taper was not necessary. It was used for this simple example since it will be used for real data. The dispersion curve for this example is exact. Figure 3.3 shows plots for the same data except that this time no cosine taper and no spectral smoothing were applied in calculating the spectral estimates. For this noise-free example the spectral ratio and dispersion curve are exact. Figures 3.4 and 3.5 are the same as figures 3.2 and 3.3 respectively, except that the analysis has been done on the traces with the added random noise. Comparison of these figures indicates that there is less scatter on the data derived from the weighted, smoothed spectral estimates. Note that the noise has caused a fair amount of scatter. This scatter is worst at high frequencies because the signal amplitude is lower there, while the noise amplitude is constant at all frequencies. Figure 3.6 is the same as figure 3.2 except that the smoothing was applied to the amplitude spectrum and the phase spectrum rather than the complex Fourier coefficients. Note that there is no apparent difference between the two methods. The method of smoothing the complex Fourier coefficients is preferred because it is computationally easier due to problems associated with unwrapping the phase curve prior to smoothing.

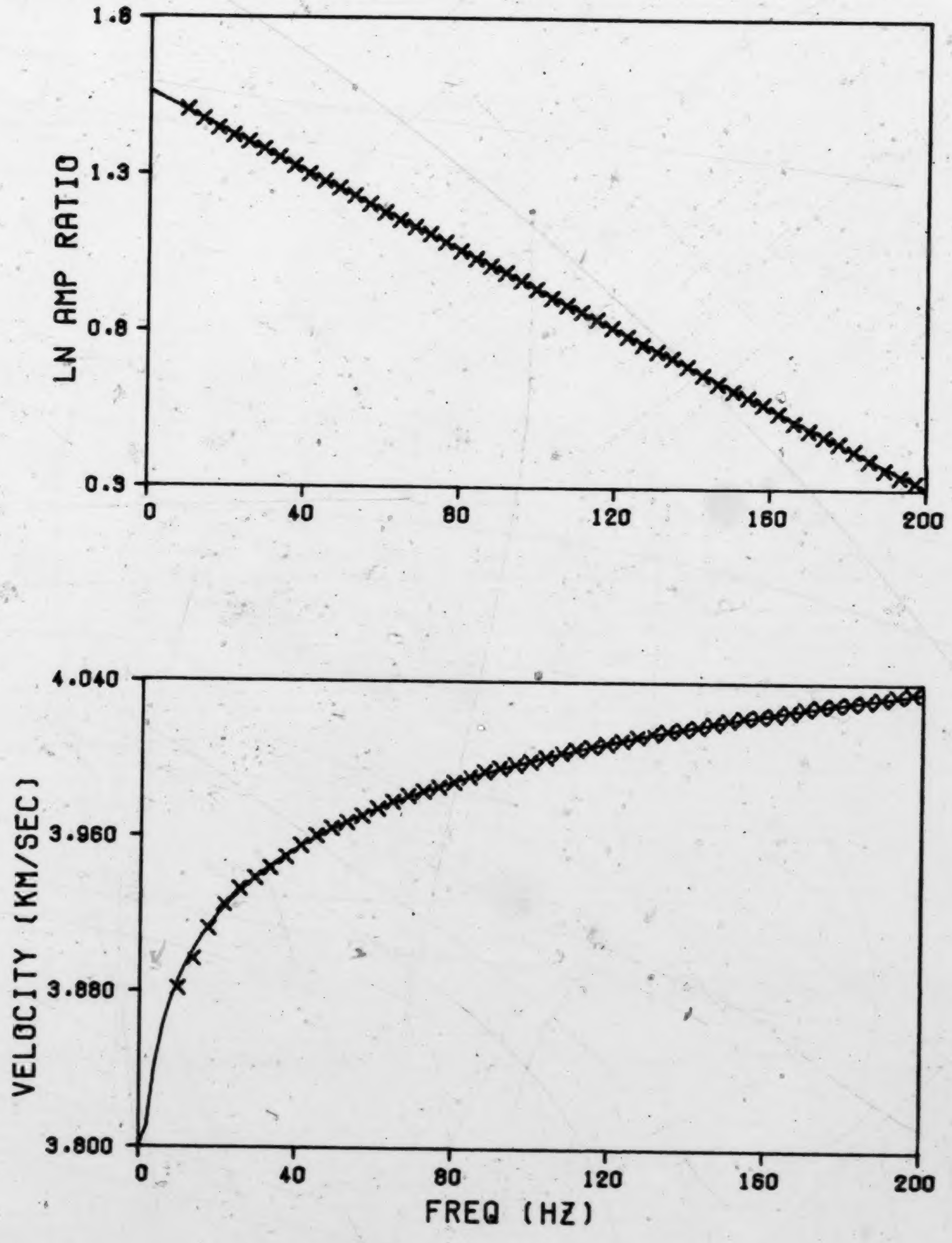

Figure 3.3 Unsmoothed Fourier spectral ratio plot and dispersion curve for noise-free test example.

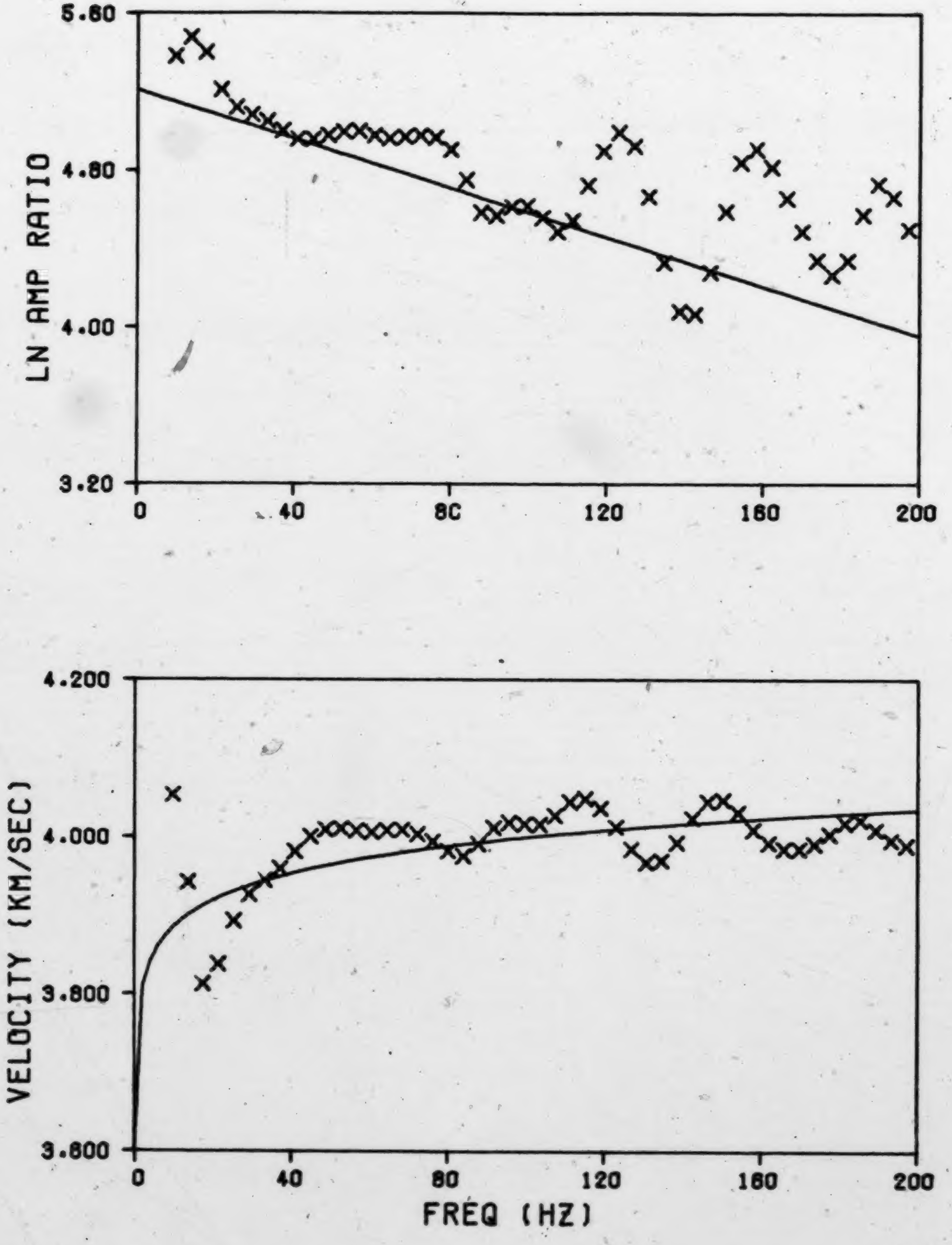

Figure 3.4 Smoothed Fourier spectral ratio plot and dispersion curve for noise-added test example.

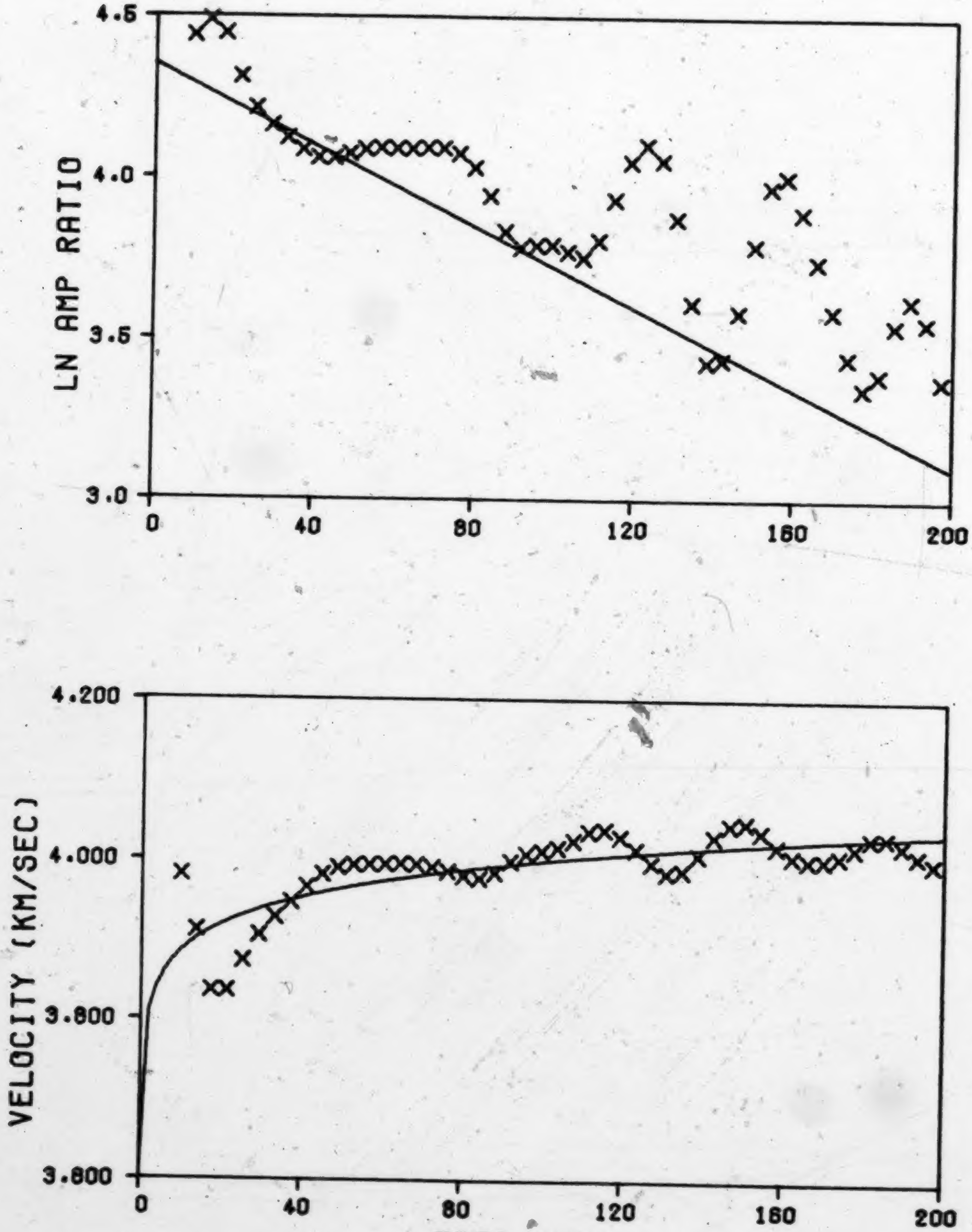

Figure 3.5 Unsmoothed Fourier spectral ratio plot and dispersion curve for noise-added test example.

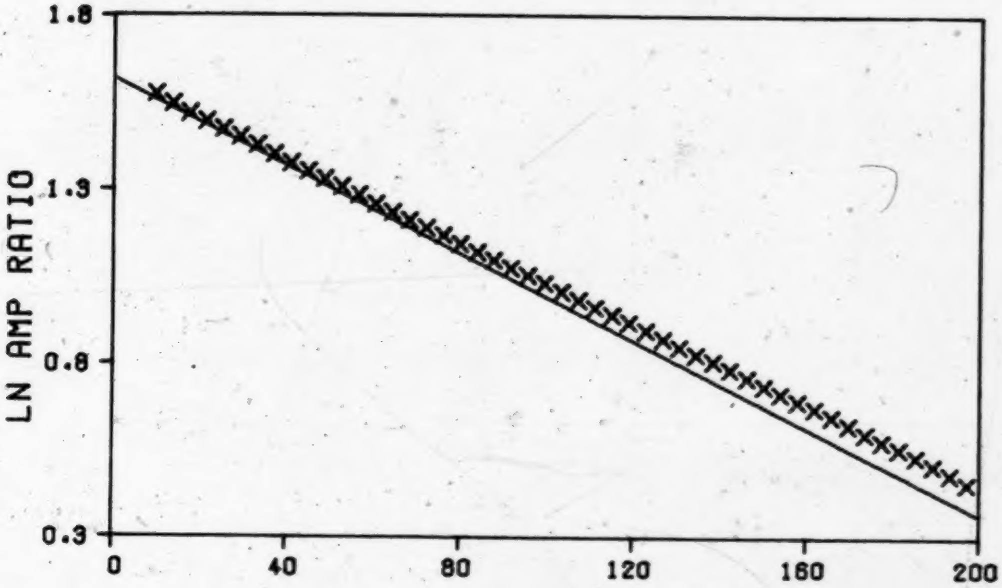

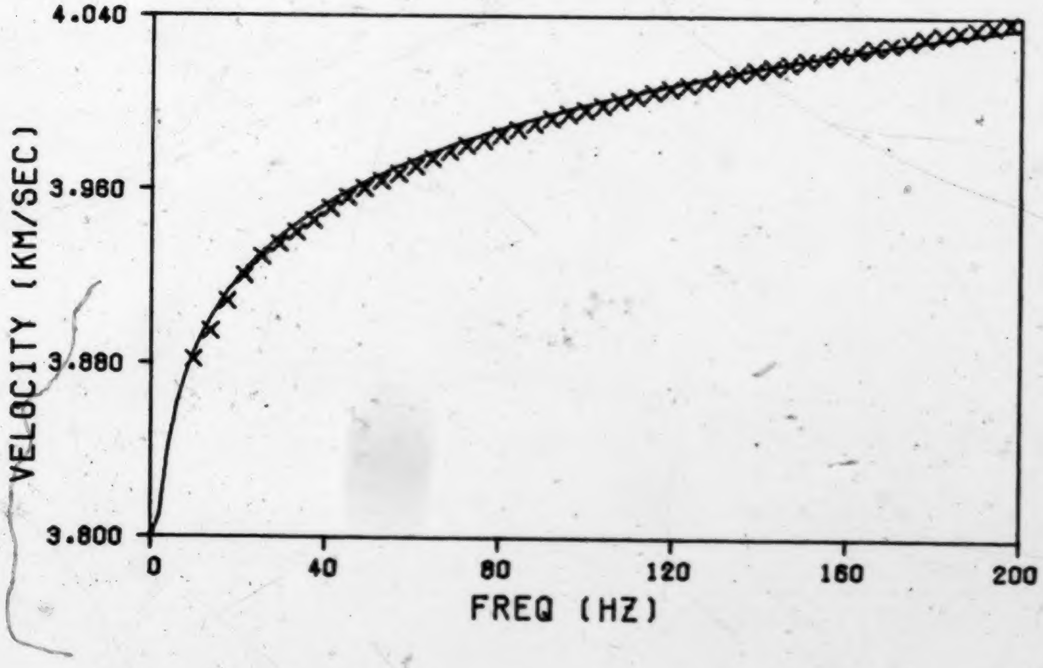

Figure 3.6 Amplitude and phase smoothed Fourier spectral ratio plot and dispersion curve for noise-added test example.

In conclusion it can be said that all of the Fourier spectral estimates give satisfactory spectral ratio plots and satisfactory estimates of the phase velocity.

3.3 AR Spectral Estimates

The AR model of a process of order p is given by

$$X(z) = Z(z)/B(z,p) \tag{3.8}$$

where X(z) is the z transform of the AR process, Z(z) is the input to the process and B(z,p) is the z transform of a polynomial of order p given by

$$B(z,p) = 1 + b(1)z + b(2)z^2 + \ldots + b(p)z^p. \tag{3.9}$$

If Z(z) is random uncorrelated noise with zero mean and variance s^2 then the AR estimate of the power spectrum of X(z) is given by

$$|X(w)|^2 = s^2/|B(w)|^2 \tag{3.10}$$

where |B(w)| is obtained by evaluating B(z,p) on the unit circle. Thus, AR spectral estimatation consists of fitting an AR model as given by equation 3.8 to the given data and evalutating the spectrum using equation 3.10. In fitting the model it is necessary to estimate the coefficients b(i) and the order p of the model from the input data.

If the autocovariance of the input process is known or can be well estimated, then the coefficients b(i) can be calculated by solving the Yule-Walker equations (pp 55 of Box and Jenkins, 1970). These equations are identical to the single channel Wiener filter equations for a unit prediction filter and could be easily solved using the recursive approach of Levinson (1947).

Another method of estimating these coefficients has been proposed by Burg (1967). This method requires no a priori knowledge of the autocovariance. The Burg method of fitting an AR model to the data leads to what has become known as the maximum entropy method or MEM spectrum as was pointed out by Van den Bos (1971). The details of calculating the MEM spectral estimate have been discussed in detail in Ables (1974), Chen and Stegen (1974), Ulrych and Bishop (1975) or chapter 16 of Kanasewich (1975). The basis of the algorithm is that successively higher order unit prediction error operators (see for example Peacock and Treitel, 1969) are fit to the data. These operators are calculated in such a way that the average of the prediction error power when the filter is run both forwards and backwards over the data is a minimum. In running the filter over the data in either direction, the filter is not allowed to run off the data. This average power is minimized with respect to the coefficient b(p) for successively increasing values of p and all calculations are done recursively (see Andersen, 1974).

A second problem to be solved in the AR spectral analysis method is that of estimating the order p of the AR model. The simplest order estimation technique involves the magnitude of the coefficient b(p). This coefficient is referred to as the partial autocorrelation function (Box and Jenkins, 1970, pp 65). When successively higher orders of AR model are fit to the data, this function will be non-zero for orders less than or equal to the true order of the process and zero for orders greater than the true order. Thus if the maginitude of the estimate of b(p) is monitored for increasing p, it may indicate the correct value of p. A more sophisticated estimation criterion has been suggested by Akaike (1969a, 1969b, 1970) and is referred to as the final prediction error or FPE. The FPE is given by

$$FPE(p) = \frac{n+p+1}{n-p-1} P(p) \qquad (3.11)$$

where n is the number of samples of the time series used to fit the model, p is the order of the model fitted and P(p) is the prediction error power for order p. This problem of order estimation has not been solved and more recent criteria have been suggested as improvements by Akaike (1976) and Parzen (1976).

The MEM spectral analysis method has been widely studied and compared to MA methods (Lacoss, 1971, Ulrych, 1972, Smylie and Ulrych, 1973, Ables, 1974, Chen and Stegen, 1974 and Fougere, 1977). In general these comparisons have focussed on sharpness of spectral peaks in defining resolution. In this respect the MEM method has been claimed to be a superior spectral analysis method. Treitel et al (1977) emphasize the very important point that these comparisons are not very meaningful unless the nature of the process producing the data is known. Only when the process is known can a particular spectral estimation method be said to be superior. Another point that also must be made is that comparisons of MEM and Fourier spectra have often been made on truncated sinusoids in the presence of random noise. Ulrych and Clayton (1976) have shown that such a process is an ARMA process and thus neither the MEM nor the Fourier spectra is correct. In fact this is an ARMA process which has poles and zeroes on the unit circle.

A relative to the MEM spectral estimate is the maximum likelihood method or MLM spectral estimate (Capon, 1969, Lacoss, 1971). Burg (1972) has shown that the reciprocal of the MLM spectrum is just the average of the reciprocals of the MEM spectra for all orders from 1 to n-1 where n is the length of the series being analyzed.

Both the MEM and MLM methods give estimates of the power spectrum and not the amplitude spectrum. However the latter is the square root of the former and so can be easily calculated. Figure 3.7 shows the plots of the logarithm of the amplitude spectral ratio against frequency for the noise-free and noise-added traces of figure 3.1. The

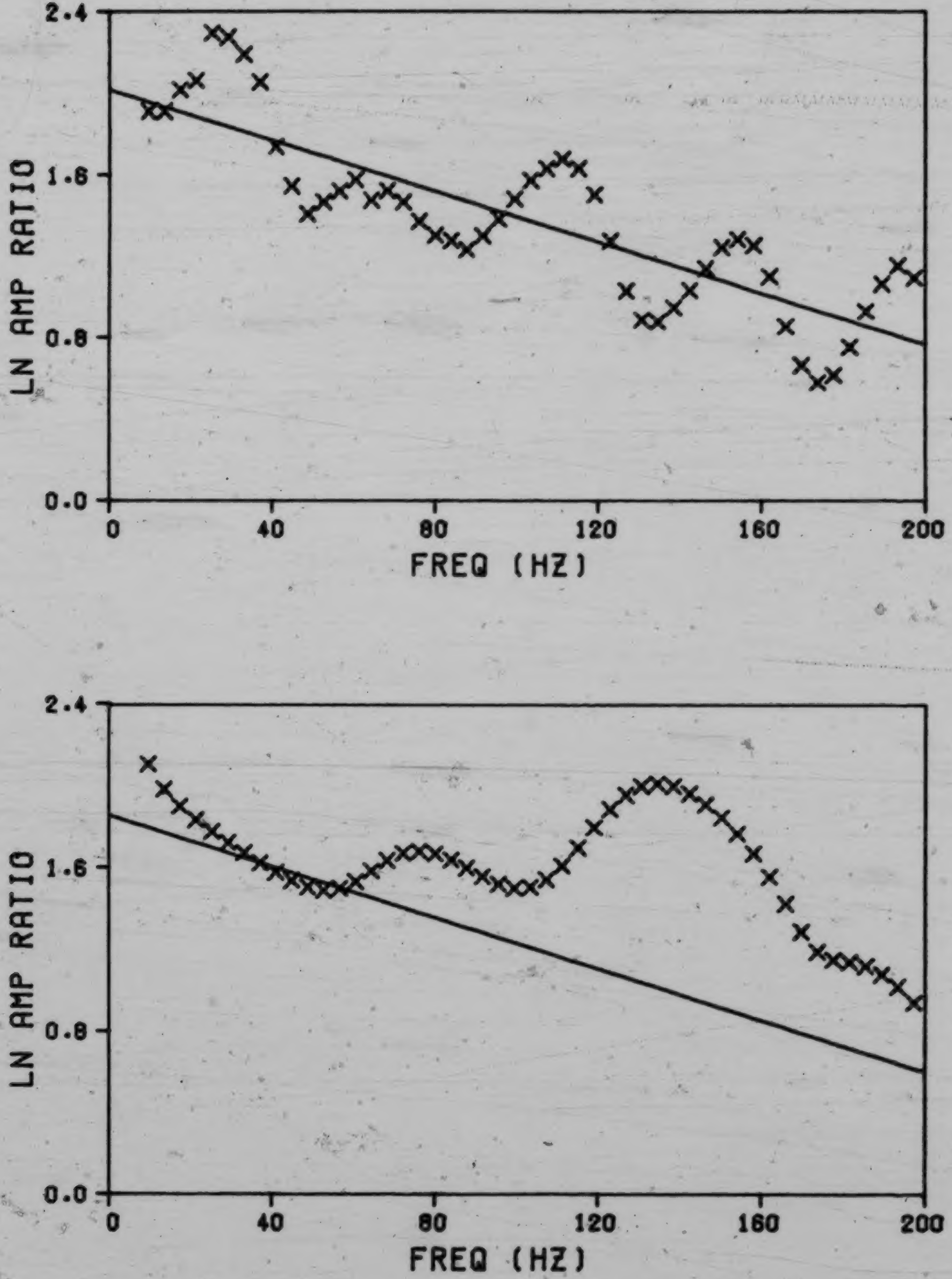

Figure 3.7 MEM spectral ratio plots for noise-free and noise-added test examples.

noise-free example is on the top and the noise-added example is on the bottom. The analysis window length was 50 samples and the order used for the AR process was 17. This order was determined using the FPE criterion. From the figure it is clear that the MEM spectral estimate gives a much poorer spectral ratio then the Fourier methods. Figure 3.8 is the same as figure 3.7 except that the MLM method was used for the spectral estimate. Clearly the MLM method gives a very unsatisfactory spectral ratio.

3.4 ARMA Spectral Estimates

The ARMA model of a process of AR order p and MA order q is given by

$$X(z) = Z(z)A(z,q)/B(z,p) \tag{3.12}$$

where X(z) is the z transform of the ARMA(p,q) process, Z(z) is the z transform of the input and A(z,q) and B(z,p) are z polynomials of orders q and p respectively as given by equations 3.7 and 3.9. If Z(z) is random noise of zero mean and variance s^2 then the ARMA spectral estimate is

$$|X(w)|^2 = s^2|A(w)|^2/|B(w)|^2 \tag{3.13}$$

where |A(w)| and |B(w)| are obtained by evaluating A(z,q) and B(z,p) on the unit circle. Fitting ARMA models to the data requires estimates of all coefficients a(i) and b(i) and also of the orders p and q. Techniques for this

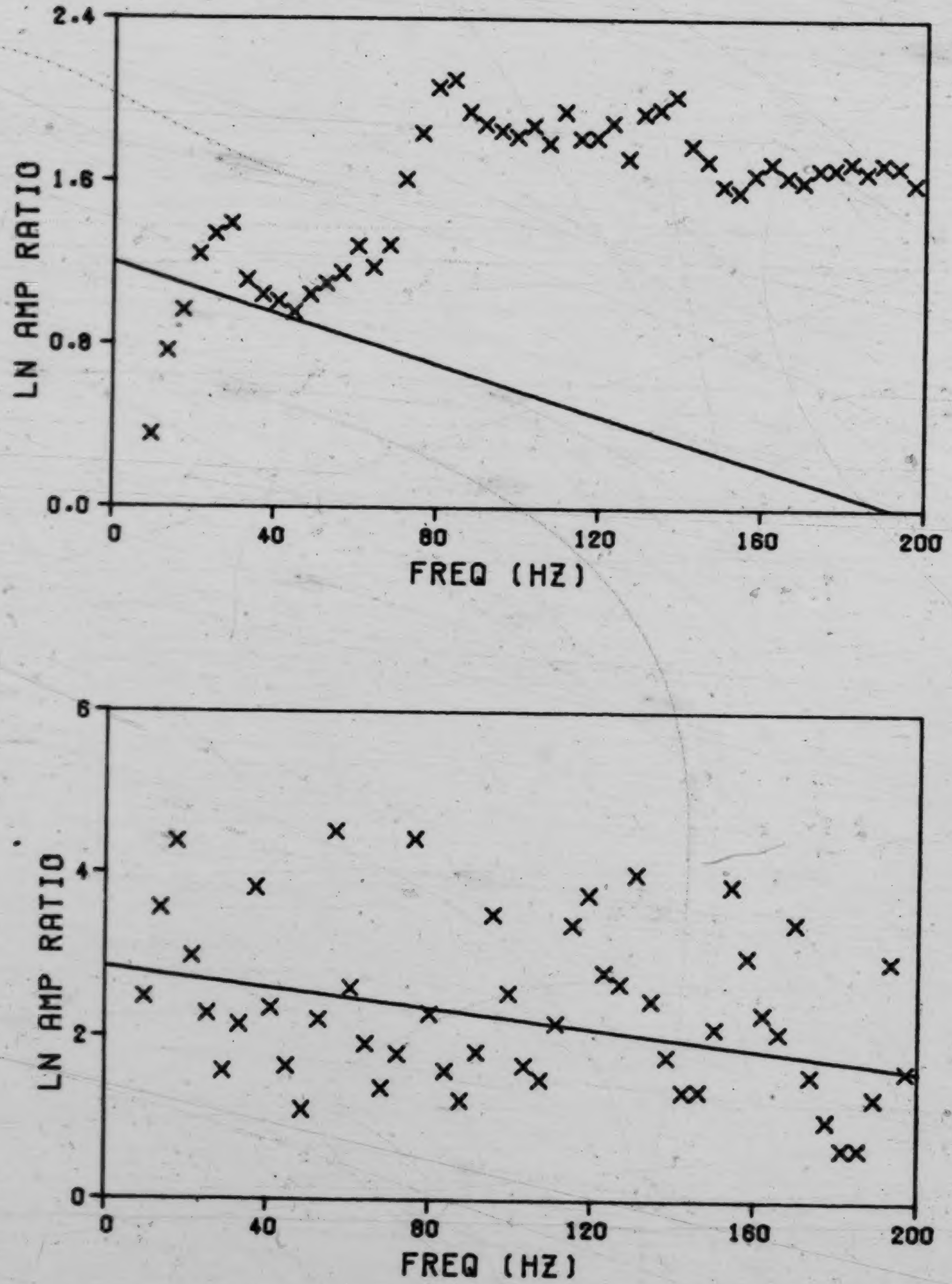

Figure 3.8 MLM spectral ratio plots for noise-free and noise-added test examples.

estimation are given in Box and Jenkins (1970) and involve a great deal of iterating and estimating of orders. Treitel et al (1977) propose an iterative algorithm for ARMA model estimating which requires an estimate of p and q and of A(z,q).

It was pointed out in a previous section that the proper spectral estimation technique depends on the model of the process. It has also been pointed out that the absorption process is essentially a moving average process if interfering reflections are ignored. The effects of such reflections are discussed in detail in the next section and it will be shown that if the proper corrections are made the absorption is essentially a moving average process in this case as well. As a result of these facts and the uncertainties involved in computing ARMA estimates, this analysis procedure has not been tested in this thesis.

3.5 Effect of Reflections on the Spectral Ratio Method

A reflection seismogram or a seismogram recorded within a series of homogeneous layers can be represented using the one dimensional plane wave model by an ARMA process if absorption is ignored (see for instance Treitel and Robinson, 1966). In this case the elastic (no absorption) seismogram Y(z) is

$$Y(z) = A(z)/B(z) \tag{3.14}$$

where A and B are z polynomials. A particular wavelet can be associated with each arrival in $Y(z)$. This particular wavelet can be written as a z transform. Since the absorption is different along different ray paths, the wavelet is not the same for each arrival.

Consider two seismograms recorded at different depths in a layered medium. The first seismogram is given by

$$X'(z) = W'(z)A'(z)/B'(z) = W'(z)Y'(z) \qquad (3.15)$$

where $W'(z)$ is a wavelet which includes the effects of the absorption and dispersion. $W'(z)$ has been treated as a constant wavelet which is not strictly correct; however, it is assumed that $X'(z)$ is short enough in time that the change in the wavelet associated with different arrivals in $X'(z)$ is negligible. In order to examine this assumption in detail consider a simple example where the receiver is located a distance d/2 above a single interface in a half space. The recorded seismogram is given in the frequency domain by

$$X'(w) = W'(w)[1+R\exp(-iwd/c-ad)] \qquad (3.16)$$

where $W'(w)$ is the Fourier transform of the wavelet $W'(z)$ which has been identified with the direct arrival at the receiver and R is the reflection coefficient of the interface. The elastic seismogram is given in the frequency domain by

$$Y'(w) = 1+r'\exp(-iwd/c') \qquad (3.17)$$

where r' is the reflection coefficient and c' is the phase velocity. Equation 3.16 can be written as

$$X'(w) = V'(w)Y'(w) \qquad (3.18)$$

where

$$V'(w) = W'(w)\frac{1+R\exp(-iwd/c-ad)}{1+r'\exp(-iwd/c')}. \qquad (3.19)$$

Examination of equation 3.19 reveals that in this case the assumption that W'(w) is a constant involves ignoring the frequency dependence of the reflection coefficient caused by the absorption, the absorption along the reflection path (distance d), and the phase change associated with the dispersion along the reflection path. If Y'(z) contains many reflections and multiples, the assumption that W'(z) is constant involves these same assumptions about all reflections and multiples which are included in Y'(z). It was shown in the previous chapter that the reflection coefficient is quite constant over 2 or 3 octaves and the phase change associated with the reflection is small. Therefore the assumption that W'(z) is a constant involves assuming that the absorption and dispersion along all reflection and multiple paths within the time window of interest are negligible. Returning to the example of two seismograms at different depths, the seismogram at the second depth is written as

$$X''(z) = W''(z)A''(z)/B''(z) = W''(z)Y''(z) \qquad (3.20)$$

where $W''(z)$ is the wavelet associated with the direct arrival at the second depth and includes the absorption and dispersion between this depth and the source. The assumption that $W''(z)$ is a constant over the analysis window involves the same assumption that the absorption and dispersion along the reflection and multiple paths within the window are negligible.

In order to measure the absorption between the two receivers it is necessary to calculate the logarithm of the ratio of the amplitude spectra of $W''(z)$ and $W'(z)$. From equations 3.15 and 3.20

$$\frac{|W''(w)|}{|W'(w)|} = \frac{|X''(w)|}{|X'(w)|}\,\frac{|Y'(w)|}{|Y''(w)|}. \qquad (3.21)$$

This equation states that it is possible to measure the absorption between two receivers in the presence of other interfering reflections and multiples. It is necessary to know the velocity and density structure so that synthetic seismograms without absorption can be calculated to use as a correction term (namely the spectral ratio $|Y'(w)|/|Y''(w)|$). Equation 3.21 is only valid as long as $W'(z)$ and $W''(z)$ can be treated as constant wavelets within the analysis windows. This is true if the absorption and dispersion are negligible along the raypaths of the interfering reflections. It is now apparent that negligible means negligible with respect to the absorption and dispersion between the two receivers.

The implication of this is that the receivers must be widely separated relative to the distance travelled by any reflections or multiples which are also present within the time limits of the analysis windows. In a similar manner it can be shown that

$$\mathrm{Arg}(W'')-\mathrm{Arg}(W') = \mathrm{Arg}(X'')-\mathrm{Arg}(X')+\mathrm{Arg}(Y')-\mathrm{Arg}(Y'') \quad (3.22)$$

where Arg indicates the phase of the complex function. In applying equation 3.22 the correction phases (Arg(Y') and Arg(Y")) are referenced to the theoretical arrival times of the direct wave at each depth. There is some error introduced by the velocity c' of equation 3.17 since this velocity is the velocity in the absence of absorption and dispersion. In practice this velocity is identified with a reference frequency at which the velocity and Q are to be measured. This is usually chosen as a frequency near the upper limit of the frequency band width of the pulse. This velocity can be approximated by measuring the first arrival times and using them to correct the integrated velocity log. Errors that this uncertanty in c' introduces are not very large. Equation 3.22 states that the dispersion can also be measured in the presence of other reflections if the information is available to calculate the correction terms. Again, the receivers must be widely separated relative to the distance travelled by the interfering reflections.

In the preceding discussion it has been assumed that the two traces were recorded at different distances from the source. If a single reflection seismogram is recorded, $X'(z)$ and $X''(z)$ would apply to different reflections at different times. The corrections given by equations 3.21 and 3.22 are still valid and the requirement of widely separated depths implies that the reflections must be widely separated in time relative to the analysis window lengths. In addition, if a different source was used for the two records, then a correction must be made for the source difference. In a practical experiment this correction could be obtained from a reference seismogram recorded in the same position relative to the two sources.

A simple model study illustrates the effect of this correction. The model used consists of three layers over a half space as shown in figure 3.9. The source is at the surface and traces are calculated at depths of 285, 585 and 615 meters. The velocities, densities, Q values and layer thicknesses are given in the figure and apply at a frequency of 100 Hz. The top traces in figure 3.10 show the synthetic traces which include the effects of absorption and dispersion at the 3 depths indicated for the model in figure 3.9. The bottom traces are the synthetic traces calculated without including the effects of absorption. The bottom traces will be used in calculating the correction to be applied for the effects of other reflections. These synthetic traces were calculated using the vertical incidence, plane wave synthetic program described in chapter 2. A 250 Hz non-zero-phase low pass Butterworth filter was

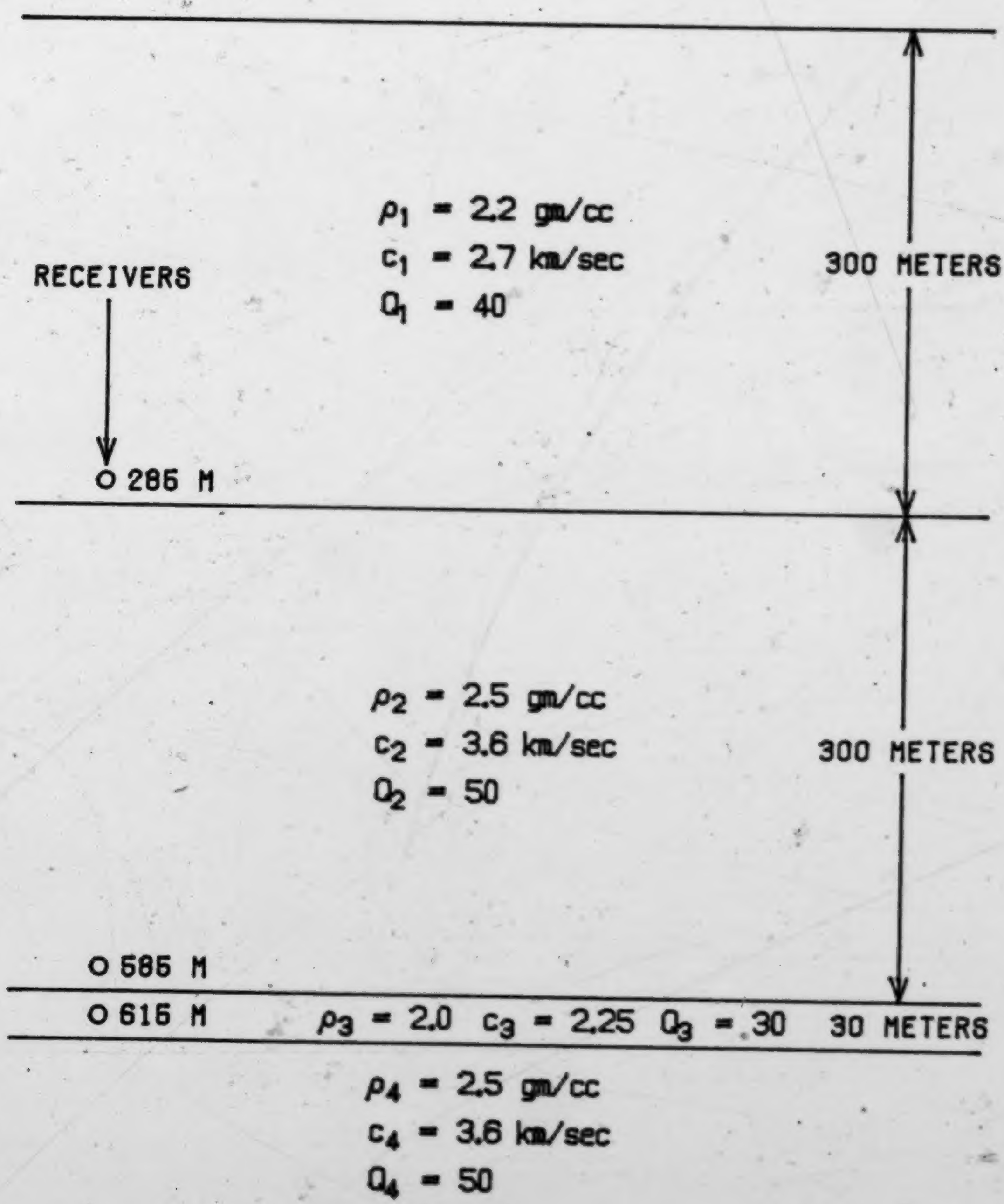
ρ1 = 2.2 gm/cc
c1 = 2.7 km/sec
Q1 = 40
RECEIVERS
300 METERS
O 285 M
ρ2 = 2.5 gm/cc
c2 = 3.6 km/sec
Q2 = 50
300 METERS
O 585 M
O 615 M
ρ3 = 2.0 c3 = 2.25 Q3 = 30
30 METERS
ρ4 = 2.5 gm/cc
c4 = 3.6 km/sec
Q4 = 50

Figure 3.9 Simple model used in illustrating the correction for reflections and multiples.

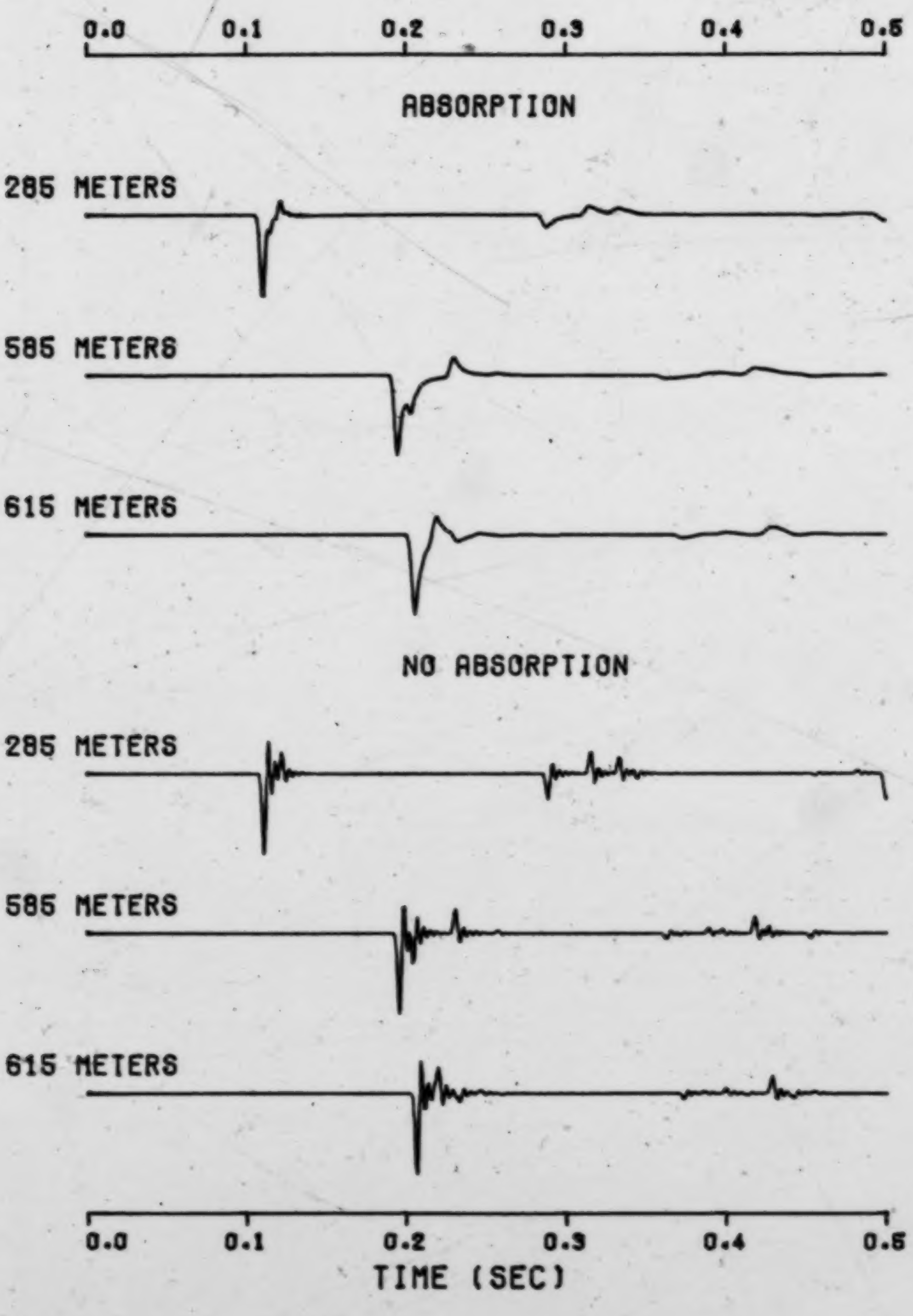

Figure 3.10 Synthetic traces with and without absorption for model in the figure 3.9.

applied to all traces in figure 3.10 and the source was a spike. From this figure it is apparent that there are reflections interfering with the direct arrivals at each depth, especially at 615 meters. Figure 3.11 shows the spectral ratio and dispersion curve calculated for the pair of traces at 285 and 615 meters from figure 3.10 when no correction was made for the effects of other reflections. A 50 msec analysis window was used and zeroes were added to bring the window length to 1024 samples for the FFT. Three points at each end of the window were weighted with the cosine bell and the complex Fourier coefficients were smoothed over a 10 Hz wide window. The sample interval of the data was one msec. The x's are the data values and the solid curves are the theoretically correct values. For clarity only every fourth point is shown in the figure. Note the interference pattern in the measured spectral ratio and dispersion curve due to the constructive and destructive interference of the interfering reflections. Figure 3.12 is the same as figure 3.11 except that the correction given by equations 3.21 and 3.22 has been applied to the data. Note that the interference pattern is no longer present and a very acceptable fit to the theoretically correct values has been obtained. At higher frequencies where the absorption is greater along the reflection paths, the correction, which neglects this absorption entirely, is not as good. The effects of the reflections are not as well corrected at high frequencies as at low frequencies. Figures 3.13 and 3.14

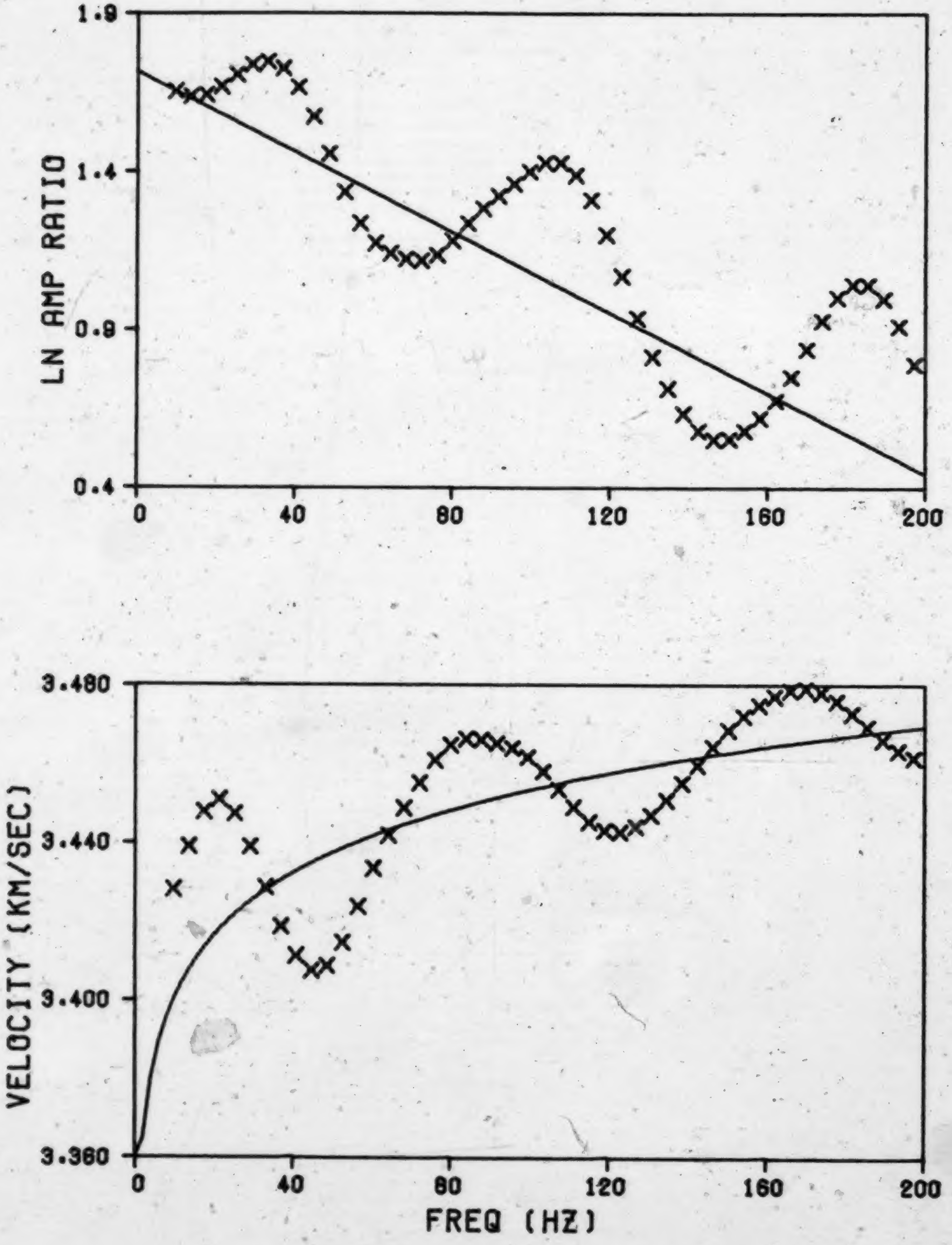

Figure 3.11 Uncorrected spectral ratio and dispersion curve for the synthetic traces at 285 and 615 meters.

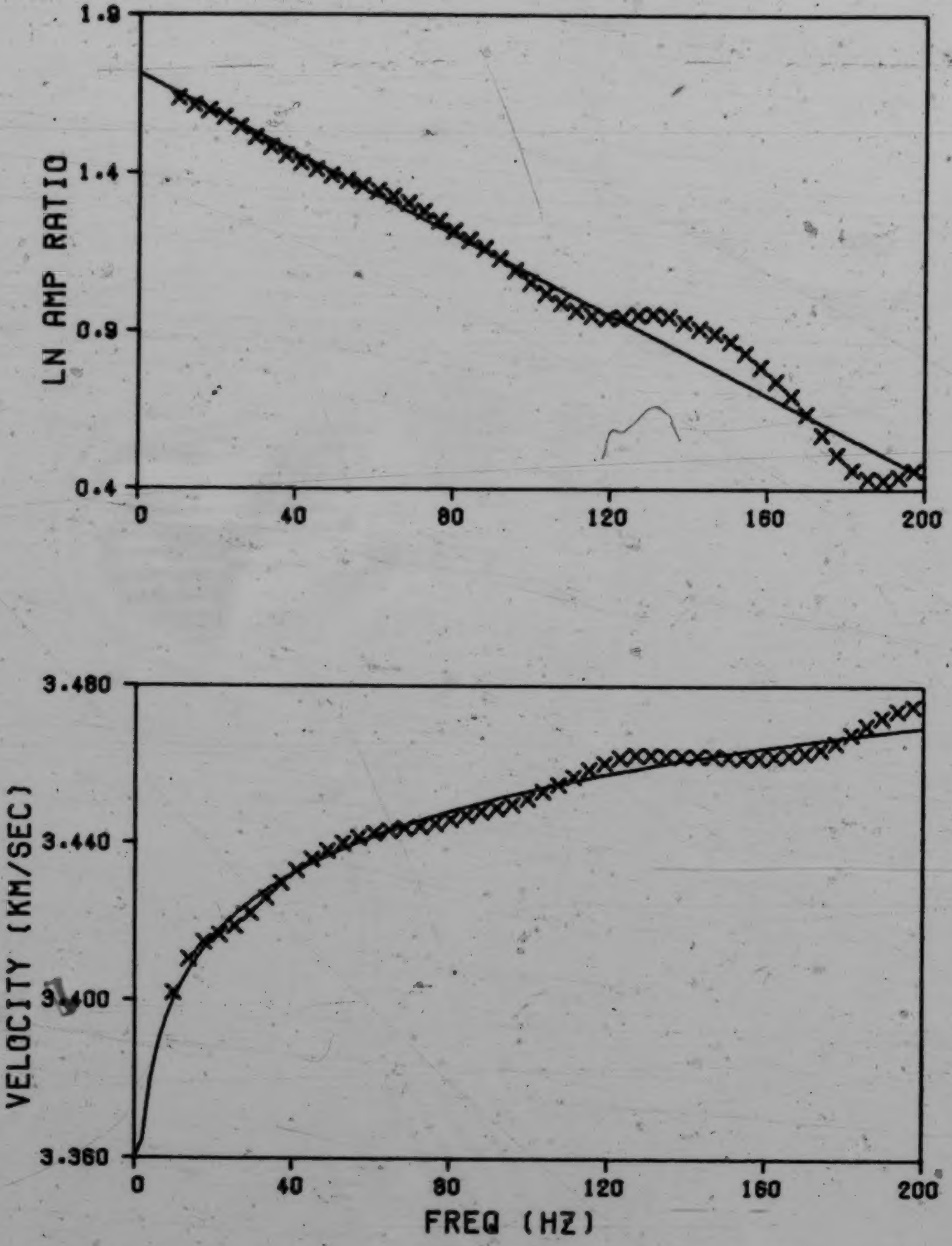

Figure 3.12 Corrected spectral ratio and dispersion curve for the synthetic traces at 285 and 615 meters.

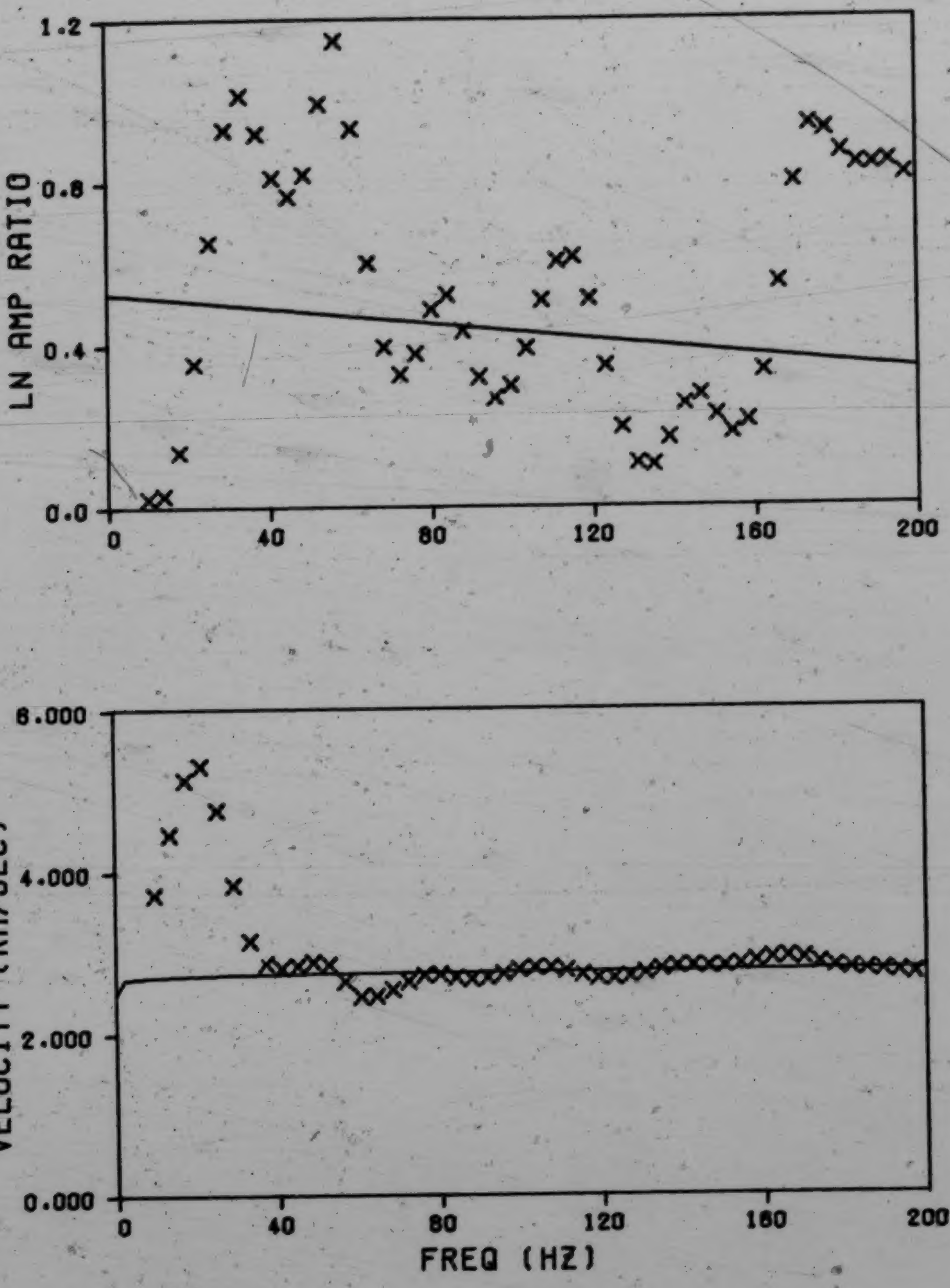

Figure 3.13 Uncorrected spectral ratio and dispersion curve for the synthetic traces at 585 and 615 meters.

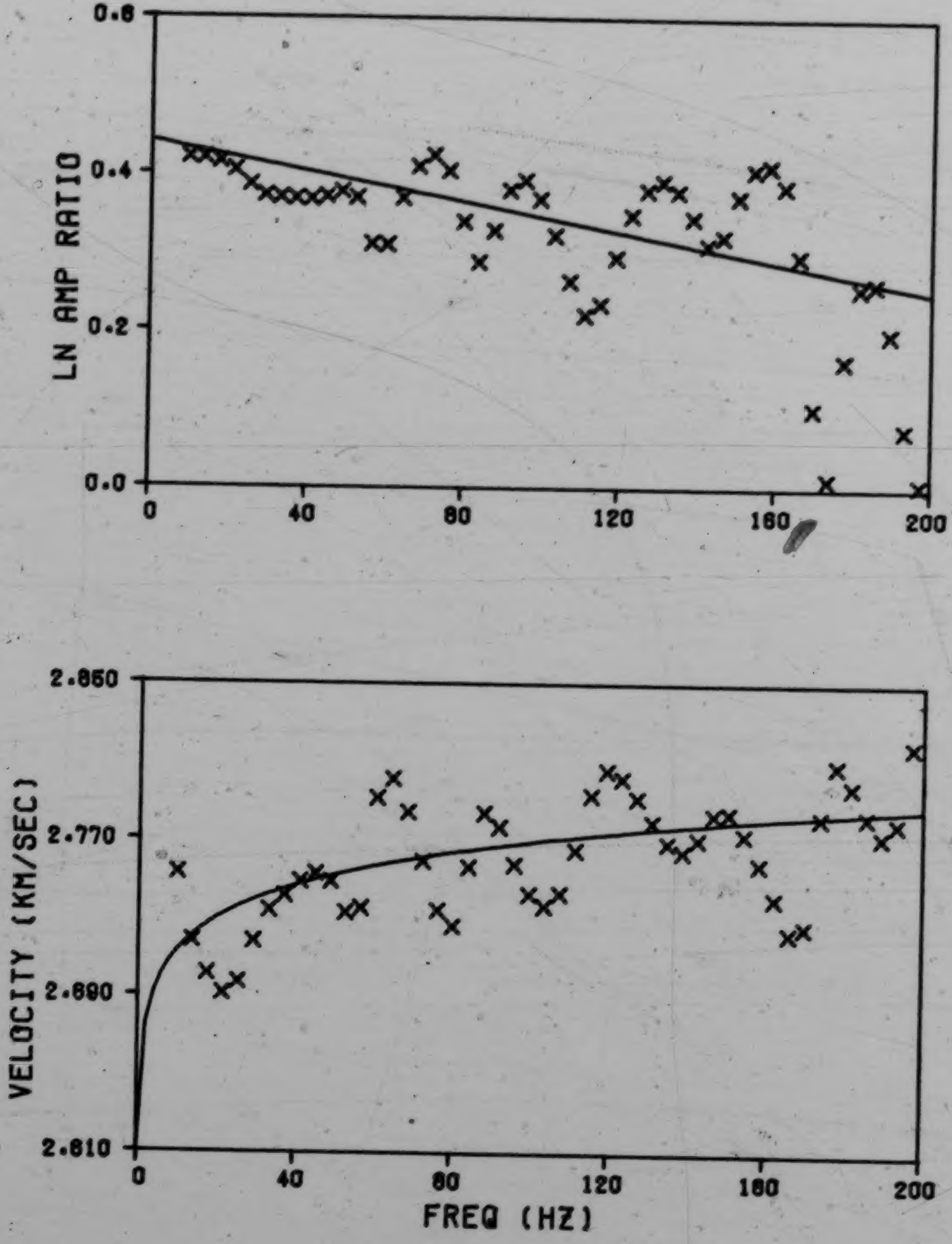

Figure 3.14 Corrected spectral ratio and dispersion curve for the synthetic traces at 585 and 615 meters.

are the same as figures 3.11 and 3.12 respectively except that the pair of traces used was for depths of 585 and 615 meters. In this case the absorption along the reflection paths is not negligible in respect to the absorption between the receivers. As a result the correction is not as effective as in the previous figure; however, it does improve the data. The large error in velocity determination at low frequency in figure 3.13 is a result of the fact that a small error in phase at low frequencies leads to a large error in the calculated velocity, particularly when the calculation is over a short distance. The spectral ratio curve and dispersion curve of the uncorrected data are unacceptable in this case. The correction has made an improvement but the corrected results are still not good. This is because the receivers are too close in relation to the analysis window lengths. This length is determined by the band width of the pulse.

In conclusion it can be said that it should be possible to measure the absorption and dispersion with the spectral ratio method. Fourier methods should be used for the spectral estimate. Corrections must be made for the effects of other reflections; however, the correction procedure leads to a limit on the depth resolution that can be obtained. Corrections must also be made for other variations such as the source. As distances between receivers become smaller errors will increase due to the effects of other reflections. If the data analysis window is made shorter in time it will tend to eliminate the effects of these reflections; however, spectral estimation will become much more uncertain if the window is shortened to the point where the pulse is truncated. The examples considered in this chapter were for transmitted pulses, but the results can also be applied to different time windows on a reflection seismogram. In the reflection case there would likely be a greater limitation on the depth resolution due to the effects of other reflections than in the transmitted pulse case. This is because other interfering reflections are of the same order of magnitude in amplitude as the main reflection, whereas for a transmitted pulse these reflections are an order of magnitude lower in amplitude than the direct pulse.

4. MEASUREMENT OF ABSORPTION AND DISPERSION FROM CHECK-SHOT SURVEYS

4.1 Model Study

In this chapter the problem of measuring absorption and dispersion from a digitally recorded check-shot survey is examined. A check shot survey is an elastic wave experiment in which an impulsive source is set off near the surface and a seismic recording is made by a geophone, or geophones, clamped at different depths in a borehole. The purpose of the survey is to obtain travel times from the surface to various depths. This information is used to correct the integrated times on velocity logs and also to aid in interpretation of seismograms. In this section a model study will be performed to assess the feasibility of using the variation of amplitude with frequency in such a survey to measure Q as a function of depth. This information could possibly be used as an aid in the detection of hydrocarbons.

The model used for this study is based on velocity and density logs obtained for a well in a sedimentary basin in northern Canada. These logs were blocked into a 263 layer model. Figure 4.1 shows the velocity-depth structure for this model and figure 4.2 shows the density model. Figure 4.3 shows the Q versus depth structure which was used for this model. The Q values were synthesized for the purpose of the study. The velocity and Q values apply at 125 Hz.

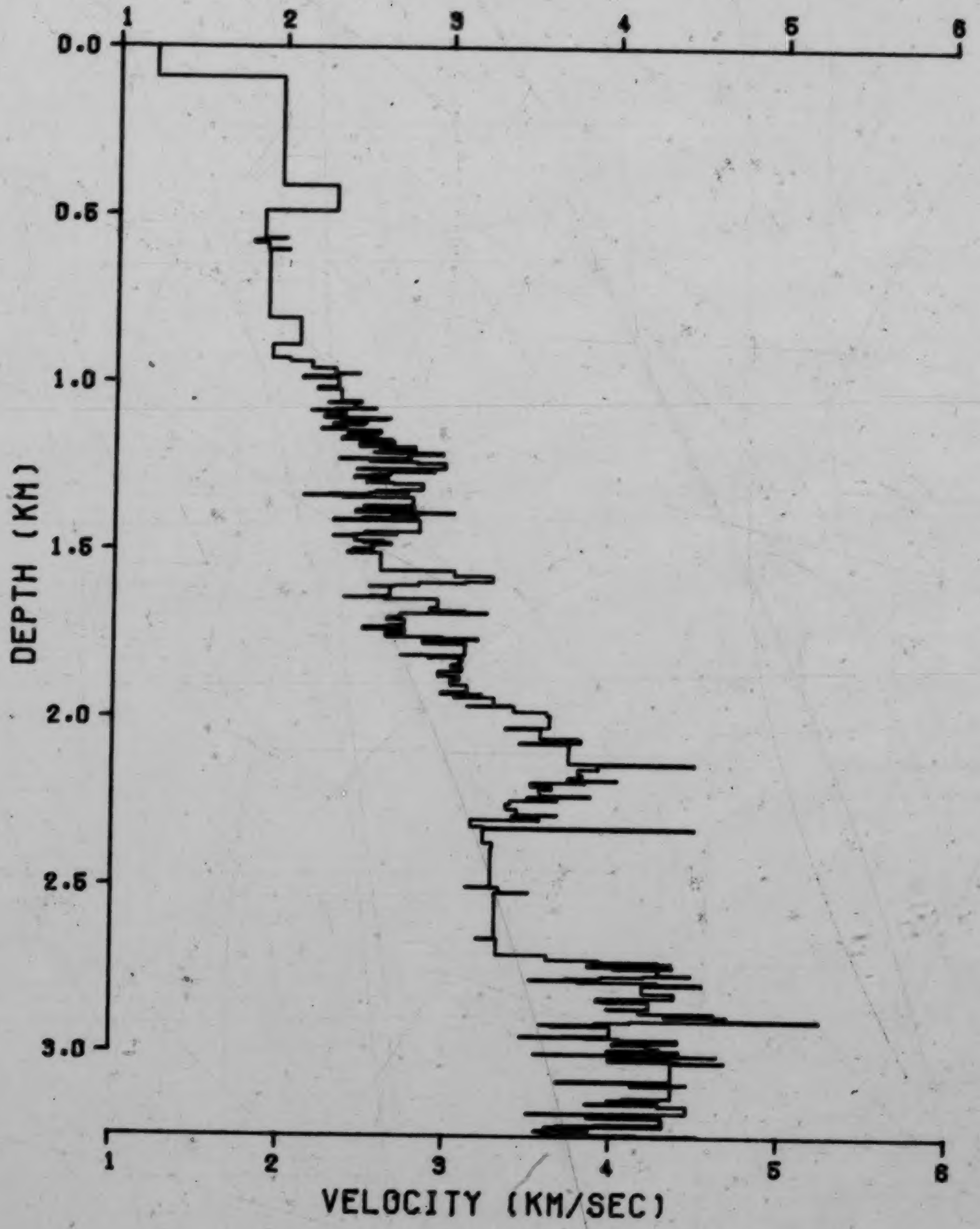

Figure 4.1 263 layer velocity model from a well in northern Canada.

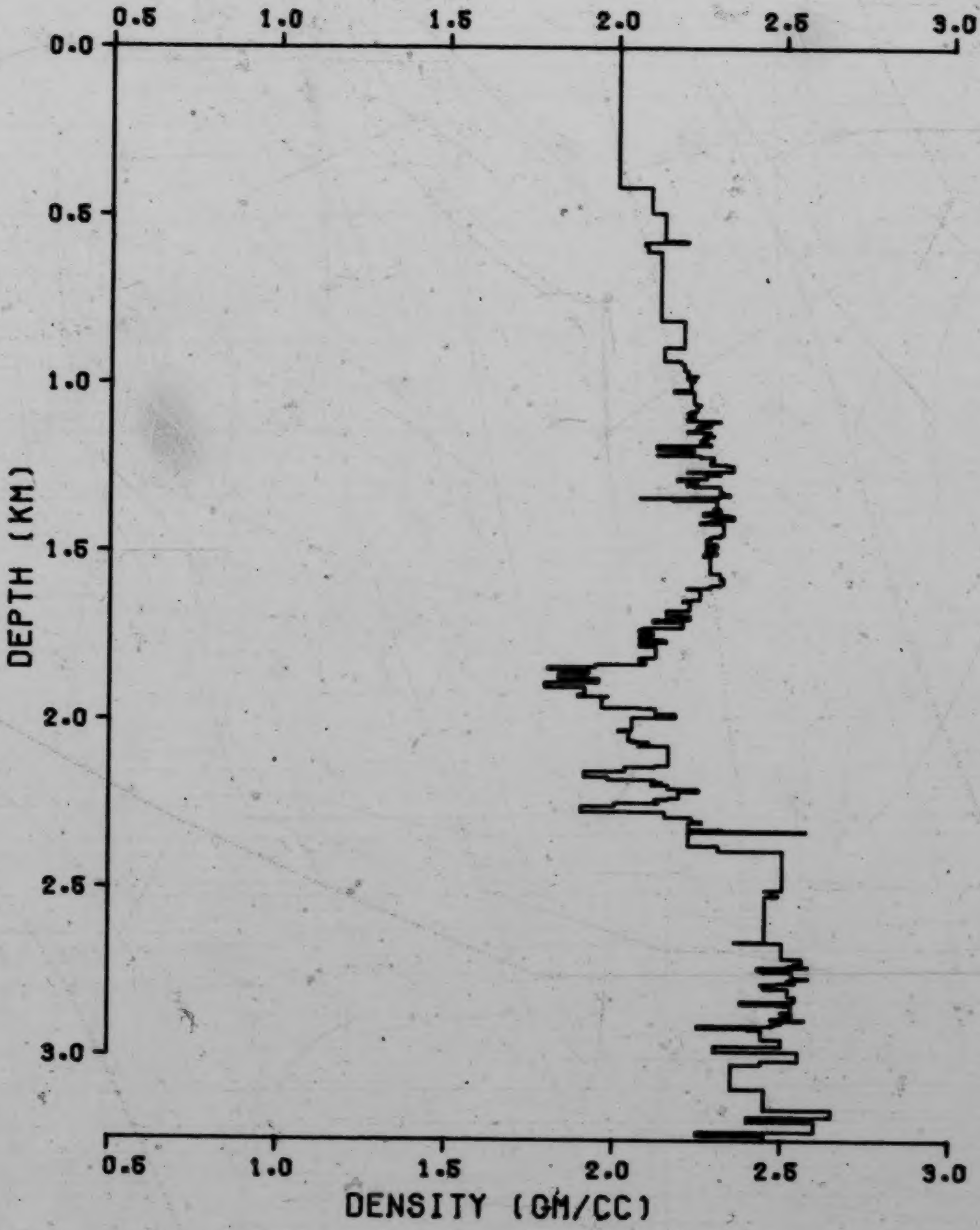

Figure 4.2 263 layer density model from a well in northern Canada.

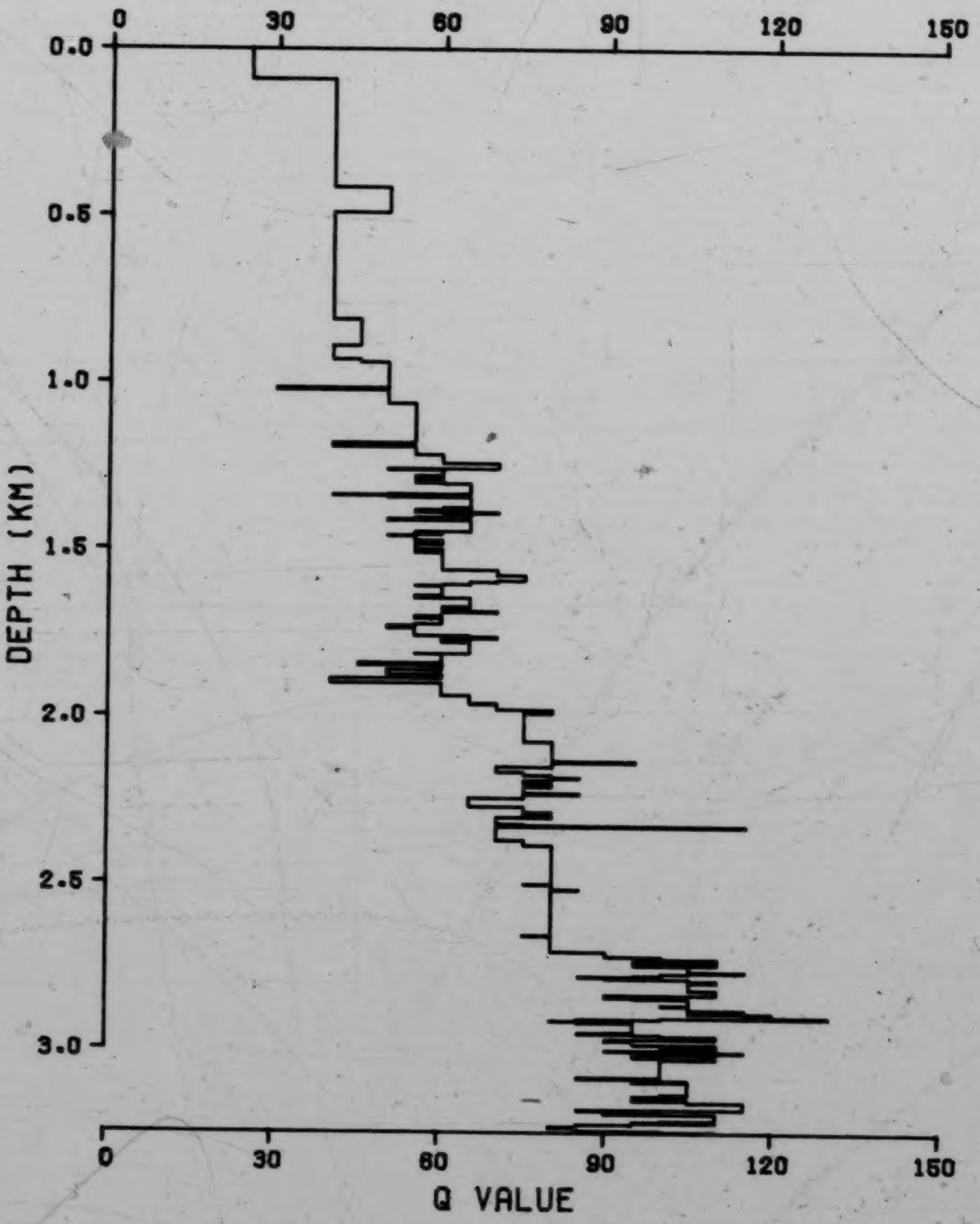

Figure 4.3 263 layer Q model for check shot model study.

In order to simulate the check shot survey synthetic traces were calculated at several depths. The source for all traces was a spike at a depth of 12 meters. The synthetic traces are 4096 points long with a 2 msec sample interval. All data was passed through a 125 Hz Butterworth low pass filter (non-zero phase) which simulated an anti-alias filter. These synthetic traces were calculated using the plane wave, vertical incidence program described in chapter 2. Figure 4.4 shows the synthetic traces calculated at the indicated depths for the model in figures 4.1 to 4.3. Figure 4.5 shows the synthetic traces calculated with no absorption and dispersion for the same model. All parameters were exactly the same as for the data in figure 4.4 except that the traces were 8192 points long. The data in figure 4.5 will be used to calculate the correction for the effects of other reflections and multiples. Figure 4.6 is the same data as in figure 4.4 except that 10% random noise has been added to the data. This data will be used to study the effects of noise on the solution.

With all of the data that is available from figure 4.4 there is more than one method that can be used to estimate the Q versus depth structure from the check shots. The simplest approach is to pick a depth interval and use the traces at the top and bottom of this interval in the calculation. This uses only two traces for each depth interval. A more sophisticated approach is to do the

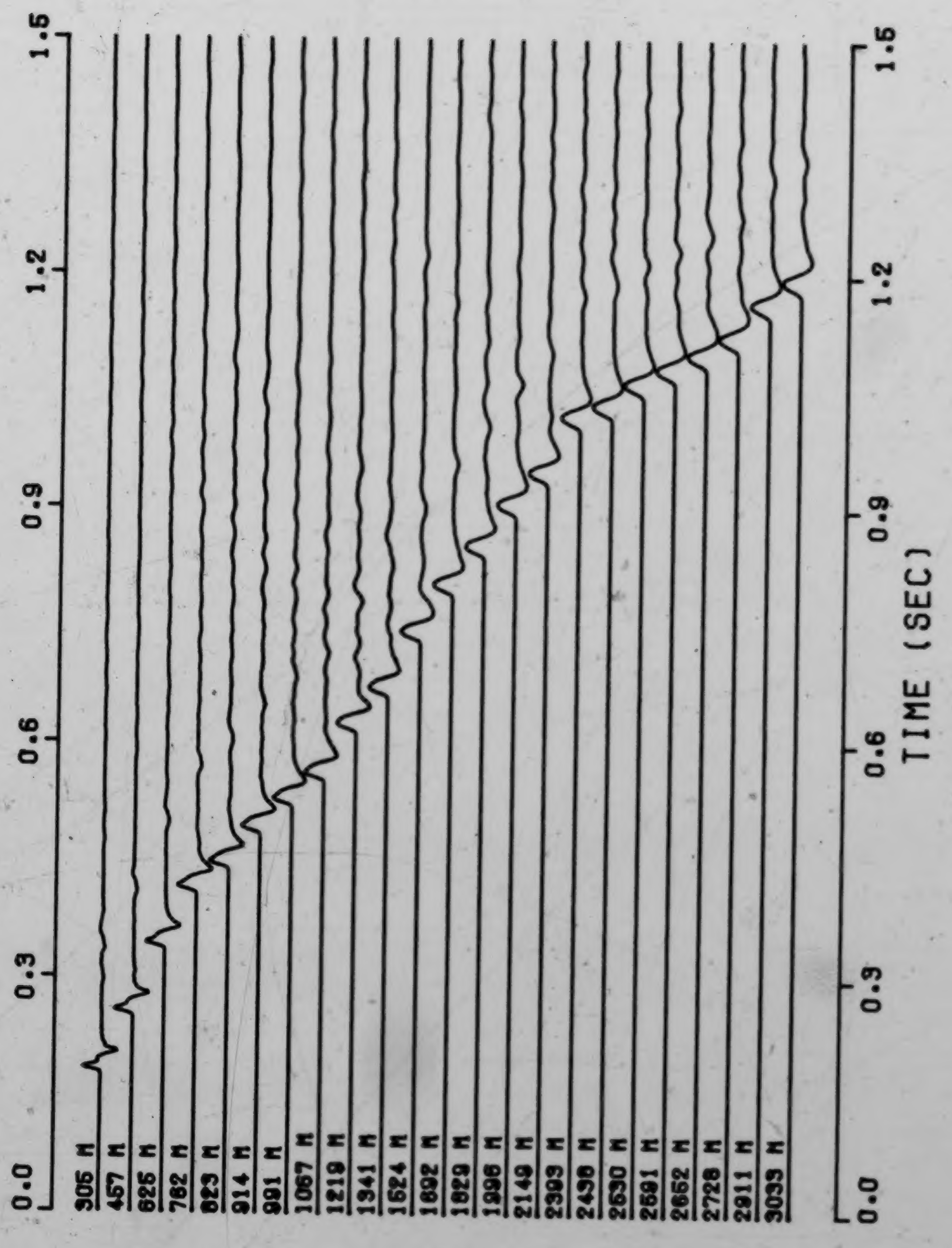

Figure 4.4 Synthetic check shot survey for model in figures 4.1 to 4.3.

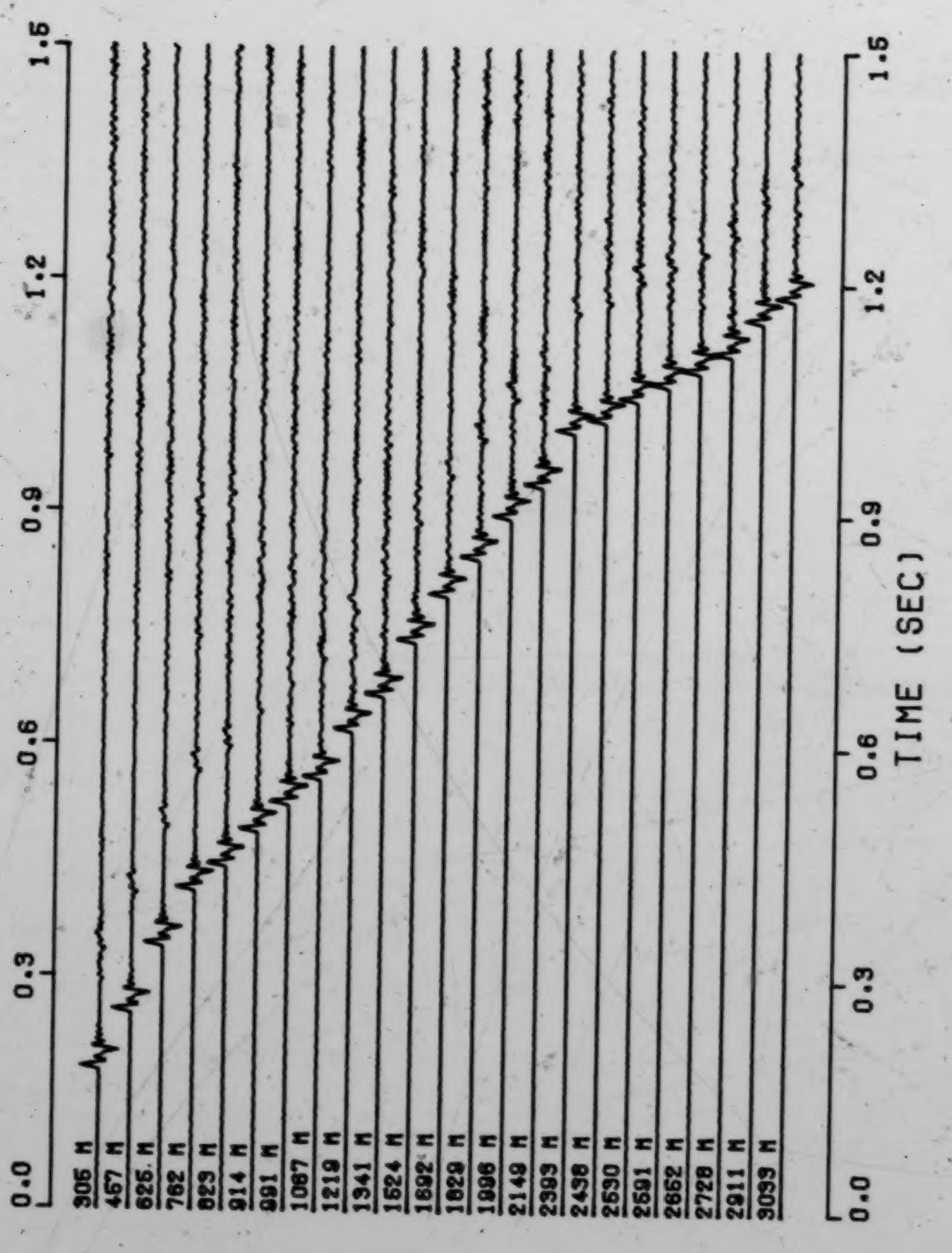

Figure 4.5 Synthetic check shot survey without including the effects of absorption and dispersion.

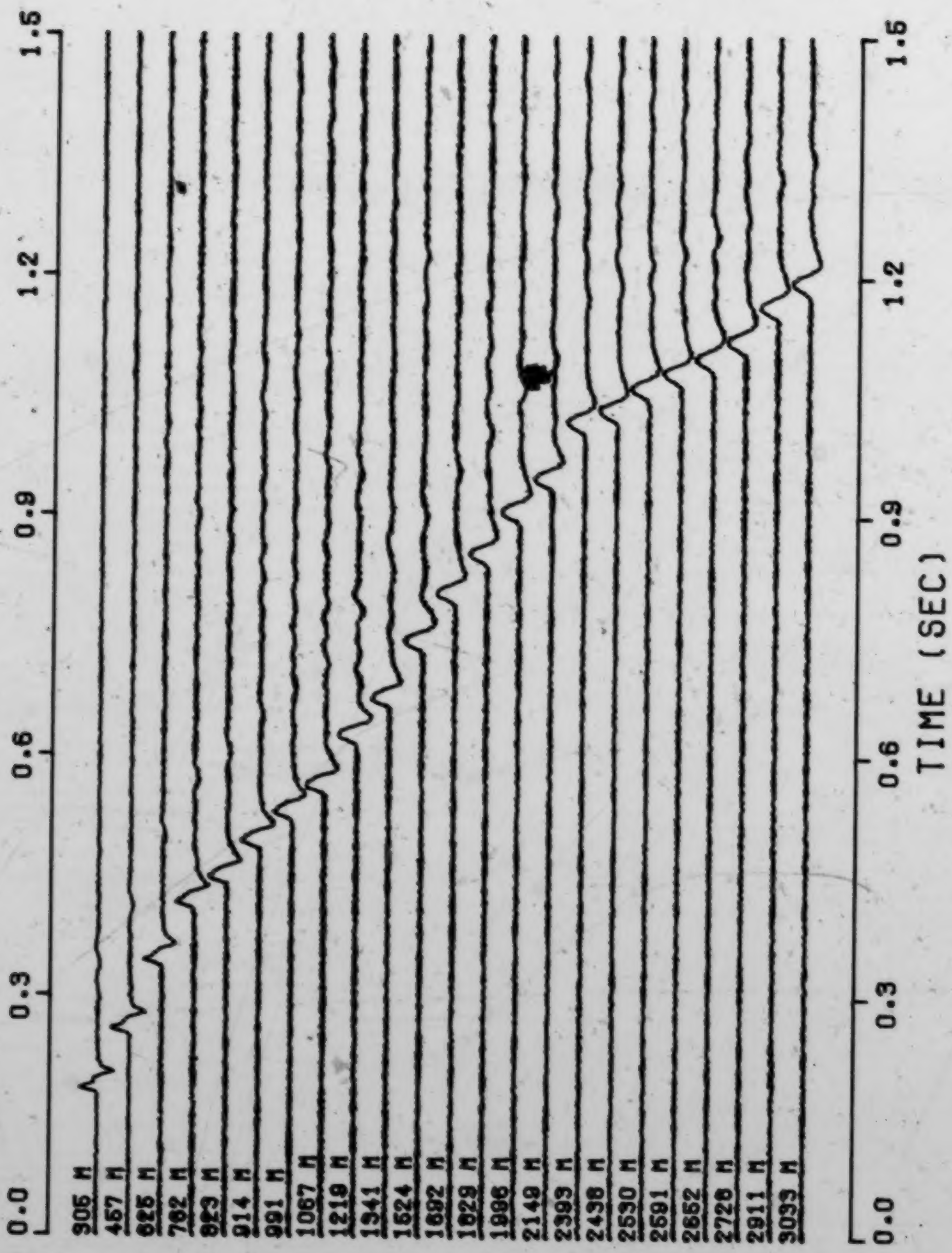

Figure 4.6 Synthetic check shot data from figure 4.4 with 10% random noise added.

spectral ratio calculation over as many pairs of traces as possible and then to analyze these results in order to obtain a least-squares solution.

The theory for the least-squares approach will now be examined briefly. Consider N+1 seismograms recorded at N+1 different depths as part of a check-shot survey. There are then N depth intervals between the N+1 traces. The quantity which is to be calculated in a least-squares sense is the true slope of the spectral ratio plot, x(i), over the i'th depth interval, where i ranges from 1 to N. From the N+1 seismograms there are a maximum of N(N+1)/2 pairs of seismograms which can be used in the spectral ratio calculation. M is the number of these possible pairs of seismograms for which the calculation has been done, and b(j) is the measured slope over the j'th interval where j ranges from 1 to M and M is larger than N. From equation 3.4 it is apparent that b(j) is just a sum of one or more of the x(i). Thus

$$CX = B \tag{4.1}$$

where X is a column vector of length N containing the unknown slopes, x(i), and B is a column vector of length M containing the measured slopes b(j). C is an MxN coefficient matrix relating the unknowns to the observations. The elements of C are all ones and zeroes and are determined from the relationships between the i'th depth intervals and the j'th interval for each observation. The least-squares solution to equation 4.1 is found by solving

$$C''CX = C''B \tag{4.2}$$

where the double prime denotes the transpose of the indicated matrix (Noble and Daniell, 1977). If a weighted least-squares solution to equation 4.1 is desired, it is obtained by solving

$$C''WCX = C''WB \tag{4.3}$$

where W is an MxM diagonal matrix whose diagonal element on row j is the weight for observation j.

The solution to equation 4.1 can be found by using the singular value decomposition of the matrix C (Noble and Daniel, 1977). The singular value decomposition of C is given by

$$C = ULV'' \tag{4.4}$$

where U is an MxN matrix whose columns are the eigenvectors associated with CC", V is an NxN matrix whose columns are the eigenvectors associated with C"C, and L is an NxN diagonal matrix whose elements are the positive square roots of the eigenvalues of C"C. By convention the elements of L are ordered from largest to smallest along the diagonal. The solution of equation 4.1 is given by

$$X = VL^{-1}U''B \tag{4.5}$$

where L^{-1} is the inverse of the matrix L. One advantage of the formulation of the problem given by equation 4.5 is that the variances of the least-squares solutions can be estimated by

$$s^2(i) = S^2 v^2(i,j)/l^2(j,j) \tag{4.6}$$

where there is an implied summation over j on the right hand side of the equation (Wiggins, 1972). S^2 is the problem variance which is estimated by

$$S^2 = |E|^2/(N-M) \tag{4.7}$$

and

$$E = CX-B. \tag{4.8}$$

The procedure used in this thesis for calculating the least-squares solution is as follows. First, several sets of spectral ratios are calculated from the available traces. Each spectral ratio plot is then examined in order to determine the frequency range over which a straight line can be fit reliably to the data. In general this frequency range becomes smaller as the depth of the traces increases because the cumulative effect of the absorption lowers the frequency above which amplitudes are large enough to give a meaningful ratio. The range also becomes smaller in the presence of several reflectors for reasons pointed out in the previous chapter. The next step is to calculate the least-squares slopes of the straight lines which were fit to the spectral ratio plots. These regression calculations give estimates of the variances of these slopes. The reciprocals of these estimates of the variances are used as the weights if the weighted solution is calculated. This means that measured slopes with large uncertainties are less heavily weighted in the least-squares calculation than those with small uncertainties. The least-squares solution is then calculated for the slopes between adjacent depths. Equation 3.4, an estimate of the phase velocity at a reference frequency, and the slope are then used to calculate Q at that frequency. The estimation of the phase velocity can be made by dividing the depth interval by the transit time or by a more exact procedure which is described below. Note that the Q value solved for in this way is actually an average value over the given interval and is not Q but Q" of equation 3.5.

Examination of the phase difference curves for each pair of depths gives the frequency at which the phase difference is zero. This examination is made after a linear trend equal to a static time difference has been removed from the phase difference curve. The velocity at this frequency (where the phase difference is zero) is then equal to the difference in depths divided by the static time difference which was removed from the phase difference curve. The Q value at this frequency is then calculated from this velocity and the slope of the spectral ratio plot for these depths using equation 3.4. Equation 1.14 is then used to correct this Q value to the desired reference frequency and equation 1.12 is used to calculate the phase velocity at this frequency. The velocities calculated at this frequency for all pairs of depths are then converted to transit times. These times are used to obtain a least squares solution for the transit times between adjacent depths in exactly the same way as a least-squares solution was obtained for the slopes. Finally, these least-squares transit times are converted to average velocities over the respective depth intervals.

Now that the procedure for calculating the Q values and phase velocities from the spectral ratio data has been described, the results of the model study will be examined. The input for this study was the set of synthetic traces of figure 4.4 and the correction traces were those of figure 4.5. For all calculations the analysis window length was 100 msec (50 samples) and 3 points at each end of the window were weighted with the cosine bell taper. Zeroes were added to bring the window length to 512 points for the FFT and the Fourier coefficients were smoothed over a window which was 10 Hz wide.

Table 4.1 lists the calculated Q values and phase velocities over the indicated depth intervals. Values in the first column were obtained by direct measurement over the indicated interval. Values in the second column are an unweighted least-squares solution while those in the third column are the weighted least-squares solution. For the

Depth Interval (meters)	Direct Measurement	Unweighted Least squares	Weighted Least squares	Actual Values
		Q Values		
305-823	41	42	41	41.3
823-1524	53	53	53	52.9
1524-2393	66	67	67	66.3
2393-3033	100	110	110	89.4
		Phase Velocities (m/sec)		
305-823	1972	1972	1972	1971
823-1524	2417	2416	2416	2416
1524-2393	3182	3182	3182	3183
2393-3033	3667	3673	3667	3674

Table 4.1 Q values and phase velocities for noise-free model measured over large interval spacing.

least-squares solutions 9 measurements were input. The fourth column in the table gives the theoretically correct values as calculated directly from the input model. All values given in the table apply at 125 Hz. The depth intervals in table 4.1 are sufficiently large that the results are quite accurate. Note that the least-squares results show no improvement over the direct measurements. The loss of accuracy over the deepest interval can be attributed partly to the decrease of frequency band width of the signal with increasing depth. Table 4.2 is the same as table 4.1 except that the depth intervals have been made smaller in an attempt to obtain better resolution. The depth intervals in this table are at about the limit of resolution that should be expected. The number of measurements used for the least-squares calculation in this table was 35. In all cases the accuracy is quite good and the least-squares results show no improvement over the direct measurements.

Table 4.3 is the same as table 4.2 except that no correction was made to the data for the effect of interfering reflections. Comparison of these tables indicates that the correction has certainly improved the results. This is particularly evident below a depth of 900 meters where there are many more reflectors.

It may appear that the least squares procedure offers a way to get increased resolution by using widely separated

Depth Interval (meters)	Direct Measurement	Unweighted Least squares	Weighted Least squares	Actual Values
		Q Values		
305-457	41	41	41	42.4
457-625	43	43	43	41.7
625-823	41	41	40	40.3
823-991	46	48	48	45.0
991-1219	50	50	50	51.4
1219-1524	61	61	61	59.9
1524-1829	64	64	65	61.5
1829-2393	68	70	68	69.2
2393-3033	100	76	76	89.4
		Phase Velocities (m/sec)		
305-457	2065	2065	2065	2063
457-625	1956	1956	1956	1956
625-823	1921	1920	1920	1917
823-991	2085	2088	2088	2091
991-1219	2422	2422	2422	2420
1219-1524	2639	2641	2641	2637
1524-1829	2812	2827	2827	2824
1829-2393	3420	3420	3417	3417
2392-3033	3667	3667	3676	3674

Table 4.2 Q values and phase velocities for noise-free model measured over small interval spacing.

Depth Interval (meters)	Direct Measurement	Unweighted Least squares	Weighted Least squares	Actual Values
		Q Values		
305-457	45	46	46	42.4
457-625	43	41	42	41.7
625-823	40	39	39	40.3
823-991	47	45	46	45.0
991-1219	36	36	36	51.4
1219-1524	71	68	70	59.9
1524-1829	45	44	44	61.5
1829-2393	86	80	81	69.2
2393-3033	75	110	110	89.4
		Phase Velocities (m/sec)		
305-457	2065	2065	2065	2063
457-625	1958	1958	1956	1956
625-823	1921	1918	1920	1917
823-991	2085	2096	2090	2091
991-1219	2416	2411	2414	2420
1219-1524	2644	2639	2641	2637
1524-1829	2830	2820	2817	2824
1829-2393	3417	3423	3420	3417
2392-3033	3667	3667	3676	3674

Table 4.3 Q values and phase velocities for noise-free model calculated without the correction for the effect of other reflections.

pairs of seismograms in calculating spectral ratios and then using the least-squares procedure to extract values over small depth intervals. Table 4.4 shows the results if this procedure is attempted. 214 measurements were used as input to the least-squares calculation and none of the measurements was made over a depth interval of thickness less than 100 msec in terms of transit time. Depth intervals with no measured Q values are those which had a positive value for the determined slope. Note that in the zones where an attempt was made to get high resolution, namely 762 to 1067 meters and 2392 to 2712 meters, the results are quite poor. This indicates that the least-squares technique cannot be used to extend the resolution beyond reasonable limits.

As a final example the data in figure 4.6 which had the added random noise was used as the synthetic check shot data and the analysis which had been done to produce tables 4.1 and 4.2 was repeated on the noisy data to produce tables 4.5 and 4.6. Comparison of the data in these tables indicates that the noise has caused larger errors in the measured Q values, as would be expected. However, the phase velocities are not affected very much by the noise. The depth intervals of table 4.6 are likely too small, as indicated by the large errors. Once again, the least-squares approach has not improved the accuracy over the direct measurements.

In conclusion, the model study has indicated that the

Depth Interval	Weighted Least-squares	Actual Values
305-457	42	42.4
457-625	43	41.7
625-762	43	40.0
762-823	38	40.8
823-914	37	43.6
914-991	70	46.9
991-1067	51	47.7
1067-1219	50	53.5
1219-1341	58	60.3
1341-1524	66	59.7
1524-1692	67	63.2
1692-1829	63	59.5
1829-1996	76	58.6
1996-2149	49	77.7
2149-2393	91	73.3
2393-2438	--	80.0
2438-2530	42	80.0
2530-2591	--	80.0
2591-2652	70	80.0
2652-2728	60	83.5
2728-2911	140	103.6
2911-3033	300	98.0

Table 4.4 Q values for noise-free model obtained by attempting to use least-squares procedure to inrease resolution.

Depth Interval (meters)	Direct Measurement	Unweighted Least squares	Weighted Least squares	Actual Values
Q Values				
305-823	40	39	39	41.3
823-1524	56	54	54	52.9
1524-2393	70	79	72	66.3
2393-3033	110	110	140	89.4
Phase Velocities (m/sec)				
305-823	1975	1984	1978	1971
823-1524	2411	2408	2408	2416
1524-2393	3155	3158	3158	3183
2393-3033	3673	3658	3636	3674

Table 4.5 Q values and phase velocities for noise-added model measured over large interval spacing.

Depth Interval (meters)	Direct Measurement	Unweighted Least squares	Weighted Least squares	Actual Values
Q Values				
305-457	44	41	40	42.4
457-625	46	46	45	41.7
625-823	31	33	32	40.3
823-991	47	69	85	45.0
991-1219	40	41	40	51.4
1219-1524	80	71	74	59.9
1524-1829	100	130	120	61.5
1829-2393	57	56	56	69.2
2393-3033	110	100	110	89.4
Phase Velocities (m/sec)				
305-457	2050	2060	2070	2063
457-625	1960	1960	1960	1956
625-823	1930	1940	1930	1917
823-991	2090	2060	2050	2091
991-1219	2440	2440	2440	2420
1219-1524	2640	2640	2630	2637
1524-1829	2820	2810	2810	2824
1829-2393	3430	3420	3410	3417
2392-3033	3670	3640	3660	3674

Table 4.6 Q values and phase velocities for noise-added model measured over small interval spacing.

spectral ratio method, with the correction for the effects of other reflections, can be used to measure the absorption and dispersion from check shot surveys. Depth resolution should be limited to intervals of the order of 300 meters in thickness and a least-squares solution does not seem to improve the resolution or the accuracy of the method.

4.2 Application to real data

In this section the measurement of absorption and dispersion from a real check shot survey will be presented. The data was recorded in a well in a sedimentary basin in northern Canada. The well is the one which was used to make the model shown in figures 4.1 to 4.3. Since the data was not digitally recorded, it was necessary to digitize it by hand from the paper recordings of the analog signal. The source was an airgun and the pressure of the gun was varied from shot to shot. Since there was no reference phone near the source, the analysis was only performed on pairs of traces for which the airgun pressure and depth were the same. It was assumed that the source was essentially identical for records which met these conditions. This greatly reduced the available data. The traces used in correcting the data were calculated using the plane wave program and the model of figures 4.1 and 4.2. The source was very close to the borehole so that the data was essentially at vertical incidence. The plane wave correction leads to small errors because geometric spreading is neglected. The geometric spreading does not change much over the length of the analysis window at the depths involved and thus these errors are insignificant.

Figure 4.7 shows 4 traces selected for the analysis. The airgun pressure and depth were the same for the traces at depths of 549 and 1193 meters and for those at 945 and 1311 meters, although the pressure and depth were not the same for all four depths. Note that the records are quite "ringy" due to the fact that the source was a single airgun. The data is also quite noisy, particularly the record at 549 meters.

Figure 4.8 shows the spectral ratio plot for the pair of records at depths of 945 and 1311 meters. The x's are the measured values and the solid line is the least-squares straight line which was fit to the data. The window length was 200 msec (100 samples) and the cosine taper was applied to 9 points at each end of the analysis window. 512 points were used for the FFT and the complex Fourier coefficients were smoothed over a window which was 10 Hz wide. The calculated Q for this plot is 67 and applies at a frequency of 125 Hz. Using the standard deviation of the slope of the regression line as an uncertainty leads to a range of 62-73 for the measured Q value. Figure 4.9 shows the dispersion curve for the depth interval of 945 to 1311 meters. The x's are the measured values and the solid line is the

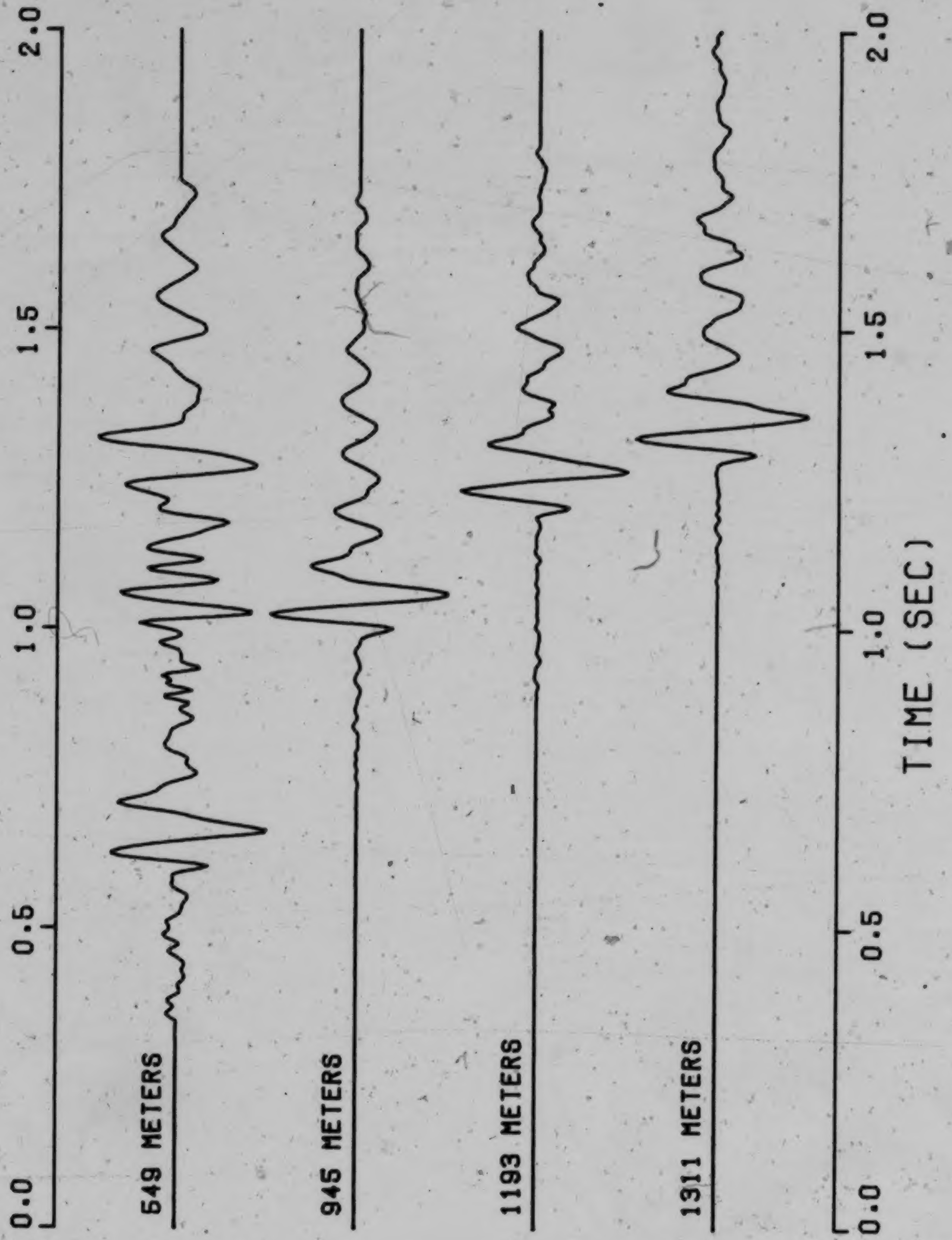

Figure 4.7 Actual check shot data from a well in a sedimentary basin in northern Canada.

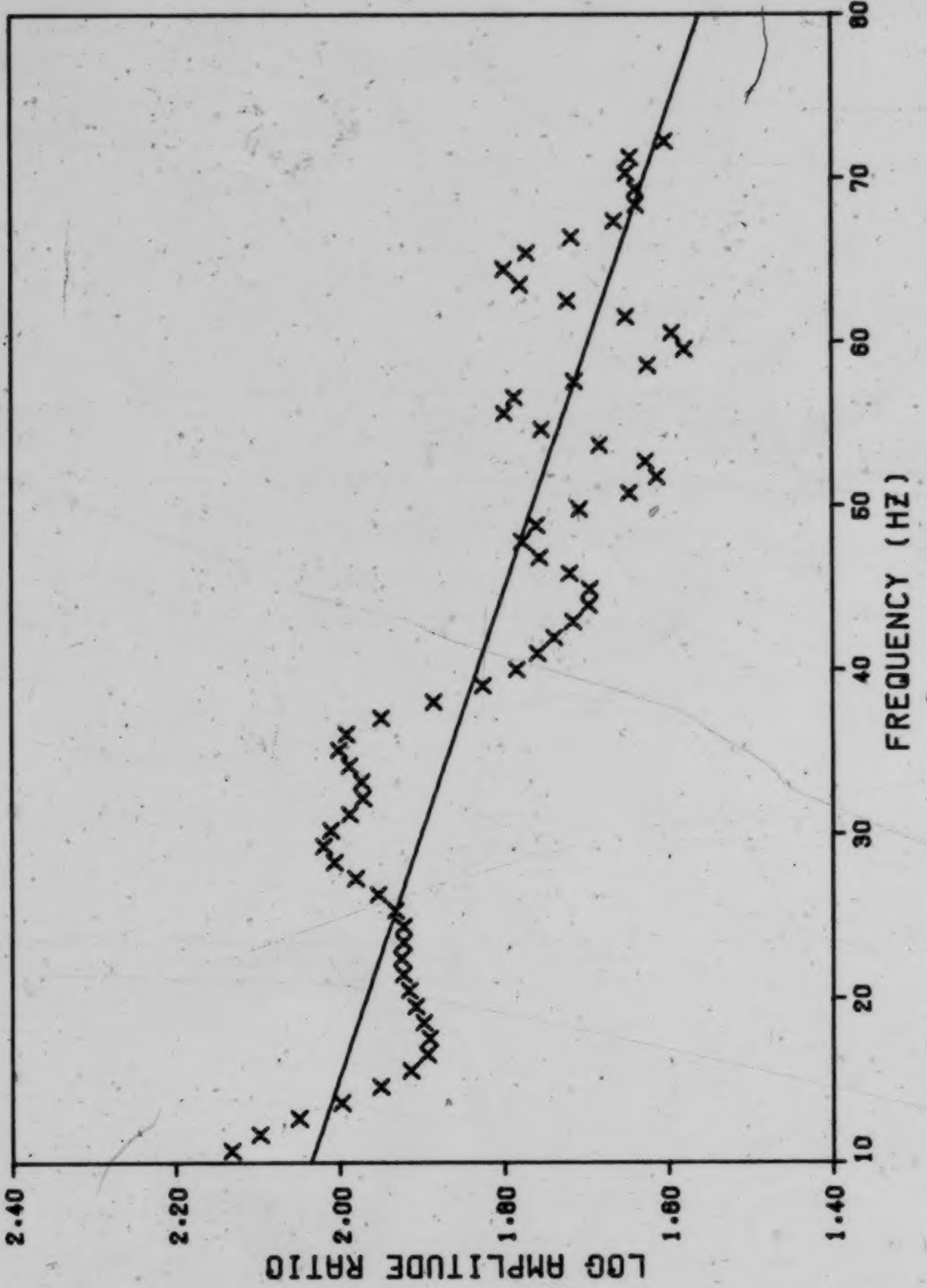

Figure 4.8 Lcg spectral ratio plot for the depth interval 945 to 1311 meters.

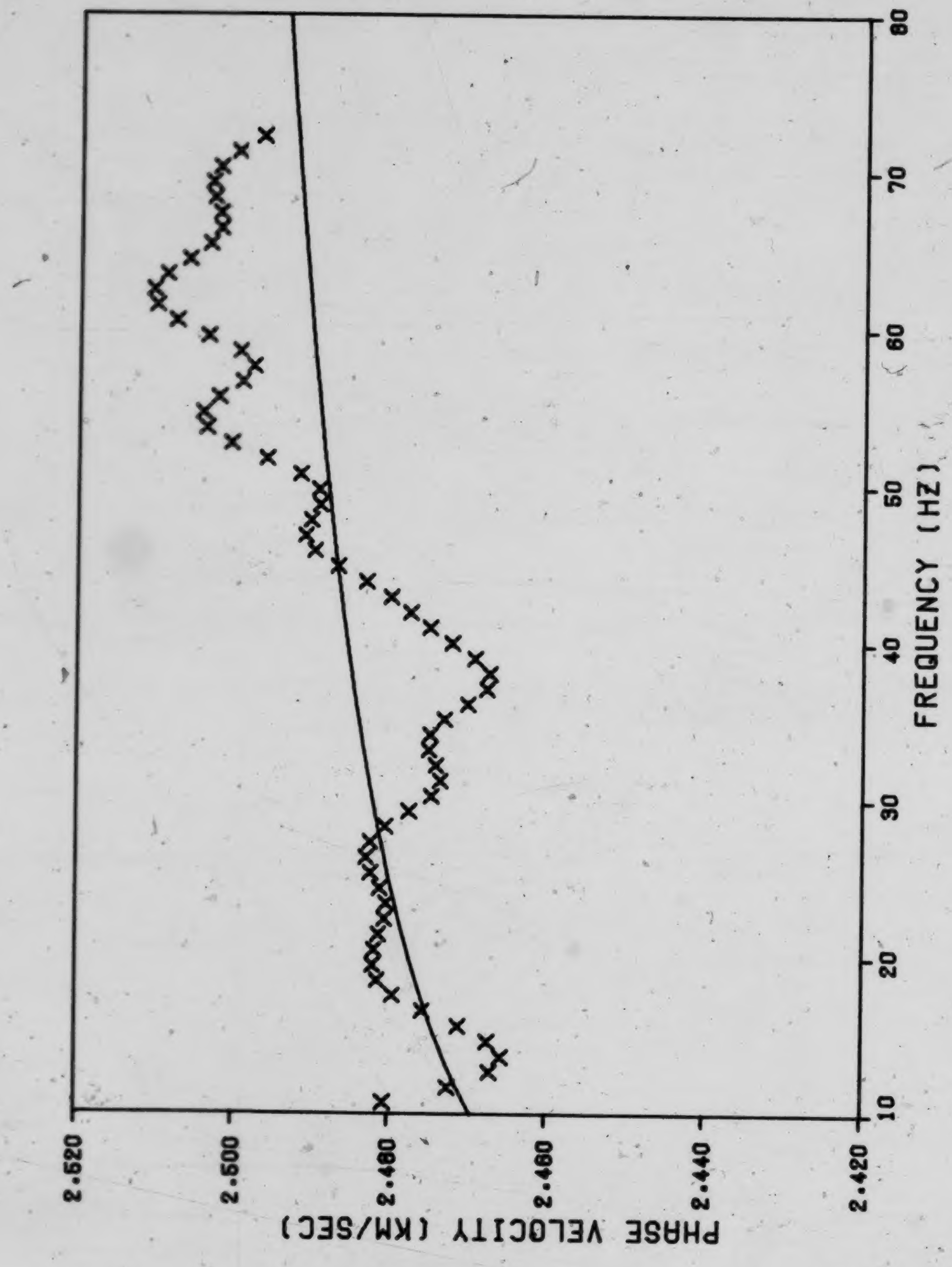

Figure 4.9 Measured dispersion curve for the depth interval 945 to 1311 meters.

theoretical curve predicted by Futterman's model for a Q value of 67 at 125 Hz. Figures 4.10 and 4.11 show the spectral ratio plot and dispersion curve respectively for the pair of traces at 549 and 1193 meters. The calculated range for the Q value is 42 to 45 and the Q value used in calculating the theoretical dispersion curve was 43. These values also apply at 125 Hz.

From figures 4.8 to 4.11 it can be concluded that the spectral ratio method has given reasonable results when applied to real data. The absorption coefficient appears to be a linear function of frequency and the data shows dispersion which is consistent with Futterman's model.

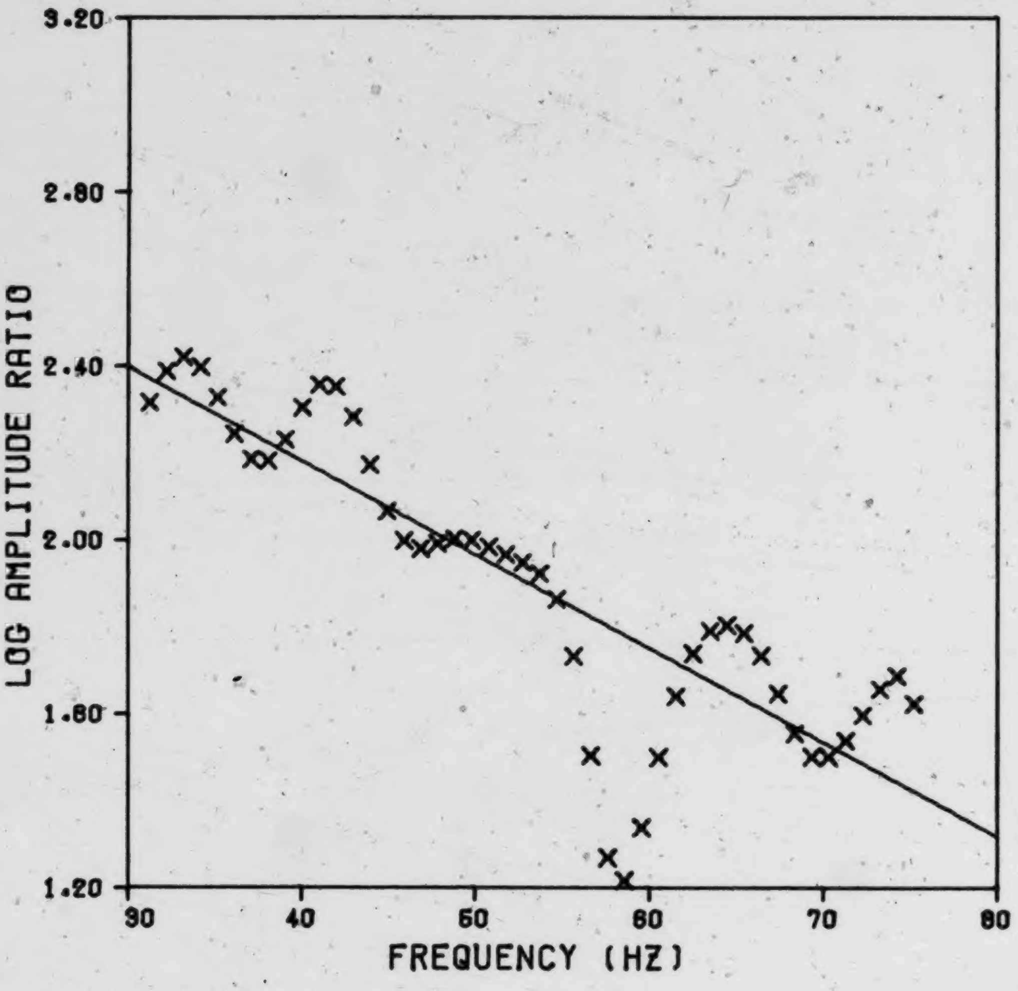

Figure 4.10 Log spectral ratio plot for the depth interval 549 to 1193 meters.

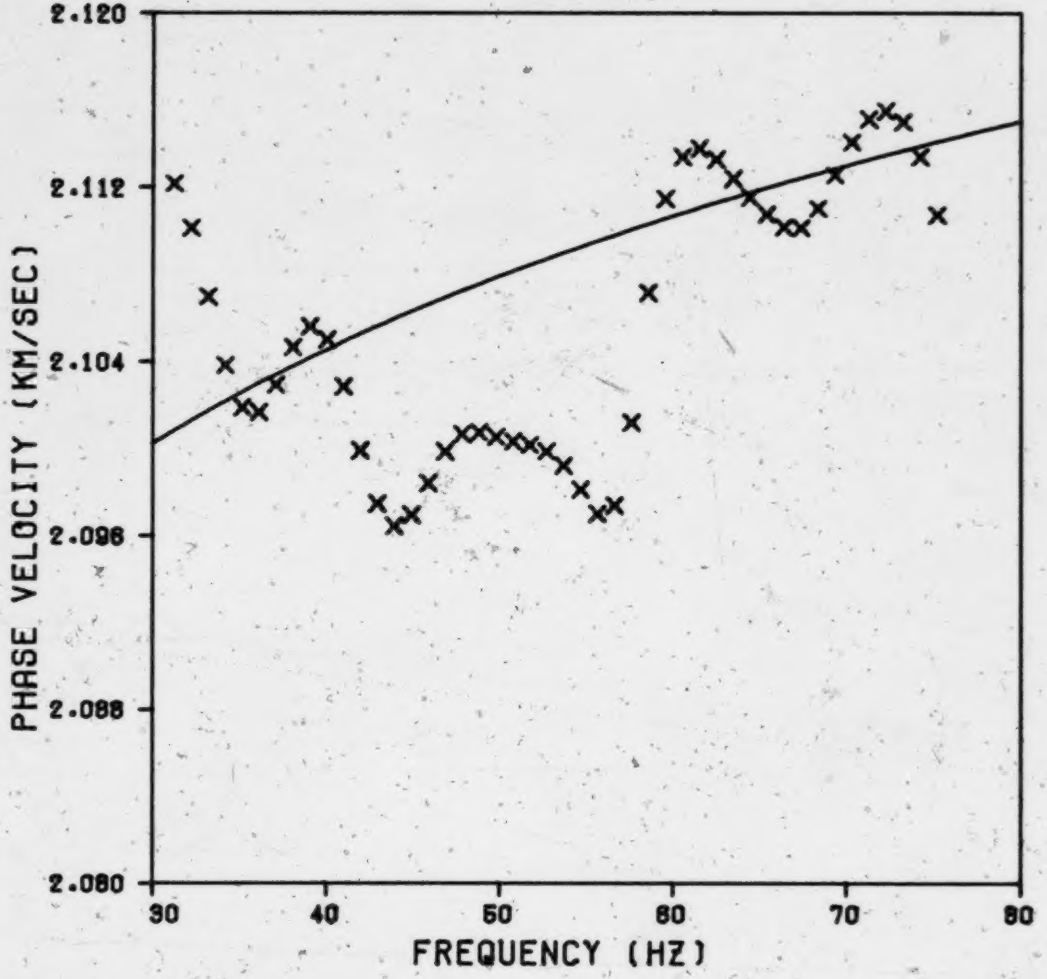

Figure 4.11 Measured dispersion curve for the depth interval 549 to 1193 meters.

5. CONCLUSIONS AND DISCUSSION

In this thesis the absorption and dispersion of seismic waves has been examined, both from a theoretical viewpoint and from actual measurements on real data. The problem of computing synthetic seismograms which include the effects of absorption and dispersion has also been examined. Methods for calculating such seismograms have been presented for plane waves at vertical incidence using a matrix method and for curved waves at non-vertical incidence using ray theory. These methods have been shown to be accurate and computationally efficient. The effect of multiples on synthetic seismograms has also been briefly examined.

The spectral ratio method was examined theoretically, as well as with the aid of model studies, and was applied to real data. Fourier spectral estimates were found to be superior to autoregressive estimates. Correction of the data for the effects of interfering reflections was shown to be an important step in the method. Resolution was found to be limited to intervals of the order of 300 meters in thickness when applying the method to check shot data.

Finally, a limited amount of real data from a check shot survey was examined for absorption and dispersion using the spectral ratio method. The spectral ratio plots supported the conclusion that the absorption coefficient is essentially a linear function of frequency. Dispersion was present in the data and was consistent with a theory proposed by Futterman (1962). Measured Q values on this data were 42±2 for the depth interval 549 to 1193 meters and 67±6 for the interval 945 to 1311 meters. This would suggest an increase of Q with depth.

The limits on resolution imposed by the spectral ratio method are a result of the frequency range of the seismic data. If measurements of absorption are to be useful in petroleum exploration where detailed resolution is often required, then it would appear that a borehole logging tool should be designed. Such a tool could operate at frequencies in the kHz range and the resolution would be over interval thicknesses of the order of one meter or less. This would then possibly make measurements of absorption a viable technique for stratigraphic interpretation or hydrocarbon detection. This is a problem which requires much more research, and it appears to be an important area to investigate.

Recently there has been a good deal of emphasis in the seismic data processing field on the correction of seismograms for any phase distortions (see for instance Lindseth, 1978 and Robinson, 1978). Since dispersion causes phase distortion, corrections should be made for this distortion. These corrections can be made if estimates of the absorption are available. Detailed resolution would not be required to make a reasonable correction for this effect.

This correction would have to be a dynamic correction, in the sense that it would change with time, since the absorption and dispersion change with time on a seismic record.

BIBLIOGRAPHY

Ables, J. G., 1974, Maximum entropy spectral analysis, Astronomy and Astrophysics Supplement, vol. 15, pp 383-393.

Akaike, H., 1969a, Fitting autoregressive models for prediction, Ann. Inst. Statist. Math., vol. 21, pp 243-247.

Akaike, H., 1969b, Power spectrum estimation through autoregressive model fitting, Ann. Inst. Statist. Math., vol. 21, pp 407-419.

Akaike, H., 1970, Statistical predictor identification, Ann. Inst. Statist. Math., vol. 22, pp 203-217.

Akaike, H., 1976, Time series analysis and control through parametric models, paper presented at Applied Time Series Analysis, a symposium sponsored by University of Tulsa, May 14-15, 1976, Tulsa, Oklahoma.

Andersen, N., 1974, On the calculation of filter coefficients for maximum entropy spectral analysis, Geophysics, vol. 39, pp 69-72.

Attewell, P. B. and Ramana, Y. V., 1966, Wave attenuation and internal friction as functions of frequency in rocks, Geophysics vol. 31, pp 1049-1056.

Auberger, Michael and Rhinehart, John S., 1961, Ultrasonic velocity and attenuation of longitudinal waves in rocks, J.G.R., vol. 66, pp. 191-199.

Averbukh, A. G. and Trapeznikova, N. A., 1972, Reflection and refraction of plane waves normally incident on the boundary of absorbing media, Izvestia (Earth Physics), pp. 74-83 (translation pages 616-621).

Azimi, Sh. A., Kalinin, A. V., Kalinin V. V. and Pivovarov, B. L., 1968, Impulse and transient characteristics of media with linear and quadratic absorption laws, Izvestia (Earth Physics), pp. 42-54 (translation pages 88-93).

Baranov, V. and Kunetz, G., 1960, Film synthéthique avec réflexions multiples; théorie et calcul practique, Geophysical Prospecting, vol. 8, pp 315-325.

Berryman, L. H., Goupillaud, P. L. and Waters, K. H., 1958, Reflections from multiple transition layers, Geophysics, vol 23, pp. 223-243.

Bhatia, A. B., 1967, Ultrasonic Absorption, Clarendon press, Oxford.

Biot, M. A., 1956, Theory of propagation of elastic waves in a fluid saturated porous solid (parts 1 and 2), J. Acoust. Soc. Am., vol 28, pp 168-191.

Biot, M. A., 1962a, Mechanics of deformation and acoustic propagation in porous media, J. App. Phys., vol. 33, pp 1482-1498.

Biot, M. A., 1962b, Generalized theory of acoustic propagation in porous dissipative media, J. Acoust. Soc. Am., vol. 34, pp 1254-1264.

Birch, Francis and Bancroft, Dennison, 1938, Elasticity and internal friction in a long column of granite, B.S.S.A., vol. 28, pp 243-254.

Blackman, R. B. and Tukey, J. W., 1959, The Measurement of Power Spectra, Dover Publications, New York.

Boltzman, L., 1876, Zur theorie der elastische nachwirkung, Ann. Phys. Chem (Poggendorff), vol. 7, pp. 624-654.

Borcherdt, Roger D., 1973, Energy and plane waves in linear viscoelastic media, J.G.R., vol. 78, pp 2442-2453.

Borcherdt, Roger D., 1977, Relflection and refraction of type-II S waves in elastic and anelastic media, B.S.S.A., vol. 67, pp. 43-67.

Born, W. T., 1941, The attenuation constant of Earth Materials, Geophysics, vol. 6, pp 132-148.

Box, George E. P. and Jenkins, Gwilym M., 1970, Time Series Analysis, Holden Day, San Francisco.

Bradley, James J. and Fort, A. Newman Jr., 1966, Internal friction in rocks, section 8 in Handbook of Physical Constants edited by Sydney P. Clark Jr., memoir 97 of Geological Society of America.

Brennan, B. J. and Stacey, F. D., 1978, Frequency dependence of elasticity of rock--test of seismic velocity dispersion, Nature, vol. 268, pp. 220-222.

Bruckshaw, J. McG. and Mahanta, P. C., 1954, Petroleum, vol 17, pp 14-18.

Burg, J. P., 1967, Maximum entropy spectral analysis, paper presented at the 37'th annual meeting of the SEG, Oklahoma City.

Burg, J. P., 1972, The relationship between maximum entropy spectra and maximum likelihood spectra, Geophysics, vol. 37, pp. 375-576.

Capon, J., 1969, High resolution frequency-wavenumber spectrum analysis, Proceeding of the IEEE, vol 57, pp 1408-1418.

Chen, W. Y. and Stegen, G. R., Experiments with maximum entropy power spectra of sinusoids, J.G.R., vol. 79, pp. 3019-3022.

Churney, Garth, 1977, Computation of Synthetic Seismograms by Ray Methods, M.Sc. thesis in the Physics Department, University of Alberta, Edmonton, Alberta.

Claerbout, J. F., 1968, Synthesis of a layered medium from its acoustic transmission response, Geophysics, vol. 33, pp. 264-269.

Clowes, R. M. and Kanasewich, E. R., 1970, Seismic attenuation and the nature of reflecting horizons within the crust, J.G.R., vol. 75, pp. 6693-6705.

Cole, B. F., 1965, Marine sediment attenuation and ocean bottom reflected sound, J. Acoust. Soc. Am., vol. 37, pp 291-297.

Collins, Francis and Lee, C. C., 1956, Seismic wave attenuation characteristics from pulse experiments, Geophysics, vol. 21, pp. 16-40.

Cooper, Henry F. Jr., 1967, Reflection and transmission of oblique plane waves at a plane interface between viscoelastic media, J. Acoust. Soc. Am., vol. 42, pp. 1064-1069.

Cooper, Henry F. Jr. and Reiss, Edward L., 1966, Reflection of plane viscoelastic waves from plane boundaries, J. Acoust. Soc. Am., vol. 39, pp 1133-1138.

Crowe, C. and Alhilali, K., 1975, Attenuation of seismic reflections as a key to lithology and pore filler, paper presented at the 60th annual meeting of the American Assocaitation of Petroleum Geologists.

Cerveny, Vlatislov and Ravindra, Ravi, 1971, Theory of Seismic Head Waves, University of Toronto Press, Toronto.

Cerveny, V., Molotkov, I. A. and Psencik, I., 1977, Ray Method in Seismology, Universita Karlova, Praha.

Darby, E. K. and Neidell, N. S., 1966, Applications of dynamic programming to the problems of plane wave propagation in a layered medium, Geophysics, vol. 31, pp. 1037-1048.

Fougere, Paul F., 1977, A solution to the problem of spontaneous line splitting in maximum entropy power spectrum analysis, J.G.R., vol. 82, pp. 1051-1054.

Futterman, Walter I., 1962, Dispersive body waves, J.G.R., vol. 67, pp. 5279-5291.

Gladwin M. T. and Stacey, F. D., 1974, Anelastic degradation of acoustic pulses in rock, Physics of Earth and Planetary Interiors, vol. 8, pp. 332-336.

Gordon, Robert B. and Nelson, Carl W., 1966, Anelastic properties of the earth, Reviews of Geophysics, vol. 4, pp. 457-474.

Goupillaud, Pierre, L., 1961, An approach to inverse filtering of near surface layer effects from seismic records, Geophysics, vol. 26, pp. 754-760.

Hamilton, Edwin L., 1972, Compressional-wave attenuation in marine sediments, Geophysics, vol. 37, pp. 620-646.

Hamilton, Edwin L., 1975, Sound attenuation as a function of depth in the sea floor, J. Acoust. Soc. Am., vol. 59, pp. 528-535.

Hampton, Loyd D., 1967, Acoustic properties of sediments, J. Acoust. Soc. Am., vol. 42, pp. 882-890.

Hart, R. S., Anderson, D. L. and Kanamori, H., 1977, The effect of attenuation on gross earth models, J.G.R., vol. 82, pp. 1647-1654.

Hron, F., 1971, Criteria for selection of phases in synthetic seismograms for layered media, B.S.S.A., vol. 61, pp. 765-780.

Hron, F., 1972, Numerical methods of ray generation in multi-layered media, in Methods in Computational Physics, vol. 12, Academic Press, New York.

Hron, F. and Kanasewich E. R., 1971, Synthetic seismograms for deep seismic sounding studies using asymptotic ray theory, B.S.S.A., vol. 61, pp. 1169-1200.

Jackson, David D. and Anderson, Don. L., 1970, Physical mechanisms of seismic attenuation, Reviews of Geophysics and Space Physics, vol. 8, pp. 1-63.

Johnston, David H., Toksoz, Nafi M. and Timur A., 1979, Attenuation of seismic waves in dry and saturated rocks: II mechanisms, Geophysics, vol. 44, pp. 691-711.

Kaiser, J. F., 1963, Design methods for sampled data filters; proceedings of the First Allerton Conference on Circuit and Systems Theory, Monticello, Illinois, pp. 221-236.

Kalinin, A. V., Azimi, Sh. A. and Kalinin, V. V., 1967, Estimate of the phase velocity dispersion in absorbing media, Izvestia (Earth Physics), pp. 78-83 (translation pages 249-251.

Kanasewich, E. R., 1975, Time Sequence Analysis in Geophysics (2nd edition), University of Alberta press, Edmonton, Alberta.

Karus, E. V., 1958, The absorption of elastic vibrations in rocks during stationary excitation, Izvestia (Geophysics series), pp 438-448 (translation pp 249-254).

Kittell, Charles, 1976, Introduction to Solid State Physics (5th edition), John Wiley and Sons, Toronto.

Klima, K., Pros, Z. and Vanek, J., 1962, Ultrasonic attenuation of longitudinal waves in solids, J.G.R., vol. 67, pp. 2078-2081.

Knopoff, L., 1956, The seismic pulse in materials possessing solid friction, 1: plane waves, B.S.S.A., vol.46, pp. 175-183.

Knopoff, L., 1959, The seismic pulse in materials possessing solid friction, 2: Lamb's problem, B.S.S.A., vol 49, pp 404-413.

Knopoff, L., 1964, Q, Reviews of Geophysics, vol. 2, pp. 625-660.

Knopoff, Leon and MacDonald, Gordon J. F., 1958, Attenuation of small amplitude stress waves in solids, Reviews of Modern Physics, vol. 30, pp 1178-1192.

Knopoff, L. and MacDonald, G. J. F., 1960, Models for acoustic loss in solids, J.G.R., vol 65, pp. 2191-2197.

Knopoff, L. and Porter, L. D., 1963, Attenuation of surface waves in a granular material, J.G.R., vol. 68, pp. 6317-6321.

Kunetz, G., 1964, Généralisation des opérateurs d'antirésonance à nombre quelconque de réflecteurs, Geophysical Prospecting, vol. 12, pp.283-289.

Kunetz, G. and D'Erceville, I., 1962, Sur certaines propriétés d'une onde acoustique plane de compression dans un milieu stratifié, Annales de Geophysique, vol. 18, pp. 351-359.

Lacoss, R. T., 1971, Data adaptive spectral analysis methods, Geophysics, vol. 36, pp. 661-675.

Lehmer, D. H., 1964, The machine tools of combinatorics, in Applied Combanitorial Mathematics, John Wiley and Sons, New York.

Levinson, N., 1947, The Wiener RMS error criterion in filter design and prediction, J. Math. Phys., vol. 25, pp. 261-278.

Lindseth, Roy O., 1978, Synthetic sonic logs: a process for stratigraphic interpretation, Geophysics, vol. 44, pp. 3-26.

Liu, Hsi-Ping, Anderson, Don L. and Kanamori, Hiroo, 1976, Velocity dispersion due to anelasticity; implications for seismology and mantle composition, Geophys. Jour. Royal Ast. Soc., vol. 47, pp. 41-58.

Lockett, F. J., 1962, The reflection and refraction of waves at an interface between viscoelastic materials, J. Mech. Phys. Solids, vol. 10, pp 53-64.

Lomnitz, C., 1957, Linear dissipation in solids, J. App. Phys., vol. 28, pp. 201-205.

McCann, C. and McCann, D. M., 1969, The attenuation of compressional waves in marine sediments, Geophysics, vol. 34, pp. 882-892.

McDonal, J. F., Angona, F. A., Mills, R. L., Sengbush, R. L., Van Nostrand, R. G. and White, J. E., 1958, Attenuation of shear and compressional waves in Pierre shale, Geophysics, vol. 23, pp. 421-439.

McKavanagh, B. and Stacey, F. D., 1974, Mechanical hysterisis in rocks at low strain amplitudes and seismic frequencies, Physics of Earth and Planetary Interiors, vol. 8, pp. 246-250.

McLeroy, E. G. and DeLoach, A., 1968, Sound speed and attenuation from 15 to 1500 kHz measured in natural sea-floor sediments, J. Acoust. Soc. Am., vol. 44, pp. 1148-1150.

Merkulova, V. M., 1966, The frequency dependence of the damping of ultrasound in rock in the megacycle region, Izvestia (Earth Physics), pp. 47-60 (translation pages 507-514).

Merkulova, V. M., 1968, Absorption of ultrasonic waves in rocks in the 10-160 kilohertz range, Izvestia (Earth Physics), pp. 20-25 (translation pages 350-353).

Merkulova, V. M. and Vasil'tsoy E. A., 1967, Measuring absorption in rocks by the bending vibration method, Izvestia (Earth Physics), pp. 75-77 (translation pages 247-248).

Noble, Ben and Daniel, James W., 1977, Applied Linear Algebra, 2nd edition, Prentice-Hall Inc, Toronto.

Nolle, A. W., Hoyer, W. A., Mifsud, J. F., Runyan, W. R. and Ward, M. B., 1963, Acoustical properties of water-filled sands, J. Acoust. Soc. Am., vol. 35, pp. 1394-1408.

Pandit, B. I. and Savage, J. C., 1973, An experimental test of Lomnitz's theory of internal friction in rocks, J.G.R., vol. 78, pp. 6097-6099.

Parzen E., 1976, Isomorphism between time series analysis and non-parametric statistical inference, paper presented at Applied Time Series Analysis, a symposium sponsored by University of Tulsa, May 14-15, 1976, Tulsa, Oklahoma.

Peacock, K. L. and Treitel, Sven, 1969, Predictive deconvolution: theory and practice, Geophysics, vol. 34, pp. 155-169.

Peselnick, Louis and Outerbridge, W. F., 1961, Internal friction in shear and shear modulus of Solenhofen limestone over a frequency range of 10^7 cycles per second, J.G.R., vol. 66, pp. 581-588.

Peselnick, Louis and Zietz, Isidore, 1959, Internal friction of fine-grained limestones at ultrasonic frequencies, Geophysics, vol. 24, pp. 285-296.

Ricker, Norman, 1953, The form and laws of propagation of seismic wavelets, Geophysics, vol. 18, pp 10-40.

Robinson, E. A., 1967, Multichannel Time Series Analysis with Digital Computer Programs, Holden Day Inc., San Francisco.

Robinson, E. A., 1968, Basic equations for synthetic seismograms using the z transform approach, Geophysics, vol. 33, pp. 521-523.

Robinson, E. A. and Treitel, Sven, 1977, The spectral function of a layered system and the determination of the wave forms at depth, Geophysical Prospecting, vol. 25, pp. 434-459.

Robinson, J. C., 1978, A technique for continuous representation of dispersion in seismic data, Geophysics, vol. 44, pp. 1345-1351.

Roderick, R. L. and Truell, Rohn, 1952, The measurement of ultrasonic attenuation by the pulse technique and some results in steel, J. App. Phys., vol. 23, pp. 267-279.

Sato, Ryosuke, 1967, Attenuation of seismic waves, Journal of Physics of the Earth, vol. 15, pp. 32-61.

Savage, J. C., 1965, Attenuation of elastic waves in granular mediums, J.G.R., vol. 70, pp. 3935-3942.

Savage, J. C., 1966, Thermoelastic attenuation of elastic waves by cracks, J.G.R., vol. 71, pp. 3929-3938.

Savage, J. C., 1976, Discussion on anelastic degradation of acoustic pulses in rock, Physics of Earth and Planetary Interiors, vol. 11, pp. 284-285.

Savage, J. C. and O'Neill, M. E., 1975, The relation between the Lomnitz and Futterman theories of internal friction, J.G.R., vol. 80, pp. 249-251.

Sherwood, J. W. C. and Trorey, A. W., 1965, Minimum-phase and related properties of the response of a horizontally stratified absorptive earth to plane acoustic waves, Geophysics, vol. 30, pp. 191-197.

Shumway, George, 1960a, Sound speed and absorption studies of marine sediments by a resonance method Pt. 1, Geophysics, vol. 25, pp. 451-467.

Shumway, George, 1960b, Sound speed and absorption studies of marine sediments by a resonance method Pt. 2, Geophysics, vol. 25, pp. 659-682.

Smylie, D. E., Clarke G. K. C. and Ulrych, T. J., 1973, Analysis of irregularities in the earth's rotation, in Methods in Computational Physics, vol. 13, Academic Press, New York.

Stacey, F. D., Gladwin, M. T., McKavanagh, B., Linde, A. T. and Hastie, L. M., 1975, Anelastic damping of acoustic and seismic pulses, Geophysical Surveys, vol. 2, pp. 131-151.

Stoll, Robert D., 1977, Acoustic waves in ocean sediments, Geophysics, vol. 42, pp. 716-725.

Stoll, Robert D. and Bryan, George M., 1970, Wave attenuation in saturated sediments, J. Acoust. Soc. Am., vol. 47, pp. 1440-1447.

Strick, E., 1967, The determination of Q, dynamic viscosity and transient creep curves from wave propagation measurements, Geophys. Jour. Royal Ast. Soc., vol. 13, pp. 197-218.

Strick, E., 1970, A predicted pedestal effect for pulse propagation in constant-Q solids, Geophysics, vol. 35, pp. 387-403.

Toksoz, Nafi M., Johnston, David H. and Timur A., 1979, Attenuation of seismic waves in dry and saturated rocks: I laboratcry measurements, Geophysics, vol. 44, pp. 691-711.

Treitel, Sven, 1959, On the attenuation of small-amplitude plane stress waves in a thermoelastic solid, J.G.R., vol. 64, pp. 661-665.

Treitel, Sven and Robinson, E. A., 1966, Seismic wave propagation in terms of communication theory, Geophysics, vol. 31, pp. 17-32.

Treitel, Sven, Gutowski, Paul, and Robinson, Enders, 1977, Emperical spectral analysis revisited, in Topics in Numerical Analysis, vol. 3, Academic Press, New York.

Trorey, A. W., 1962, Theoretical seismograms with frequency and depth dependent absorption, Geophysics, vol. 27, pp. 766-785.

Tullos, Frank N. and Reid, Alton C., 1969, Seismic attenuation of gulf coast sediments, Geophysics, vol. 34, pp. 516-528.

Ulrych, T. J., 1972, Maximum entropy power spectrum of truncated sinsusoids, J.G.R., vol. 77, pp. 1396-1400.

Ulrych, T. J. and Bishop T. N., 1975, Maximum entropy spectral analysis and autoregressive decomposition, Reviews of Geophysics and Space Physics, vol. 13, pp. 183-200.

Ulrych, T. J. and Clayton, R. W., 1976, Time series modelling and maximum entropy, Physics of Earth and Planetary Interiors, vol. 12, pp. 188-200.

Usher, M. J., 1962, Elastic behaviour of rocks at low frequencies, Geophysical Prospecting, vol. 10, pp. 119-127.

Van den Bos, 1971, An alternative interpretation of maximum entropy spectral analysis, IEEE Transactions on Information Theory, vol. IT-17, pp. 493-494.

Van Melle, F. A., 1954, Note on the primary disturbance in shale, B.S.S.A., vol. 44, pp. 123-125.

Vered, M. and Ben-Menahem, A., 1974, Applications of synthetic seismograms to the study of low-magnitude earthquakes and crustal structures in the northern Red Sea region, B.S.S.A., vol. 64, pp. 1221-1237.

Walsh, J. B., 1966, Seismic wave attenuation in rock due to friction, J.G.R., vol. 71, pp. 2591-2599.

White, J. E., 1965, Seismic Waves: Radiation, Transmission and Attenuation, McGraw Hill, Toronto.

White, J. E., 1966, Static friction as a source of seismic attenuation, Geophysics, vol. 31, pp. 333-339.

Wiggins, Ralph A., 1972, The general linear inverse problem: implications of surface waves and free oscillations for earth structure, Reviews of Geophysics and Space Physics, vol. 10, pp. 251-285.

Winkler, Kenneth, Nur, Amos and Gladwin, Michael, 1979, Friction and seismic attenuation in rocks, Nature, vol. 277, pp. 528-531.

Wood, A. B. and Weston, D. E., 1964, The propagation of sound in mud, Acustica, vol. 14, pp. 156-162.

Wuenschel, P. C., 1960, Seismogram synthesis including multiples and transmission coefficients, Geophysics, vol. 25, pp. 106-129.

Wuenschel, Paul C., 1965, Dispersive body waves--an experimental study, Geophysics, vol. 30, pp. 539-551.

Wyllie, M. R. J., Gardner, G. H. F. and Gregory A. R., 1962, Studies of elastic wave attenuation in porous media, Geophysics, vol. 27, pp. 569-589.

Zener, Clarence, 1937, Internal friction in solids, Physical Review, vol. 52, pp. 230-235.

Zener, Clarence, 1948, Elasticity and anelasticity of metals, University of Chicago Press.

APPENDIX A: LISTING OF PROGRAMS

```
      SUBROUTINE LSR4F(X1,X2,X3,X4,Y1,Y2,Y3,Y4,RAT,DIF,NX,
     .NY,MPTS)
C
C       SUBROUTINE BY DAVE GANLEY OCT 24, 1977.
C
C       THIS SUBROUTINE WILL CALCULATE THE NATURAL LOGARITHM
C       OF THE SPECTRAL RATIO AND/OR THE PHASE DIFFERENCE FOR
C       ANY NUMBER OF PAIRS OF SEISMIC TRACES.  THE SPECTRAL
C       RATIO (PHASE DIFFERENCE) IS CORRECTED BY DIVIDING BY
C       THE RATIO (SUBTRACTING THE PHASE DIFERENCE) OF 2 OTHER
C       TRACES ON A SECOND INPUT TAPE.  DIFFERENT TIME WINDOWS
C       CAN BE USED FOR EACH TRACE.   THE RESULTS ARE OUTPUT
C       IN GRAPHICAL FORM ON THE LINE PRINTER AND INTO A
C       SEQUENTIAL FILE ON LOGICAL UNIT 3.
C
C       A FAST FOURIER TRANSFORM IS USED TO CALCULATE SPECTRA.
C       THE DATA CAN BE WEIGHTED WITH A COSINE TAPER AT THE
C       ENDS AND THE SPECTRA CAN BE SMOOTHED.  THIS SMOOTHING
C       CAN BE APPLIED TO THE COMPLEX FOURIER COEFFICIENTS
C       OR TO THE AMPLITUDE AND PHASE.
C
C       INPUTS ARE:
C          X1,X2,X3,X4 = ARRAYS OF LENGTH NX
C          Y1,Y2,Y3,Y4 = ARRAYS OF LENGTH NY
C          NX = NUMBER OF DATA POINTS IN A BLOCK ON TAPE
C          NY = NUMBER OF POINTS TO USE IN FFT
C               (MUST BE A POWER OF 2)
C          MPTS = DO THE CALCULATION FOR THE FIRST MPTS
C                 FREQUENCY VALUES
C
C       OUTPUTS ARE:
C          RAT = NATURAL LOG OF SPECTRAL RATIO (LENGTH IS MPTS)
C          DIF = PHASE DIFFERENCE (LENGTH IS MPTS)
C
C       SUBROUTINES CALLED:
C          1. FFTR2 (FOURIER TRANSFORM ON 2 REAL TIME SERIES)
C          2. AMPPHZ (CALCULATES AMPLITUDE AND PHASE FROM
C                    FOURIER COEFFICIENTS OR VICE VERSA)
C          3. DANIEL (APPLY DANIELL SPECTRAL WINDOW)
C          4. UNWRAP (ATTEMPT TO UNWRAP PHASE CURVE)
C          5. GRAF (PLOT A LINE PRINTER GRAPH)
C          6. TAPER (APPLY COSINE BELL)
C          7. SKIP (SYSTEM ROUTINE TO SKIP TRACES ON TAPE)
C
      DIMENSION X1(NX),X2(NX),X3(NX),X4(NX)
      DIMENSION Y1(NY),Y2(NY),Y3(NY),Y4(NY)
      DIMENSION RAT(MPTS),DIF(MPTS)
      DATA IBLOCK/1/
      COMMON /LSRCOM/ L2NY,DT,DF,IWL,IC,IWT,ISM,FSWID
```

```
C++++
C     L2NY = SUCH THAT NY=2**L2NY
C     DT = SAMPLE INTERVAL IN MILLISECONDS
C          (SAME FOR BOTH TAPES)
C     DF = SPACING BETWEEN FREQUENCY VALUES IN HERTZ
C     IWL = TIME WINDOW LENGTH IN SAMPLES.
C           (SAME FOR ALL WINDOWS)
C     IC = 1 CALCULATE LOG OF SPECTRAL RATIO AND PHASE
C            DIFFERENCE
C        = 2 CALCULATE LOG OF SPECTRAL RATIO ONLY
C        = 3 CALCULATE PHASE DIFFERENCE ONLY
C     IWT = NUMBER OF POINTS AT EACH END OF DATA TO WEIGHT
C           WITH COSINE TAPER
C     ISM = 1 MEANS DO NOT SMOOTH SPECTRAL ESTIMATE
C         = 2 MEANS SMOOTH AMPLITUDE AND PHASE SPECTRA
C         = 3 MEANS TO SMOOTH COMPLEX FOURIER COEFFICIENTS
C     FSWID = WIDTH OF WINDOW TO USE FOR SMOOTHING (IN HERTZ)
C++++
      IWLP1=IWL+1
      MY=NY/2
      MYP1=MY+1
      MYP2=MY+2
      MYM1=MY-1
      MPTS1=MPTS-1
      IRL=0
      IR1L=0
      IR2L=0
      JRL=0
      JR1L=0
      JR2L=0
   10 READ (5,1,END=99) IR1,IWS1,IR2,IWS2,JR1,JWS1,JR2,JWS2
     .,DELT,IP1,IP2,JP1,JP2
    1 FORMAT (5X,8I5,F5.0,4I1)
C****
C     IR1 = NUMBER OF THE BLOCK ON TAPE 1 CONTAINING TRACE 1
C     IWS1 = WINDOW START FOR TRACE 1 IN MILLISECONDS
C     IP1 = 1 MEANS PLOT TRACE 1 DATA WINDOW ON LINE PRINTER
C     IR2, IWS2, IP2 = SAME AS ABOVE FOR TRACE 2 (ON TAPE 1)
C     JR1 = NUMBER OF THE BLOCK ON TAPE 2 CONTAINING TRACE 3
C     JWS1 = WINDOW START FOR TRACE 3 IN MILLISECONDS
C     JP1 = 1 MEANS PLOT TRACE 3 DATA WINDOW ON LINE PRINTER
C     JR2, JWS2, JP2 = SAME AS ABOVE FOR TRACE 4 (ON TAPE 2)
C     DELT = ACTUAL TIME DIFFERENCE (MSEC) BETWEEN ARRIVALS
C            FOR THE TWO CORRECTION TRACES (3 AND 4).  THIS
C            IS NEEDED TO REMOVE A LINEAR TREND FROM THE
C            PHASE DIFFERENCE WHICH IS CAUSED BY THE FACT
C            THAT THE TIME DIFFERENCE BETWEEN TRACES 3 AND 4
C            MUST BE A MULTIPLE OF THE SAMPLE INTERVAL WHEN
C            IT SHOULD BE DELT.  IF DELT=0.0 THIS CORRECTION
C            IS IGNORED.
C
C     IR2 MUST BE GREATER THAN IR1 AND JR2 GREATER THAN JR1
C     IT IS ASSUMED THAT FOR A GIVEN IR1 OR IR2 THE SAME
C     JR1 OR JR2 WILL CORRESPOND TO IT FOR ALL CALCULATIONS.
```

```
C      THERE CAN BE A DIFFERNET NUMBER OF TRACES ON TAPE 1 AND
C      TAPE 2 SO THAT IR1 AND IR2 DO NOT EQUAL JR1 AND JR2.
C
C      THE RATIO IS  (TRACE 2 / TRACE 1 ) * (TRACE 3 / TRACE 4)
C      DIFFERENCE IS (TRACE 2 - TRACE 1) - (TRACE 4 - TRACE 3)
C
C      IF THE SAME TRACE IS USED ON TWO CONSECUTIVE CARDS THE
C      WINDOW MUST BE THE SAME
C****
      IF (IR2.LE.IR1) GO TO 92
      IF (JR2.LE.JR1) GO TO 93
C
C      CALCULATE WINDOW STARTING POINTS
C
      T1=(IWL-1)*DT
      WRITE (6,2) T1,IR1,IWS1,IR2,IWS2,JR1,JWS1,JR2,JWS2,DELT
    2 FORMAT ('1WINDOW LENGTH IS ',F7.2,' MSEC',2(/,6X,
     .'TAPE 1 RECORD ',I3,' WINDOW START IS ',I5,' MSEC'),
     .2(/,6X,'TAPE 2 RECORD ',I3,' WINDOW START IS ',
     .' MSEC'),/' PHASE WILL BE CORRECTED TO TIME DIFFERENCE'
     .,' OF ',F7.2,' MSEC BETWEEN CORRECTION TRACES.')
      IWS1=IWS1/DT+1.5
      IWS2=IWS2/DT+1.5
      JWS1=JWS1/DT+1.5
      JWS2=JWS2/DT+1.5
C
C-----------------------------------------------------------
C
C      LOCATE AND READ THE FOUR INPUT RECORDS AND
C      CALCULATE AMPLITUDE AND/OR PHASE SPECTRA
C
      IF (IR1.EQ.IR1L) GO TO 22
      IF (IR1.NE.IR2L) GO TO 31
C
C      NEW TRACE 1 IS TRACE 2 FROM LAST CALCULATION
C      NEW TRACE 3 IS THUS TRACE 4 FROM LAST CALCULATION
C
         DO 21 I=1,NY
         Y1(I)=Y2(I)
   21    Y3(I)=Y4(I)
      IR1L=IR1
      IWS1L=IWS2L
      JR1L=JR1
      JWS1L=JWS2L
C
C      READ A NEW TRACE 2 IF TRACE 1 WAS USED ON LAST
C      CALCULATION.  ALSO READ THE NEW TRACE 4.
C
   22 IWS1=IWS1L
      JWS1=JWS1L
      NSKIP=IR2-IRL-1
      IF (NSKIP.NE.0) CALL SKIP(0,NSKIP,1,&91,&91,&91)
      READ (1) X2
      IRL=IR2
      IR2L=IR2
      IWS2L=IWS2
      J=IWS2
          DO 24 I=1,IWL
          Y2(I)=X2(J)
   24     J=J+1
      NSKIP=JR2-JRL-1
      IF (NSKIP.NE.0) CALL SKIP(0,NSKIP,2,&91,&91,&91)
      READ (2) X4
      JRL=JR2
      JR2L=JR2
      JWS2L=JWS2
      J=JWS2
          DO 25 I=1,IWL
          Y4(I)=X4(J)
   25     J=J+1
      IF (IWL.EQ.NY) GO TC 27
          DO 26 I=IWLP1,NY
          Y2(I)=0.0
   26     Y4(I)=0.0
C
C      CALCULATE SPECTRA FOR NEW TRACES 2 AND 4
C
   27 IF (IWT.EQ.0) GO TO 28
      CALL TAPER(Y2,IWL,IWT)
      CALL TAPER(Y4,IWL,IWT)
   28 CALL FFTR2(L2NY,Y2,Y4)
      GO TO (29,29),ISM
      CALL DANIEL(Y2,NY,FSWID,DT)
      CALL DANIEL(Y4,NY,FSWID,DT)
   29 CALL AMPPHZ(L2NY,Y2,IC,PDC2,PFN2)
      CALL AMPPHZ(L2NY,Y4,IC,PDC4,PFN4)
      GO TO (60,30,60),ISM
   30 CALL UNWRAP(Y2(MYP2),MYM1)
      CALL UNWRAP(Y4(MYP2),MYM1)
      CALL DANIEL(Y2,NY,FSWID,DT)
      CALL DANIEL(Y4,NY,FSWID,DT)
      GO TO 60
C
C       NEW TRACES 1 AND 2 (AND THUS 3 AND 4) TO BE READ
C
   31 IF (IR2.EQ.IR2L) GO TO 50
      NSKIP=IR1-IRL-1
      IF (NSKIP.NE.0) CALL SKIP(0,NSKIP,1,&91,&91,&91)
      READ (1) X1
      IRL=IR1
      IR1L=IR1
      IWS1L=IWS1
      J=IWS1
          DO 33 I=1,IWL
          Y1(I)=X1(J)
   33     J=J+1
      NSKIP=JR1-JRL-1
      IF (NSKIP.NE.0) CALL SKIP(0,NSKIP,2,&91,&91,&91)
      READ (2) X3
      JRL=JR1
      JR1L=JR1
      JWS1L=JWS1
      J=JWS1
          DO 35 I=1,IWL
          Y3(I)=X3(J)
 35       J=J+1
      NSKIP=IR2-IRL-1
      IF (NSKIP.NE.0) CALL SKIP(0,NSKIP,1,&91,&91,&91)
      READ (1) X2
      IRL=IR2
      IR2L=IR2
      IWS2L=IWS2
      J=IWS2
          DO 37 I=1,IWL
          Y2(I)=X2(J)
 37       J=J+1
      NSKIP=JR2-JRL-1
      IF (NSKIP.NE.0) CALL SKIP(0,NSKIP,2,&91,&91,&91)
      READ (2) X4
      JRL=JR2
      JR2L=JR2
      JWS2L=JWS2
      J=JWS2
          DO 39 I=1,IWL
          Y4(I)=X4(J)
 39       J=J+1
      IF (IWL.EQ.NY) GO TC 46
          DO 41 I=IWLP1,NY
          Y1(I)=0.0
          Y2(I)=0.0
          Y3(I)=0.0
 41       Y4(I)=0.0
C
C      CALCULATE SPECTRA FOR 4 NEW TRACES
C
 46   IF (IWT.EQ.0) GO TO 47
      CALL TAPER(Y1,IWL,IWT)
      CALL TAPER(Y2,IWL,IWT)
      CALL TAPER(Y3,IWL,IWT)
      CALL TAPER(Y4,IWL,IWT)
 47   CALL FFTR2(L2NY,Y1,Y2)
      CALL FFTR2(L2NY,Y3,Y4)
      GO TO (48,48),ISM
      CALL DANIEL(Y1,NY,FSWID,DT)
      CALL DANIEL(Y2,NY,FSWID,DT)
      CALL DANIEL(Y3,NY,FSWID,DT)
      CALL DANIEL(Y4,NY,FSWID,DT)
 48   CALL AMPPHZ(L2NY,Y1,IC,PDC1,PFN1)
      CALL AMPPHZ(L2NY,Y2,IC,PDC2,PFN2)
      CALL AMPPHZ(L2NY,Y3,IC,PDC3,PFN3)
      CALL AMPPHZ(L2NY,Y4,IC,PDC4,PFN4)
      GO TO (60,49,60),ISM
```

```
   49 CALL UNWRAP(Y1(MYP2),MYM1)
      CALL UNWRAP(Y2(MYP2),MYM1)
      CALL UNWRAP(Y3(MYP2),MYM1)
      CALL UNWRAP(Y4(MYP2),MYM1)
      CALL DANIEL(Y1,NY,FSWID,DT)
      CALL DANIEL(Y2,NY,FSWID,DT)
      CALL DANIEL(Y3,NY,FSWID,DT)
      CALL DANIEL(Y4,NY,FSWID,DT)
      GO TO 60
C
C      READ A NEW TRACE 1 IF TRACE 2 WAS USED ON LAST
C      CALCULATION.  ALSO READ THE NEW TRACE 3.
C
   50 IWS2=IWS2L
      NSKIP=IR1-IRL-1
      IF (NSKIP.NE.0) CALL SKIP(0,NSKIP,1,&91,&91,&91)
      READ (1) X1
      IRL=IR1
      IR1L=IR1
      IWS1L=IWS1
      J=IWS1
          DO 52 I=1,IWL
          Y1(I)=X1(J)
   52     J=J+1
      NSKIP=JR1-JRL-1
      IF (NSKIP.NE.0) CALL SKIP(0,NSKIP,2,&91,&91,&91)
      READ (2) X3
      JRL=JR1
      JR1L=JR1
      JWS1L=JWS1
      J=JWS1
          DO 54 I=1,IWL
          Y3(I)=X3(J)
   54     J=J+1
      IF (IWL.EQ.NY) GO TC 56
          DO 55 I=IWLP1,NY
          Y1(I)=0.0
   55     Y3(I)=0.0
C
C      CALCULATE SPECTRA OF NEW TRACES 1 AND 3
C
   56 IF (IWT.EQ.0) GO TO 57
      CALL TAPER(Y1,IWL,IWT)
      CALL TAPER(Y2,IWL,IWT)
   57 CALL FFTR2(L2NY,Y1,Y3)
      GO TO (58,58),ISM
      CALL DANIEL(Y1,NY,FSWID,DT)
      CALL DANIEL(Y3,NY,FSWID,DT)
   58 CALL AMPPHZ(L2NY,Y1,IC,PDC1,PFN1)
      CALL AMPPHZ(L2NY,Y3,IC,PDC3,PFN3)
      GO TO (60,59,60),ISM
   59 CALL UNWRAP(Y1(MYP2),MYM1)
      CALL UNWRAP(Y3(MYP2),MYM1)
      CALL DANIEL(Y1,NY,FSWID,DT)
      CALL DANIEL(Y3,NY,FSWID,DT)
C
C----------------------------------------------------------------
C
C      CALCULATE NATURAL LOGARITHM OF RATIO OF AMPLITUDE
C      SPECTRA
C
   60 GO TO (61,61,65),IC
   61 RMIN=0.0
          DO 63 I=1,MPTS
          RAT(I)=ALOG(Y2(I)/Y1(I)*Y3(I)/Y4(I))
          IF (RAT(I).LT.RMIN) RMIN=RAT(I)
   63     CONTINUE
          DO 64 I=1,MPTS
   64     RAT(I)=RAT(I)-RMIN
C
C      CALCULATE PHASE DIFFERENCE
C
      GO TO (65,70),IC
   65     DC 66 I=2,MPTS
          J=I+MY
   66     DIF(I)=Y2(J)-Y1(J)+Y3(J)-Y4(J)
      DIF(1)=PDC2-PDC1+PDC3-PDC4
      IF (MPTS.EQ.MYP1) DIF(MPTS)=PFN2-PFN1+PFN3-PFN4
      PFACT=((JWS2-JWS1)*DT-DELT)*0.36*DF
      IF (DELT.EQ.0.0) PFACT=0.0
      IF (PFACT.EQ.0.0) GO TO 68
          DO 67 I=2,MPTS
          PCOR=PFACT*(I-1)
   67     DIF(I)=DIF(I)+PCOR
   68 IF (ISM.EQ.2) GO TO 70
          DO 69 I=1,MPTS
          IF (DIF(I).LE.-540.0) DIF(I)=DIF(I)+720.0
          IF (DIF(I).GT.540.0) DIF(I)=DIF(I)-720.0
          IF (DIF(I).LE.-180.0) DIF(I)=DIF(I)+360.0
          IF (DIF(I).GT.180.0) DIF(I)=DIF(I)-360.0
   69     CONTINUE
C
C----------------------------------------------------------------
C
C      PLOT INPUT TRACES IF REQUESTED AND
C      PLOT RATIOS AND/OR DIFFERENCES
C      OUTPUT RATIOS AND DIFFERENCES TO LOGICAL UNIT 3
C
    3 FORMAT ('1PLOT OF BLOCK ',I5,' TAPE 1')
    4 FORMAT ('1PLOT OF BLOCK ',I5,' TAPE 2')
    5 FORMAT ('1CORRECTED RATIO/DIFFERENCE OF BLOCK ',I3,
     .' TC BLOCK ',I3,' IS BLOCK ',I3,' ON TAPE')
C
   70 IF (IP1.NE.1) GO TO 72
      WRITE (6,3) IR1
      T1=(IWS1-1)*DT
      CALL GRAF(T1,DT,X1(IWS1),IWL,3)
   72 IF (IP2.NE.1) GO TO 74
```

```
      WRITE (6,3) IR2
      T1=(IWS2-1)*DT
      CALL GRAF(T1,DT,X2(IWS2),IWL,3)
   74 IF (JP1.NE.1) GO TO 76
      WRITE (6,4) JR1
      T1=(JWS1-1)*DT
      CALL GRAF(T1,DT,X3(JWS1),IWL,3)
   76 IF (JP2.NE.1) GO TO 80
      WRITE (6,4) JR2
      T1=(JWS2-1)*DT
      CALL GRAF(T1,DT,X4(JWS2),IWL,3)
   80 GO TO (81,81,83),IC
   81 WRITE (6,5) IR2,IR1,IBLOCK
      WRITE (3) RAT
      IBLOCK=IBLOCK+1
      CALL GRAF(0.0,DF,RAT,MPTS,1)
   83 GO TO (85,10,85),IC
   85 WRITE (6,5) IR2,IR1,IBLOCK
      WRITE (3) DIF
      IBLOCK=IBLOCK+1
      CALL GRAF(0.0,DF,DIF,MPTS,2)
      GO TO 10
C
C-----------------------------------------------------------
C
C       ERROR MESSAGES
C
   91 WRITE (6,96)
      RETURN
   92 WRITE (6,97) IR1,IR2
      RETURN
   93 WRITE (6,98) JR1,JR2
      RETURN
   96 FORMAT ('-BAD RETURN FROM SKIP IN LSR2F')
   97 FORMAT ('-IR2 MUST BE GREATER THAN IR1 ',I5,5X,I5)
   98 FORMAT ('-JR2 MUST BE GREATER THAN JR1 ',I5,5X,I5)
   99 RETURN
      END
      SUBRCUTINE DANIEL(X,N,FWIND,DT)
C
C     SUBROUTINE BY DAVE GANLEY DECEMBER 12, 1977.
C
C     THIS SUBROUTINE CALCULATES A DANIELL-LIKE SPECTRAL
C     ESTIMATE FROM THE PERICDCGRAM.  THIS IS DONE BY
C     AVERAGING ALL FREQUENCIES WITHIN A WINDOW CENTRED
C     ABOUT THE DESIRED FREQUENCY.  SINCE REAL AND
C     IMAGINARY COEFFICIENTS (OR AMPLITUDE AND PHASE VALUES)
C     ARE AVERAGED THIS IS NOT A DANIELL POWER SPECTRAL
C     ESTIMATE.  ALSO NOTE THAT AT FREQUENCIES WITHIN HALF
C     OF THE WINDOW WIDTH OF DC CR NYQUIST FREQUENCIES THE
C     ESTIMATES ARE CALCULATED BY AVERAGING OVER FEWER
C     VALUES.
C
C     INPUTS:
C       X = INPUT FOURIER TRANSFORM AS OUTPUT BY FFTR1 OR
C            AMPPHZ.  ON CUTPUT X CONTAINS THE SMOOTHED
C            SPECTRAL ESTIMATE IN THE SAME FORMAT.
C       N = LENGTH OF X (N IS 2**M WHERE M IS AN INTEGER)
C       FWIND = WINDOW WIDTH IN FREQUENCY DOMAIN (HERTZ)
C       DT = SAMPLE INTERVAL CF ORIGINAL TIME SERIES (MSEC)
C
      DIMENSION X(N)
      DIMENSION Y(1024)
      IF (N.LE.1024) GO TO 10
      WRITE (6,1)
    1 FORMAT ('1N CANNOT EXCEED 1024 IN SUBRCUTINE DANIELL')
      STOP 8
   10 N2=N/2
      N22=N2+2
      NP2=N+2
      DF=1000.0/(N*DT)
      M2=FWIND/(2.0*DF)+.5
      M21=M2+1
      M=2*M2+1
      XM=M
      XM1=M-1
      FWID=2.0*M2*DF
      WRITE (6,2) M,FWID
    2 FORMAT (' ',I3,' PCINTS USED IN DANIELL WINDOW '
     -,'WHICH IS A WIDTH OF ',F6.2,' HERTZ')
      IF (M2.EQ.0) RETURN
          DO 19 I=1,N
   19     Y(I)=X(I)
      KE=0
          DO 49 I=1,M2
          II=N22-I
          L=I+N2
          LL=II+N2
          JE=M21-I
          I21=2*I-1
          II21=N22-I21
          L21=I21+N2
      LL21=NP2-I21
      XF=XM-JE
      XF1=XF-1.0
      IF (I.EQ.1) GO TO 30
      KE=I-1
          DO 29 K=1,KE
          X(I)=X(I)+Y(I+K)+Y(I-K)
          X(II)=X(II)+Y(II+K)+Y(II-K)
          X(L)=X(L)+Y(L+K)
          X(LL)=X(LL)+Y(LL-K)
          IF (K.EQ.KE) GO TO 29
          X(L)=X(L)+Y(L-K)
          X(LL)=X(LL)+Y(LL+K)
29        CONTINUE
30        DO 39 J=1,JE
          X(I)=X(I)+Y(I21+J)
          X(II)=X(II)+Y(II21-J)
          IF (I.EQ.1) GO TO 39
          X(L)=X(L)+Y(L21+J)
          X(LL)=X(LL)+Y(LL21-J)
39        CONTINUE
      X(I)=X(I)/XF
      X(II)=X(II)/XF
      IF (I.EQ.1) GO TO 49
      X(L)=X(L)/XF1
      X(LL)=X(LL)/XF1
49    CONTINUE
   IE=N22-M21
   IF (M21.GT.IE) RETURN
   L=M21+N2
      DO 59 I=1,M2
      X(M21)=X(M21)+Y(M21+I)+Y(M21-I)
      IF (M.GT.N2.AND.I.EQ.M2) GO TO 59
      X(L)=X(L)+Y(L+I)
      IF (I.EQ.M2) GO TO 59
      X(L)=X(L)+Y(L-I)
59    CONTINUE
   X(M21)=X(M21)/XM
   X(L)=X(I)/XM1
   IF (M.GT.N2) X(L)=X(L)*XM1/(XM1-1.0)
   IF (IE.EQ.M21) RETURN
   L=IE+N2
      DO 69 I=1,M2
      X(IE)=X(IE)+Y(IE+I)+Y(IE-I)
      X(L)=X(L)+Y(L-I)
      IF (I.NE.M2) X(L)=X(L)+Y(L+I)
69    CONTINUE
   X(IE)=X(IE)/XM
   X(L)=X(L)/XM1
   IE=IE-1
   IS=M21+1
   IF (IS.GT.IE) RETURN
      DO 89 I=IS,IE
      L=I+N2
```

```
                 DO 79 J=1,M2
                 X(I)=X(I)+Y(I+J)+Y(I-J)
                 X(L)=X(L)+Y(L+J)+Y(L-J)
 79              CONTINUE
           X(I)=X(I)/XM
           X(L)=X(L)/XM
 89        CONTINUE
      RETURN
      END
      SUBROUTINE UNWRAP(X,N)
C
C     ROUTINE BY DAVE GANLEY DECEMBER 16, 1977.
C
C     THIS A SIMPLE ROUTINE TO USE TO TRY AND UNWRAP A
C     PHASE CURVE WHERE THE PHASE VALUES ARE RESTRICTED
C     TO THE PRINCIPAL BAND (-180 TO 180).  IT ASSUMES
C     THAT THE CURVE IS REASONABLY SMOOTH AND THAT A
C     CHANGE IN PHASE BETWEEN ADJACENT POINTS OF 180 DEGREES
C     INDIDCATES A MULTIPLE OF 360 DEGREES HAS BEEN LEFT OFF
C     PHASE VALUES FROM THIS POINT ON.  IF THE PHASE JUMPS
C     AROUND BY PLUS OR MINUS 180 DEGREES THEN THIS ROUTINE
C     WILL NOT WORK PROPERLY.
C
C     X IS THE PHASE CURVE (OF LENGTH N) ON INPUT AND IS
C     THE UNWRAPPED CURVE ON OUTPUT
C
      DIMENSION X(N)
      D1=0.0
      DO 9 I=2,N
      IF (I.GT.4) D1=(X(I-1)-X(I-4))/3.0
      IF (ABS(X(I)-X(I-1)-D1).LT.180.0) GO TO 9
      JS=I
      IF (X(I).GT.X(I-1)) GO TO 4
         DO 2 J=JS,N
 2       X(J)=X(J)+360.0
      GO TO 7
 4       DO 5 J=JS,N
 5       X(J)=X(J)-360.0
 7    WRITE (6,8) JS
 8    FORMAT (' PHASE CURVE ALTERED BY MULTIPLE OF 360 '
     -,'BEYOND POINT ',I4)
 9    CONTINUE
      RETURN
      END
      SUBROUTINE TAPER(X,N,M)
C
C      SUBROUTINE BY DAVE GANLEY, MARCH 8, 1978.
C
C      THIS SUBROUTINE WILL APPLY A COSINE TAPER TO EACH
C      END OF AN INPUT TIME SERIES.
C
C      INPUTS ARE:
C         X = TIME SERIES
C         N = LENGTH OF X
C         M = NUMBER OF POINTS AT EACH END OF X TO WEIGHT
C              (MAXIMUM IS 25)
C
C      OUTPUT IS:
C         X = TAPERED TIME SERIES
C
      DIMENSION W(25),X(1)
      DATA ML/0/
      IF (M.GT.25) GO TO 4
      IF (2*M.GT.N) GO TO 6
      IF (M.EQ.ML) GO TO 2
      T1=3.1415927/(M+1)
      DO 1 I=1,M
      T2=T1*I
    1 W(I)=.5-COS(T2)/2.0
    2 NP1=N+1
          DO 3 I=1,M
          J=NP1-I
          X(I)=X(I)*W(I)
    3     X(J)=X(J)*W(I)
      RETURN
    4 WRITE (6,5)
    5 FORMAT ('1 TAPER CAN ONLY WEIGHT UP TO 25 TERMS')
      STCP 16
    6 WRITE (6,7)
    7 FORMAT ('1M CANNOT BE LARGER THAN N/2 IN TAPER')
      STOP 16
      END
      SUBROUTINE AMPPHZ(LOG2N,X,IC,PDC,PFN)
C
C
C************************************************************
C
C     WRITTEN BY DAVE GANLEY ON MAY 19, 1977.
C
C          THIS SUBROUTINE CALCULATES AMPLITUDE AND/OR PHASE
C     SPECTRA FROM THE REAL AND IMAGINARY PARTS OF A
C     FREQUENCY SPECTRUM OR VICE VERSA.  THE INPUT (OUTPUT)
C     ARRAY X IS OF LENGTH 2**LCG2N WITH THE REAL PARTS OF
C     THE FOURIER COEFFICIENTS FOR FREQUENCIES ZERC TO
C     NYQUIST IN THE FIRST N/2+1 POSITIONS OF X.  THE
C     IMAGINARY PARTS OF THE COEFFICIENTS ARE IN POSITIONS
C     IN POSITIONS N/2+2 TO N AND ARE NOT STORED FOR DC OR
C     NYQUIST FREQUENCY (WHERE THEY ARE ZERO).  THE OUTPUT
C     (INPUT) ARRAY HAS AMPLITUDES IN THE FIRST N/2+1
C     POSITIONS AND PHASES (IN DEGREES) IN THE LAST N/2-1
C     POSITICNS.  PHASES FOR DC AND NYQUIST FREQUENCIES
C     ARE RETURNED (SPECIFIED) IN PDC AND PFN.
C
C     IC = 1 INPUT IS FOURIER COEFFICIENTS.
C            OUTPUT IS AMPLITUDE AND PHASE.
C        = 2 INPUT IS FOURIER COEFFICIENTS.
C            OUTPUT IS AMPLITUDE CNLY.
C        = 3 INPUT IS FOURIER COEFFICIENTS.
C            OUTPUT IS PHASE ONLY.
C        = -1 INPUT AMPLITUDE AND PHASE.
C             OUTPUT IS FOURIER COEFFICIENTS.
C
C************************************************************
C
C
      DIMENSION X(1)
      IF (LCG2N.LT.1) RETURN
      M=1
        DO 9 I=2,LOG2N
    9   M=2*M
      N=2*M
      MP1=M+1
      IF (IC.LT.1) GO TO 400
      GO TO (100,200,300),IC
C
C     CALCULATE AMPLITUDE AND PHASE SPECTRUM
C
  100 IF (X(1).GE.0.0) GO TO 105
      X(1)=-X(1)
      PDC=180.0
      GO TO 110
  105 PDC=0.0
  110 IF (X(MP1).GE.0.0) GO TO 115
      X(MP1)=-X(MP1)
      PFN=180.0
      GO TO 120
  115 PFN=0.0
  120 IF (LOG2N.EQ.1) RETURN
         DO 129 I=2,M
         A=X(I)
         B=X(I+M)
         X(I)=SQRT(A*A+B*B)
  129    X(I+M)=57.29578*ATAN2(B,A)
      RETURN
C
C     CALCULATE AMPLITUDE SPECTRUM ONLY
C
  200 IF (X(1).LT.0.0) X(1)=-X(1)
      IF (X(MP1).LT.0.0) X(MP1)=-X(MP1)
      IF (LOG2N.EQ.1) RETURN
         DO 209 I=2,M
         A=X(I)
         B=X(I+M)
  209    X(I)=SQRT(A*A+B*B)
      RETURN
C
C     CALCULATE PHASE SPECTRUM ONLY
C
  300 IF (X(1).LT.0.0) GO TO 305
      PDC=0.0
      GO TO 310
  305 PDC=180.0
  310 IF (X(MP1).LT.0.0) GO TO 315
      PFN=0.0
      GO TO 320
  315 PFN=180.0
  320 IF (LOG2N.EQ.1) RETURN
         DO 329 I=2,M
         A=X(I)
         B=X(I+M)
  329    X(I+M)=57.29578*ATAN2(B,A)
      RETURN
C
C     CALCULATE FOURIER COEFFICIENTS FROM AMPLITUDE AND PHASE
C
  400 X(1)=X(1)*COS(PDC/57.29578)
      X(MP1)=X(MP1)*COS(PFN/57.29578)
      IF (LOG2N.EQ.1) RETURN
         DO 409 I=2,M
         A=X(I)
         B=X(I+M)/57.29578
         X(I)=A*COS(B)
  409    X(I+M)=A*SIN(B)
      RETURN
      END
```

```
C
C     PROGRAM BY DAVE GANLEY, NOVEMBER 14, 1977.
C
C     THIS PROGRAM WILL DO A LEAST-SQUARES FIT OF A STRAIGHT
C     LINE TO DATA OUTPUT BY MY SPECTRAL RATIO PROGRAM FOR
C     THE PURPOSE OF ESTIMATING Q.  IT CAN ALSO OUTPUT THE
C     DISPERSION CURVE CORRESPONDING TO THE PHASE DIFFERENCE
C     CURVE OUTPUT BY THE SPECTRAL RATIO PROGRAM AND PRODUCE
C     LINE PRINTER GRAPHS AND CALCOMP PLOTS.
C
C     SUBROUTINES CALLED:
C         1. SLOPE
C         2. GRAF (MAKES LINE PRINTER PLOTS)
C         3. UNWRAP
C         4. CALCOMP PLOTTER ROUTINES
C
      DIMENSION X(257),Y(260),C(103),F(103)
      DATA PI/3.141593/,IBL/0/
      READ (5,1) N,DF,FN,ICALC
C****
C     N = NUMBER OF POINTS IN A RECORD ON TAPE
C         (LOGICAL UNIT 1)
C         N CANNOT EXCEED 257
C     DF = FREQUENCY INTERVAL (HZ) BETWEEN INPUT POINTS
C     FN = NYQUIST FREQUENCY FOR THIS DATA
C     ICALC = 1 MEANS THAT CALCOMP PLOTS ARE TO BE MADE
C****
    1 FORMAT (5X,I5,F10.0,F5.0,I5)
      IF (N.GT.257) GO TO 91
C
         DO 9 I=1,N
    9    X(I)=(I-1)*DF
      IF (ICALC.NE.1) GO TO 10
      CALL PLOTS
      CALL PLOT(2.0,2.0,-3)
   10 READ (5,2,END=99) IB,ISA,ILA,IQPC,ISP,ILP,DELZ,DELT
     -,FZERO,PSTAT,ICPC,ICPL,IQPI
C****
C     IB = NUMBER OF BLOCK CONTAINING LOG SPECTRAL RATIO DATA
C          THIS REFERS TO LOGICAL UNIT 1
C     ISA = FIRST POINT TO USE IN ANALYSIS OF AMPLITUDE DATA
C     ILA = LAST POINT TO USE IN ANALYSIS OF AMPLITUDE DATA
C     IQPC = 1 MEANS PLOT AMPLITUDE DATA AND REGRESSION LINE
C           ON CALCOMP
C     ISP = FIRST POINT TO USE IN ANALYSIS OF PHASE DATA
C         = 0 OR BLANK MEANS DON'T CALCULATE DISPERSION CURVE
C           IF A DISPERSION CURVE IS TO BE CALCULATED THEN
C           THE PHASE CURVE MUST BE IN THE BLOCK IMMEDIATELY
C           BEHIND THAT CONTAINING THE AMPLITUDE DATA.
C     ILP = LAST POINT TO USE IN ANALYSIS OF PHASE DATA
C     DELZ = DISTANCE BETWEEN RECEIVERS FOR THIS DIFFERENCE
C     DELT = TIME DIFFERENCE BETWEEN ANALYSIS WINDOW STARTS
C           FOR THIS PHASE DIFFERENCE.
C     FZERO = LOWEST FREQUENCY AT WHICH PHASE CURVE IS ZERO.
```

```
C              AT THIS FREQUENCY PHASE VELOCITY IS DELZ/DELT.
C              THIS IS USED IN PLOTTING THE DISPERSION CURVE.
C      PSTAT = REMOVE A PHASE OF PSTAT*FREQUENCY DEGREES FROM
C              THE PHASE CURVE BEFORE ANALYSIS.
C      ICPC = 1 MEANS TO PLOT DISPERSION DATA AND THEORETICAL
C             DISPERSION CURVE ON CALCOMP PLOTTER.
C      ICPL = 1 MEANS PLOT DISPERSION CURVE ON LINE PRINTER
C      IQPL = 1 MEANS PLOT Q VERSUS FREQUENCY CURVE ON PRINTER
C****
     2 FORMAT (5X,6I5,4F5.0,3I5)
       IF (ISA.EQ.0) ISA=1
       IF (ILA.EQ.0) ILA=N
       IF (ISA.GE.ILA) GO TO 93
       IF (FZERO.EQ.0.0) FZERO=FN
C
C      CALCULATE SLOPE OF LOG SPECTRAL RATIO PLOT
C
       NSKIP=IB-IBL-1
       IF (NSKIP.NE.0) CALL SKIP(0,NSKIP,1,&95,&95,&95)
       READ (1) (Y(I),I=1,N)
       IBL=IB
       MA=ILA-ISA+1
       CALL SLOPE(X(ISA),Y(ISA),MA,S,SD,YI,YID)
       WRITE (6,3) IB,ISA,ILA,S,SD,YI,YID
     3 FORMAT ('1BLOCK ',I3,' POINTS ',I3,' TO ',I3,/,6X,
      .'SLOPE = ',E10.4,5X,' STD DEV = ',E10.4,/,6X,
      .'INTERCEPT = ',E10.4,5X,'STD DEV = ',E10.4)
       IF (ICPC.NE.1) GO TO 25
C
C      MAKE CALCOMP PLOT OF AMPLITUDE DATA
C
       IT1=X(ISA)/10.0
       IT1=10*IT1
       IT2=X(ILA)/10.0+1.0
       IT2=IT2*10
       IT3=IT2-IT1+1
       T=1.0
       IF (IT3.GT.101) T=2.0
       IF (IT3.GT.201) T=4.0
    13 IF (IT3.GT.401) STOP 13
       IT3=IT3/T+.8
           DO 15 I=1,IT3
           F(I)=(I-1)*T+IT1
           C(I)=-(YI+F(I)*S)
           IF (C(I).GT.0.0) C(I)=0.0
    15     CONTINUE
       F(IT3+1)=F(1)
       F(IT3+2)=10.*T
       FLEN=(F(IT3)-F(1))/F(IT3+2)
       Y(ILA+1)=-C(1)
       CALL SCALE(Y(ISA),7.0,MA+1,1)
       C(IT3+1)=-Y(ILA+2)-7.0*Y(ILA+3)
       C(IT3+2)=Y(ILA+3)
       CALL AXIS2(0.0,0.0,'LOG OF AMPLITUDE',-16,7.0,0.0,
     .-C(IT3+1),-C(IT3+2),1.0)
      CALL AXIS2(7.0,0.0,'FREQUENCY (HZ)',-14,FLEN,90.0,
     .F(IT3+1),F(IT3+2),1.0)
      CALL PLOT(7.0,FLEN,3)
      CALL PLOT(0.0,FLEN,2)
      CALL PLOT(0.0,0.0,2)
      CALL SYMBOL(-1.0,0.0,0.20,'BLOCK',90.0,5)
      T=IB+.05
      CALL NUMBER(-1.0,1.2,0.20,T,90.0,-1)
      T=(C(1)-C(IT3+1))/C(IT3+2)
      CALL PLOT(T,0.0,3)
      CALL LINE(C,F,IT3,1,0)
          DO 19 I=ISA,ILA
          XP=(Y(I)+C(IT3+1))/(-C(IT3+2))
          YP=(X(I)-F(IT3+1))/F(IT3+2)
   19     CALL SYMBOL(XP,YP,0.10,4,90.0,-1)
      IF (ICPC.NE.1.OR.ISP.EQ.0) GO TO 22
      CALL PLOT(0.0,15.0,-3)
      GC TO 25
   22 CALL PLOT(10.0,0.0,-3)
   25 IF (ISP.EQ.0) GO TC 10
C
C     CALCULATE DISPERSION CURVE
C
      IF (ILP.EQ.0) ILP=ILA
      IF (ISP.GE.ILP) GO TO 93
      READ (1) (Y(I),I=1,N)
      IBL=IBL+1
      WRITE (6,4)
    4 FORMAT ('-FREQUENCY',5X,'PHASE VELOCITY')
C
C     IN CALCULATING THE DISPERSION CURVE FROM THE PHASE
C     SPECTRUM I AM USING RCUTINE UNWRAP TO UNWRAP THE PHASE
C     CURVE IF IT IS LIMITED TO THE PRINCIPAL BAND (-180 TO
C     180). I AM ALSO REMOVING A LINEAR TREND BY SUBTRACTING
C     PSTAT*FREQUENCY DEGREES FROM THE PHASE CURVE.
C
      CALL UNWRAP(Y,N)
      DELT=DELT-PSTAT/360.0
          DO 29 I=ISP,ILP
          PHZ=Y(I)-X(I)*PSTAT
          Y(I)=DELZ/(DELT-PHZ/(360.0*X(I)))
   29     WRITE (6,5) X(I),Y(I)
    5 FORMAT (' ',E12.6,5X,E10.4)
      IF (ICPC.NE.1) GO TO 40
C
C     MAKE CALCOMP PLOT CF DISPERSION CURVE
C
      MP=ILP-ISP+1
      IT1=X(ISP)/10.0
      IT1=10*IT1
      IT2=X(ILP)/10.0+1.0
      IT2=IT2*10
      IT3=IT2-IT1+1
      T=1.0
      IF (IT3.GT.101) T=2.0
      IF (IT3.GT.201) T=4.0
   32 IF (IT3.GT.401) STOP 32
      IT3=IT3/T+.8
      QR=-PI*DELT/S
      CR=DELZ/DELT
      F(1)=IT1
      C(1)=-CR/(1.0+ALOG(FZERO*1000.0)/(PI*QR))
      IF (F(1).NE.0.0) C(1)=-CR/(1.0-ALOG(F(1)/FZERO)/(PI*QR))
          DO 35 I=2,IT3
          F(I)=(I-1)*T+IT1
   35     C(I)=-CR/(1.0-ALOG(F(I)/FZERO)/(PI*QR))
      F(IT3+1)=F(1)
      F(IT3+2)=10.*T
      FLEN=(F(IT3)-F(1))/F(IT3+2)
      Y(ILP+1)=-C(IT3)
      CALL SCALE(Y(ISP),3.0,MP+1,1)
      C(IT3+1)=-Y(ILP+2)-3.0*Y(ILP+3)
      C(IT3+2)=Y(ILP+3)
      IF (C(1).GT.(C(IT3+1)+7.0*C(IT3+2))) C(1)=C(IT3+1)
     .+7.0*C(IT3+2)
      CALL AXIS2(0.0,0.0,'VELOCITY',-8,7.0,0.0,-C(IT3+1),
     .-C(IT3+2),1.0)
      CALL AXIS2(7.0,0.0,'FREQUENCY (HZ)',-14,FLEN,90.0,
     .F(IT3+1),F(IT3+2),1.0)
      CALL PLOT(7.0,FLEN,3)
      CALL PLOT(0.0,FLEN,2)
      CALL PLOT(0.0,0.0,2)
      CALL SYMBOL(-1.0,0.0,0.20,'BLCCK',90.0,5)
      T=IBL+.05
      CALL NUMBER(-1.0,1.2,0.20,T,90.0,-1)
      T=(C(1)-C(IT3+1))/C(IT3+2)
      CALL PLOT(T,0.0,3)
      CALL LINE(C,F,IT3,1,0)
          DO 39 I=ISP,ILP
          XP=(Y(I)+C(IT3+1))/(-C(IT3+2))
          YP=(X(I)-F(IT3+1))/F(IT3+2)
   39     CALL SYMBOL(XP,YP,0.10,4,90.0,-1)
      IF (IQPC.EQ.1) CALL PLOT(0.0,-15.0,-3)
      CALL PLOT(10.0,0.0,-3)
C
C     PLCT DISPERSION CURVE ON LINE PRINTER
C
   40 IF (ICPL.NE.1) GO TO 42
      F1=DF*(ISP-1)
      MP=ILP-ISP+1
      DELT=DELT+PSTAT/360.0
      WRITE (6,6) IBL,DELZ,DELT,FZERO,PSTAT
    6 FORMAT ('1DISPERSION CURVE FOR BLOCK ',I3,/,6X,
     .'DELZ = ',F10.4,5X,'DELT = ',F10.4,5X,'FZERO = ',
     .F6.1,5X,'PSTAT = ',F10.4)
      CALL GRAF(F1,DF,Y(ISP),MP,1)
C
```

```
C     PLOT Q VERSUS FREQUENCY CURVE ON LINE PRINTER
C
   42 IF (IQPL.NE.1) GO TO 10
      IF (ISA.LT.ISP) ISA=ISP
      IF (ILA.GT.ILP) ILA=ILP
      MA=ILA-ISA+1
         DO 44 I=ISA,ILA
   44    Y(I)=-PI*DELZ/(Y(I)*S)
      F1=DF*(ISA-1)
      WRITE (6,7) IB
    7 FORMAT ('1Q VERSUS FREQUENCY CURVE FOR BLOCK ',I3)
      CALL GRAF(F1,DF,Y(ISA),MA,1)
      GO TO 10
   91 WRITE (6,92)
   92 FORMAT ('1N CANNOT EXCEED 257')
      GO TO 99
   93 WRITE (6,94)
   94 FORMAT ('1ISA (ISP) MUST BE LESS THAN ILA (ILP)')
      GO TO 99
   95 WRITE (6,96)
   96 FORMAT ('1BAD RETURN FROM SKIP')
   99 IF (ICALC.EQ.1) CALL PLOT(0.0,0.0,999)
      STOP
      END
      SUBROUTINE SLOPE(X,Y,N,S,SD,B,BD)
C
C     SUBROUTINE BY DAVE GANLEY, NOV 14, 1977.
C
C     THIS SUBROUTINE WILL CALCULATE THE LEAST SQUARES
C     ESTIMATE OF THE EQUATION OF A STRAIGHT LINE THROUGH
C     N DATA POINTS.
C
C     INPUTS:
C          X = ARRAY OF X COORDINATES OF THE POINTS
C          Y = ARRAY OF Y COORDINATES OF THE POINTS
C          N = NUMBER OF INPUT POINTS (N MUST BE AT LEAST 3)
C
C     OUTPUTS:
C          S = LEAST SQUARES ESTIMATE OF THE SLOPE
C          SD = ESTIMATE OF THE STANDARD DEVIATION OF SLOPE
C          B = LEAST SQUARES ESTIMATE OF THE Y INTERCEPT
C          SB = ESTIMATE OF THE STANDARD DEVIATION OF B
C
C     THEORY TAKEN FROM ELEMENTS OF STATISTICAL INFERENCE BY
C     DAVID V HUNSTBERGER (PUB BY ALLYN AND BACON, 1967) ON
C     PAGES 255 TO 263.
C
      DIMENSION X(N),Y(N)
      IF (N.LT.3) GO TO 6
      XN=N
      XN2=XN-2.0
      SUMX=0.0
      SUMX2=0.0
      SUMY=0.0
      SUMY2=0.0
      SUMXY=0.0
          DO 1 I=1,N
          SUMX=SUMX+X(I)
          SUMX2=SUMX2+X(I)*X(I)
          SUMY=SUMY+Y(I)
          SUMY2=SUMY2+Y(I)*Y(I)
    1     SUMXY=SUMXY+X(I)*Y(I)
      SXY=SUMXY-SUMX*SUMY/XN
      SX2=SUMX2-SUMX*SUMX/XN
      SY2=SUMY2-SUMY*SUMY/XN
      S=SXY/SX2
      SD=(SY2-S*SXY)/(SX2*XN2)
      B=(SUMY-S*SUMX)/XN
      BD=(SD*SX2+SD*SUMX*SUMX/XN)/XN
      SD=SQRT(SD)
      BD=SQRT(BD)
      RETURN
    6 WRITE (6,7)
    7 FORMAT ('1 SUBROUTINE SLOPE REQUIRES N GREATER THAN 2')
      STOP 7
      END
```

```
C
C     LOGSMOOTH1 WRITTEN BY DAVE GANLEY JULY 5, 1977.
C
C     THIS PROGRAM WAS WRITTEN TO SMOOTH WELL LOGS AND TO
C     ALLOW FOR THE CORRECTION OF THE RAW LOGS BASED ON
C     INTEGRATED MEASUREMENTS  (IE CHECK SHOTS FOR A
C     VELOCITY LOG).  THIS CORRECTION IS MADE PRIOR TO
C     SMOOTHING.
C
C     INPUT FILES:
C        1 IS THE RAW LOG (SEQUENTIAL FILE)
C        2 IS THE INTEGRATED CORRECTION VALUES
C     OUTPUT FILES
C        3 IS THE SMOOTHED LOG (SEQUENTIAL)
C        4 CCNTAINS LAYER THICKNESSES AND LOG VALUES OF
C          SMOOTHED LOG
C        8 IS THE ADJUSTED LCG FRCM INTEGRATED VALUES
C          (SEQUENTIAL)
C        9 IS THE FILTERED ADJUSTED LOG (SEQUENTIAL)
C
C
C     SUBROUTINES CALLED:
C        1. LCPASS
C
      DIMENSION XLOG(12001),XLINT(240),IDEPI(240),XLOGI(240)
      READ (5,1) N,IDS,DCUT,XP
      IF (N.GT.12000) GO TO 91
    1 FORMAT (2I5,2F5.0)
C****
C     N = NUMBER OF INPUT LOG VALUES
C     IDS = DEPTH OF FIRST LOG VALUE
C     DCUT = A GIVEN LAYER THICKNESS IN FEET WHICH SPECIFIES
C            THE CUTOFF THICKNESS FOR A LOW PASS FILTER.
C            LAYERS THINNER THAN DCUT WILL BE FILTERED OUT.
C          = 0.0 PERFORM NO FILTERING
C     XP = PERCENT CHANGE IN XLCG THAT IS RECOGNIZED AS A
C          A NEW LAYER
C****
      READ (1) (XLOG(I),I=1,N)
C****
C     XLOG = LOG VALUES EVERY FOOT FROM IDS TO THE BOTTOM OF
C            LOG.  A MAXIMUM OF 12000 VALUES ARE ALLOWED.
C            THE LOG VALUE APPLIES TO PRECEDING FOOT.
C****
      WRITE (6,2) N,IDS,DCUT,XP
    2 FORMAT ('1',I5,' LOG VALUES READ FROM A START DEPTH OF'
     .,I5,/' CUTOFF THICKNESS = ',F5.2,/' PER CENT CHANGE = '
     .,F5.2)
      XP=XP/100.0
         DO 15 I=1,240
         NI=I
   15    READ (2,8,END=20) IDEPI(I),XLOGI(I)
    8 FORMAT (I5,F10.0)
C****
```

```
C       IDEPI,XLOGI = INTEGRATED VALUE OF XLOG TO A DEPTH OF
C                     IDEPI STARTING FROM THE TOP OF THE LOG.
C                     A MAXIMUM OF 240 VALUES ARE ALLOWED.
C****
      NI=240
      GO TO 21
   20 NI=NI-1
      IF (NI.EQ.0) GO TO 30
C
C     ADJUST LOG BASED ON INPUT INTEGRATED LOG VALUES
C
   21 WRITE (6,3) NI
    3 FORMAT ('-',I3,' INTEGRATED VALUES OF LOG READ')
      XI=0.0
      XLI=0.0
      J=0
      JL=1
      IDI=IDS-1
          DO 29 I=1,NI
          XLOGI(I)=XLOGI(I)-XLI
   23     IDI=IDI+1
          J=J+1
          XI=XI+XLOG(J)
          IF (IDEPI(I).EQ.IDI) GO TO 25
          GO TO 23
   25     XFACT=(XLOGI(I)-XI)/(J-JL+1)
              DO 27 K=JL,J
   27         XLOG(K)=XLOG(K)+XFACT
          XLI=XLOGI(I)+XLI
          JL=J+1
          XI=0.0
   29     WRITE (6,4) IDEPI(I),XFACT
    4 FORMAT ('OCORRECTION FACTOR TO A DEPTH OF ',I5,' IS '
     .,F10.6)
      WRITE (8) (XLOG(I),I=1,N)
C
C     INTEGRATE LOG IN 50 FOOT INTERVALS PRIOR TO FILTERING
C
   30 IF (DCUT.EQ.0.0) GO TO 50
      LE=50
      J=1
          DO 39 I=1,N,50
          IF ((J+49).GT.N) LE=N-J+1
          K=1+I/50
          XLINT(K)=0.0
              DO 35 L=1,LE
              XLINT(K)=XLINT(K)+XLOG(J)
   35         J=J+1
   39     CONTINUE
C
C     FILTER LOG
C
      DFCUT=.5/DCUT
      CALL LOPASS(DFCUT,1000.0,1,XLOG,N)
```

```
C
C     ADJUST LOG AFTER FILTERING TO AGREE WITH INTEGRATIONS
C     OVER 50 FOOT INTERVALS MADE BEFORE FILTERING
C
      WRITE (6,10)
   10 FORMAT ('1')
      LE=50
      J=1
         DO 49 I=1,N,50
         IF ((J+49).GT.N) LE=N-J+1
         K=1+I/50
         XI=0.0
            DO 43 L=1,LE
            XI=XI+XLOG(J)
   43       J=J+1
         XFACT=XLINT(K)/XI
         ID=J+IDS-2
         WRITE (6,4) ID,XFACT
         J=J-LE
            DO 47 L=1,LE
            XLOG(J) =XLOG(J)*XFACT
   47       J=J+1
   49    CONTINUE
      WRITE (9) (XLOG(I),I=1,N)
C
C     BLOCK LOG INTO LAYERS
C
   50 WRITE (6,10)
      XI=0.0
      IDI=0
      IS=1
      ID=IDS-1
      XLOG(N+1)=XLOG(N)
      IDIL=0
      XIL=0.0
      XAL=0.0
         DO 59 I=1,N
         XI=XI+XLOG(I)
         IDI=IDI+1
         XA=XI/IDI
         XT=ABS(XLOG(I+1)-XA)
         IF (XT/XA.LT.XP) GO TO 59
         XT=ABS(XA-XAL)
         IF (XT.GE.XP*XAL) GO TO 53
         IDIL=IDI+IDIL
         XIL=XIL+XI
         XAL=XIL/IDIL
         IDI=0
         XI=0.0
         GO TO 59
   53    IE=I-IDI
         IF (IE.EQ.0) GO TO 57
            DO 55 J=IS,IE
   55       XLOG(J)=XAL
```

```
         WRITE (6,5) ID,IDIL,XAL
    5    FORMAT (' DEPTH TO TOP = ',I5,' THICKNESS = ',I5,
     .   ' LOG VALUE = ',F12.6)
         WRITE (4,6) IDIL,XAL
    6    FORMAT (I5,F10.4)
   57    ID=ID+IDIL
         IS=IS+IDIL
         IDIL=IDI
         XIL=XI
         XAL=XA
         IDI=0
         XI=0.0
   59    CONTINUE
      XT=ABS(XA-XAS)
      IF (XT.GE.XP*XAS) GO TO 61
      IDI=IDI+IDIL
      XI=XI+XIL
      XA=XI/IDI
      GO TO 65
   61 IE=I-IDI
         DO 63 J=IS,IE
   63    XLOG(J)=XAL
      WRITE (6,5) ID,IDIL,XAL
      WRITE (4,6) IDIL,XAL
      IS=IS+IDIL
      ID=ID+IDIL
   65 IE=I-1
         DO 67 J=IS,IE
   67    XLOG(J)=XA
      WRITE (6,5) ID,IDI,XA
      WRITE (4,6) IDI,XA
      WRITE (3) (XLOG(I),I=1,N)
      WRITE (6,7)
    7 FORMAT ('-SMOOTHED LOG WRITTEN TO OUTPUT FILE')
      GO TO 99
   91 WRITE (6,92)
   92 FORMAT ('1 A MAXIMUM OF 12000 LOG VALUES IS ALLOWED')
   99 STOP
      END
      SUBROUTINE LOPASS(FC,DELT,IG,X,N)
C
C           SUBROUTINE BY DAVE GANLEY ON JULY 4, 1977.
C
C           THE PURPOSE OF THIS SUBROUTINE IS TO DESIGN AND
C     APPLY A RECURSIVE BUTTERWORTH LOW PASS FILTER
C     (KANASEWICH, TIME SERIES ANALYSIS IN GEOPHYSICS,
C     UNIVERSITY OF ALBERTA PRESS, 1975; SHANKS, JOHN L.,
C     RECURSION FILTERS FOR DIGITAL PROCESSING, GEOPHYSICS,
C     VOL 32, PP 33-51,, 1967).
C
C           THE FILTER WILL HAVE 8 POLES IN THE S PLANE AND
C     IS APPLIED IN FORWARD AND REVERSE DIRECTIONS SO AS
C     TO HAVE ZERO PHASE SHIFT.  THE GAIN AT CUTOFF
C     FREQUENCY WILL BE -6 DB AND THE ROLLOFF WILL BE ABOUT
C     96 DB PER OCTAVE.  A BILINEAR Z TRANSFORM IS USED
C     IN DESIGNING THE FILTER TO PREVENT ALIASING PROBLEMS.
C
      COMPLEX P(8),S(8)
      DIMENSION D(8),X(1),XC(3),XD(3),XE(3)
      DATA FCOLD/0.0/,TWOPI/6.2831853/
C
C     THIS SECTION CALCULATES THE FILTER AND WILL BE SKIPPED
C     IF FC IS THE SAME AS IT WAS ON THE PREVIOUS CALL.
C
C        FC = CUTOFF FREQUENCY (6 DB DOWN)
C        DELT = SAMPLE INTERVAL IN MILLISECONDS
C        IG = 1 MEANS TO REMOVE THE FILTER GAIN SO
C             THAT THE GAIN IS UNITY
C        X = DATA VECTOR TO BE FILTERED
C        N = LENGTH OF X
C
      IF (FC.EQ.FCOLD) GO TO 31
      FCOLD=FC
      WRITE (6,1) FC,DELT
    1 FORMAT ('1 LOW PASS FILTER DESIGN FOR A CUTOFF ',
     .'FREQUENCY OF ',F8.3,' HERTZ.',//' SAMPLE INTERVAL IS '
     .,F5.2,' MILLISECONDS.')
      DT=DELT/1000.0
      TDT=2.0/DT
      FDT=4.0/DT
      FDT2=TDT*TDT
      P(1)=CMPLX(-.19509032,.98078528)
      P(2)=CMPLX(-.19509032,-.98078528)
      P(3)=CMPLX(-.55557023,.83146961)
      P(4)=CMPLX(-.55557023,-.83146961)
      P(5)=CMPLX(-.83146961,.55557023)
      P(6)=CMPLX(-.83146961,-.55557023)
      P(7)=CMPLX(-.98078528,.19509032)
      P(8)=CMPLX(-.98078528,-.19509032)
      WC=TWOPI*FC
      WC=TDT*TAN(WC/TDT)
      DO 19 I=1,8
   19 S(I)=P(I)*WC
```

```
      WRITE (6,2) S
    2 FORMAT ('-S PLANE POLES ARE AT:',/' ',8(/' ',E12.6,
     .' + I ',E12.6))
      G=1.0/WC
      G=G*G
      G=G*G
      G=G*G
      DO 29 I=1,7,2
      T1=REAL(S(I))
      T2=AIMAG(S(I))
      T2=T1*T1+T2*T2
      A=FDT2+T2-T1*FDT
      D(I)=(T2-FDT2)*2.0/A
      D(I+1)=(FDT2+T2+T1*FDT)/A
   29 G=G*A
      G=G*G
      WRITE (6,3)
    3 FORMAT ('-FILTER IS (1+Z)**8 / B1*B2*B3*B4')
      WRITE (6,4) D
    4 FORMAT (4(/' B(I) = 1 + ',E12.6,' Z + ',E12.6,' Z**2'))
      WRITE (6,5) G
    5 FORMAT ('-FILTER GAIN IS ',E12.6)
      IF (IG.EQ.1) WRITE (6,6)
    6 FORMAT ('-FILTER GAIN IS REMOVED TO GIVE UNITY GAIN')
C
C     APPLY FILTER IN FORWARD DIRECTION
C
   31 XM2=X(1)
      XM1=X(2)
      XM=X(3)
      XC(1)=XM2
      XC(2)=XM1+2.0*XM2-D(1)*XC(1)
      XC(3)=XM+2.0*XM1+XM2-D(1)*XC(2)-D(2)*XC(1)
      XD(1)=XC(1)
      XD(2)=XC(2)+2.0*XC(1)-D(3)*XD(1)
      XD(3)=XC(3)+2.0*XC(2)+XC(1)-D(3)*XD(2)-D(4)*XD(1)
      XE(1)=XD(1)
      XE(2)=XD(2)+2.0*XD(1)-D(5)*XE(1)
      XE(3)=XD(3)+2.0*XD(2)+XD(1)-D(5)*XE(2)-D(6)*XE(1)
      X(1)=XE(1)
      X(2)=XE(2)+2.0*XE(1)-D(7)*X(1)
      X(3)=XE(3)+2.0*XE(2)+XE(1)-D(7)*X(2)-D(8)*X(1)
      DO 39 I=4,N
      XM2=XM1
      XM1=XM
      XM=X(I)
      K=I-((I-1)/3)*3
      GO TO (34,35,36),K
   34 M=1
      M1=3
      M2=2
      GO TO 37
   35 M=2
      M1=1
      M2=3
      GO TO 37
   36 M=3
      M1=2
      M2=1
   37 XC(M)=XM+2.0*XM1+XM2-D(1)*XC(M1)-D(2)*XC(M2)
      XD(M)=XC(M)+2.0*XC(M1)+XC(M2)-D(3)*XD(M1)-D(4)*XD(M2)
      XE(M)=XD(M)+2.0*XD(M1)+XD(M2)-D(5)*XE(M1)-D(6)*XE(M2)
   39 X(I)=XE(M)+2.0*XE(M1)+XE(M2)-D(7)*X(I-1)-D(8)*X(I-2)
C
C     FILTER IN REVERSE DIRECTION
C
      XM2=X(N)
      XM1=X(N-1)
      XM=X(N-2)
      XC(1)=XM2
      XC(2)=XM1+2.0*XM2-D(1)*XC(1)
      XC(3)=XM+2.0*XM1+XM2-D(1)*XC(2)-D(2)*XC(1)
      XD(1)=XC(1)
      XD(2)=XC(2)+2.0*XC(1)-D(3)*XD(1)
      XD(3)=XC(3)+2.0*XC(2)+XC(1)-D(3)*XD(2)-D(4)*XD(1)
      XE(1)=XD(1)
      XE(2)=XD(2)+2.0*XD(1)-D(5)*XE(1)
      XE(3)=XD(3)+2.0*XD(2)+XD(1)-D(5)*XE(2)-D(6)*XE(1)
      X(N)=XE(1)
      X(N-1)=XE(2)+2.0*XE(1)-D(7)*X(N)
      X(N-2)=XE(3)+2.0*XE(2)+XE(1)-D(7)*X(N-1)-D(8)*X(N)
      DO 49 I=4,N
      XM2=XM1
      XM1=XM
      J=N-I+1
      XM=X(J)
      K=I-((I-1)/3)*3
      GO TO (44,45,46),K
   44 M=1
      M1=3
      M2=2
      GO TO 47
   45 M=2
      M1=1
      M2=3
      GO TO 47
   46 M=3
      M1=2
      M2=1
   47 XC(M)=XM+2.0*XM1+XM2-D(1)*XC(M1)-D(2)*XC(M2)
      XD(M)=XC(M)+2.0*XC(M1)+XC(M2)-D(3)*XD(M1)-D(4)*XD(M2)
      XE(M)=XD(M)+2.0*XD(M1)+XD(M2)-D(5)*XE(M1)-D(6)*XE(M2)
   49 X(J)=XE(M)+2.0*XE(M1)+XE(M2)-D(7)*X(J+1)-D(8)*X(J+2)
      IF (IG.NE.1) RETURN
      DC 59 I=1,N
   59 X(I)=X(I)/G
      RETURN
      END
```

```
C
C     LOGSMOOTH2 BY DAVE GANLEY ON AUGUST 16, 1977.
C
C     THIS PROGRAM IS MEANT TO BE USED WITH LOGSMOOTH1.
C     LOGSMOOTH1 WILL PRODUCE A SMOOTHED LOG AND THIS
C     PROGRAM WILL ELIMINATE THIN LAYERS IN A ZONE OF
C     MONOTONIC CHANGE IN LOG VALUE.  THIS IS DONE BY
C     AVERAGING THESE THIN LAYERS INTO ADJACENT LAYERS.
C
      DIMENSION X(1200),ID(1200),Y(1200),JD(1200)
      READ (5,1) IDC,XP,IDS
C****
C     IDC = CRITICAL THICKNESS.  LAYERS OF THIS THICKNESS
C           OR LESS ARE ELIMINATED IN A ZONE OF MONOTONIC
C           CHANGE IN LOG VALUE.
C     XP = PER CENT CHANGE BETWEEN LAYERS THAT WAS USED IN
C          BLOCKING THE LOG ORIGINALLY.  CHANGES IN LOG
C          VALUE LESS THAN THIS PER CENT WERE NOT RECOGNIZED
C          AS DIFFERENT LAYERS
C     IDS = START DEPTH OF LOG
C****
    1 FORMAT (I5,F5.0,I5)
      WRITE (6,5) IDC,XP
    5 FORMAT ('ID = ',I5,' PER CENT = ',F7.1,//)
      XP=XP/100.0
      IDC2=2*IDC
         DO 9 I=1,1201
         NI=I
         READ (1,2,END=10) ID(I),X(I)
C****
C     ID = LAYER THICKNESS FOR BLOCKED LOG PRODUCED BY
C          LOGSMOOTH1
C     X = LOG VALUE FOR LAYER OF THICKNESS ID
C****
    9    CONTINUE
    2 FORMAT (I5,F10.3)
      WRITE (6,3)
    3 FORMAT ('1 LOGSMOOTH2 CAN ONLY HANDLE 1200 LAYERS')
      STOP
   10 N=NI-1
      J=1
      I=0
   39    I=I+1
         IF (I.GT.N) GO TO 40
   11    IF (ID(I).LE.IDC) GO TO 13
   12    Y(J)=X(I)
         JD(J)=ID(I)
         J=J+1
         GO TO 39
   13    IF (I.EQ.1.OR.I.EQ.N) GO TO 12
         XS=X(I)-X(I-1)
         IF (XS*(X(I+1)-X(I)).LT.0.0) GO TO 12
         IDI=ID(I)
         XI=X(I)*ID(I)
```

```
          K=I+1
 15          IF (ID(K).GT.IDC) GO TO 17
             IF (IDI+ID(K).GT.IDC2) GO TO 17
             XST=X(K)-X(K-1)
             IF (XS*XST.LT.0.0) GO TO 17
             XI=XI+X(K)*ID(K)
             IDI=IDI+ID(K)
             K=K+1
             IF (K.GT.N) GO TO 17
             GO TO 15
 17       XA=XI/IDI
          XT=XA-Y(J-1)
          IF (XT.LT.0.0) GO TO 21
          XT=XT/XA
          GO TO 23
 21       XT=-XT/Y(J-1)
 23       IF (XT.GT.XP) GO TO 25
          Y(J-1)=(Y(J-1)*JD(J-1)+XA*IDI)/(IDI+JD(J-1))
          JD(J-1)=JD(J-1)+IDI
          GO TO 38
 25       IF (K.GT.N) GO TO 37
          XT=XA-X(K)
          IF (XT.LT.0.0) GO TO 27
          XT=XT/XA
          GO TO 29
 27       XT=-XT/X(K)
 29       IF (XT.GT.XP) GO TO 31
          X(K)=(X(K)*ID(K)+XA*IDI)/(IDI+ID(K))
          ID(K)=ID(K)+IDI
          GO TO 38
 31       IDI2=IDI/2
          Y(J-1)=(Y(J-1)*JD(J-1)+XA*IDI2)/(IDI2+JD(J-1))
          JD(J-1)=JD(J-1)+IDI2
          X(K)=(X(K)*ID(K)+XA*IDI2)/(IDI2+ID(K))
          ID(K)=ID(K)+IDI2
          IF (IDI.EQ.2*IDI2) GC TO 38
 34       IF (AES(XA-X(K)).GT.ABS(XA-Y(J-1))) GO TO 35
          X(K)=(X(K)*ID(K)+XA)/(1.0+ID(K))
          ID(K)=ID(K)+1
          GO TO 38
 35       Y(J-1)=(Y(J-1)*JD(J-1)+XA)/(1.0+JD(J-1))
          JD(J-1)=JD(J-1)+1
          GO TO 38
 37       Y(J)=XI/IDI
          JD(J)=IDI
          J=J+1
 38       I=K-1
          GC TO 39
 40   IDS=IDS-1
      J=J-1
          DO 49 I=1,J
          WRITE (2,2) JD(I),Y(I)
          WRITE (6,4) IDS,JD(I),Y(I)
          IDS=IDS+JD(I)
 49       CONTINUE
```

```
49    CONTINUE
 4 FORMAT (' DEPTH TO TOP = ',I5,' THICKNESS = ',I5,
  .' LOG VALUE = ',F12.6)
   STOP
   END
```

44733

National Library of Canada
Canadian Theses Division
Ottawa, Canada
K1A 0N4

Bibliothèque nationale du Canada
Division des thèses canadiennes

PERMISSION TO MICROFILM — AUTORISATION DE MICROFILMER

- Please print or type — Écrire en lettres moulées ou dactylographier

Full Name of Author — Nom complet de l'auteur

DAVID CHARLES GANLEY

Date of Birth — Date de naissance Dec. 7, 1949	Country of Birth — Lieu de naissance Canada

Permanent Address — Résidence fixe

40 Silverdale Crescent N.W
Calgary, Alberta
T3B 3P2

Title of Thesis — Titre de la thèse

The Seismic Measurement of Absorption and Dispersion.

University — Université

University of Alberta

Degree for which thesis was presented — Grade pour lequel cette thèse fut présentée

Ph. D.

Year this degree conferred — Année d'obtention de ce grade 1980	Name of Supervisor — Nom du directeur de thèse Dr E. R. Kanasewich

Permission is hereby granted to the NATIONAL LIBRARY OF CANADA to microfilm this thesis and to lend or sell copies of the film.

The author reserves other publication rights, and neither the thesis nor extensive extracts from it may be printed or otherwise reproduced without the author's written permission.

L'autorisation est, par la présente, accordée à la BIBLIOTHÈQUE NATIONALE DU CANADA de microfilmer cette thèse et de prêter ou de vendre des exemplaires du film.

L'auteur se réserve les autres droits de publication; ni la thèse ni de longs extraits de celle-ci ne doivent être imprimés ou autrement reproduits sans l'autorisation écrite de l'auteur.

Date June 9, 1980	Signature D C Ganley

NL-91 (4/77)

National Library of Canada
Collections Development Branch

Canadian Theses on
Microfiche Service

Bibliothèque nationale du Canada
Direction du développement des collections

Service des thèses canadiennes
sur microfiche

NOTICE

The quality of this microfiche is heavily dependent upon the quality of the original thesis submitted for microfilming. Every effort has been made to ensure the highest quality of reproduction possible.

If pages are missing, contact the university which granted the degree.

Some pages may have indistinct print especially if the original pages were typed with a poor typewriter ribbon or if the university sent us a poor photocopy.

Previously copyrighted materials (journal articles, published tests, etc.) are not filmed.

Reproduction in full or in part of this film is governed by the Canadian Copyright Act, R.S.C. 1970, c. C-30. Please read the authorization forms which accompany this thesis.

THIS DISSERTATION
HAS BEEN MICROFILMED
EXACTLY AS RECEIVED

AVIS

La qualité de cette microfiche dépend grandement de la qualité de la thèse soumise au microfilmage. Nous avons tout fait pour assurer une qualité supérieure de reproduction.

S'il manque des pages, veuillez communiquer avec l'université qui a conféré le grade.

La qualité d'impression de certaines pages peut laisser à désirer, surtout si les pages originales ont été dactylographiées à l'aide d'un ruban usé ou si l'université nous a fait parvenir une photocopie de mauvaise qualité.

Les documents qui font déjà l'objet d'un droit d'auteur (articles de revue, examens publiés, etc.) ne sont pas microfilmés.

La reproduction, même partielle, de ce microfilm est soumise à la Loi canadienne sur le droit d'auteur, SRC 1970, c. C-30. Veuillez prendre connaissance des formules d'autorisation qui accompagnent cette thèse.

LA THÈSE A ÉTÉ
MICROFILMÉE TELLE QUE
NOUS L'AVONS REÇUE

Ottawa, Canada
K1A 0N4

NL-339 (Rev. 8/80)

THE UNIVERSITY OF ALBERTA

THE SEISMIC MEASUREMENT OF ABSORPTION AND DISPERSION

by

© DAVID CHARLES GANLEY

A THESIS

SUBMITTED TO THE FACULTY OF GRADUATE STUDIES AND RESEARCH

IN PARTIAL FULFILMENT OF THE REQUIREMENTS FOR THE DEGREE

OF DOCTOR OF PHILOSOPHY

IN

PHYSICS

DEPARTMENT OF PHYSICS

EDMONTON, ALBERTA

SPRING, 1980

THE UNIVERSITY OF ALBERTA

FACULTY OF GRADUATE STUDIES AND RESEARCH

The undersigned certify that they have read, and recommend to the Faculty of Graduate Studies and Research, for acceptance, a thesis entitled THE SEISMIC MEASUREMENT OF ABSORPTION AND DISPERSION submitted by DAVID CHARLES GANLEY in partial fulfilment of the requirements for the degree of DOCTOR OF PHILOSOPHY in PHYSICS.

E. R. Kanasewich
Supervisor

L. W. Jackson

G. L. Cumming

A. B. Bhatia

Don L. Anderson
External Examiner

Date Nov 8, 1979

DEDICATION

This thesis is dedicated to Kathleen Teresa Ganley.

ABSTRACT

The absorption and dispersion of seismic waves has been examined theoretically and by measurements on seismic check shot data. A matrix method which includes the effects of absorption and dispersion has been described for calculating plane wave synthetic seismograms at vertical incidence. Non-vertical incidence, curved wave synthetic seismograms which include the effects of absorption and dispersion have been calculated using modifications to existing ray theory. The effect of multiples on seismograms has been briefly examined. The spectral ratio method for measuring absorption and dispersion has been described and studies of various spectral estimation techniques have been carried out. A correction term to remove the effects of interfering reflections has been shown to be necessary and has been included as part of the spectral ratio method. A model study of the feasability of measuring absorption and dispersion from seismic check shot surveys indicates that it should be possible to make these measurements reliably over intervals of the order of 300 meters in thickness. Actual check shot data has been examined and supports the conclusion that the absorption coefficient is a linear function of frequency. This data exhibited dispersion which is consistent with this conclusion. Measured Q values on this data were 42±2 for the depth interval 549 to 1193 meters and 67±6 for the interval 945 to 1311 meters.

ACKNOWLEDGEMENTS

I would like to thank my supervisor, Dr. E. R. Kanasewich for his encouragement and quidance during the course of this study.

I would also like to thank Esso Resources Ltd. who provided the check shot data and well logs from northern Canada and Union Oil Company of Canada Ltd. who provided well logs and seismic data in Alberta.

Financial support for various parts of this research was supplied by grants from the Natural Sciences and Engineering Research Council of Canada and Imperial Oil Ltd.

The author was partially supported by an Izaak Walton Killam Memorial Scholarship and a University of Alberta Graduate Teaching Assistantship. The plane wave synthetic seismogram program was written while the author was employed at the Amoco Production Research Center in Tulsa, Oklahoma. He wishes to thank Amoco Production Company for permission to include it as part of his thesis and for financial support through a consulting agreement.

I also wish to acknowledge the patience and understanding of my wife, Maureen, during my studies.

Table of Contents

Chapter Page

1. INTRODUCTION.......................................1

1.1 General Remarks...................................1

1.2 Experimental Measurements of Q....................2

1.3 Absorption Models................................24

1.4 Absorption Mechanisms............................39

2. SYNTHETIC SEISMOGRAMS.............................49

2.1 Plane Waves at Vertical Incidence Including Absorption.......................................49

2.2 Synthetic Seismograms Without Absorption by Ray Methods..72

2.3 Synthetic Seismograms With Absorption by Ray Methods..90

3. THE SPECTRAL RATIO METHOD........................124

3.1 Introduction.....................................124

3.2 MA Spectral Estimation...........................126

3.3 AR Spectral Estimates............................137

3.4 ARMA Spectral Estimates..........................142

3.5 Effect of Reflections on the Spectral Ratio Method...144

4. MEASUREMENT OF ABSORPTION AND DISPERSION FROM CHECK-SHOT SURVEYS.................................159

4.1 Model Study......................................159

4.2 Application to real data.........................180

5. CONCLUSIONS AND DISCUSSION.......................188

BIBLIOGRAPHY...191

APPENDIX A: LISTINGS OF PROGRAMS.....................207

LIST OF TABLES

Table Page

1.1 Summary of Experimental Measurements of Q.........23

1.2 References for Table 1.1..........................25

2.1 Partitions of N for N= 1 to 8.....................76

2.2 Comparison of required storage locations for the methods of Hron (1972) and Churney (1977)..79

2.3 Comparison of CPU times and number of phases for 20 layer model.................................88

2.4 Values of |A(g)|cos(g)/|A(0)|.....................100

2.5 17 layer model near Fox Creek, Alberta...........114

2.6 Frequency dependence of ray parameter, spreading and dispersion approximation...........115

2.7 Accuracy of single frequency approximation.......117

2.8 Accuracy of two frequency approximation..........119

4.1 Q values and phase velocities for noise-free model measured over large interval spacing.......172

4.2 Q values and phase velocities for noise-free model measured over small interval spacing.......174

4.3 Q values and phase velocities for noise-free model calculated without the correction for the effect of other reflections.....................175

4.4 Q values for noise-free model obtained by attempting to use least-squares procedure to inrease resolution..................................177

4.5 Q values and phase velocities for noise-added model measured over large interval spacing...............................178

4.6 Q values and phase velocities for noise-added model measured over small interval spacing....................................179

LIST OF FIGURES

Figure Page

2.1 The reflection and transmission at a boundary....53

2.2 The relationship of waves at the top and bottom of a layer....57

2.3 The relationship of upgoing and downgoing waves at an interface....58

2.4 The reflection and transmission of layers between the source and surface as viewed from the surface....68

2.5 The reflection and transmission of layers between the source and surface as viewed from the source....69

2.6 Illustration of ray codes....75

2.7 Flow chart of ray code generation scheme using permuted partitions....80

2.8 20 layer velocity-depth model near Edmonton, Alberta....83

2.9 Comparison of synthetic seismograms for 20 layer model....85

2.10 35 Hz damped sine wave wavelet....87

2.11 Primaries only synthetics for the model near Edmonton, Alberta....89

2.12 Primaries plus surface multiples synthetics for the model near Edmonton, Alberta....91

2.13 Non-vertical reflection and transmission of P waves....95

2.14 Reflection coefficient P1P1....107

2.15 Reflection coefficient P2P2....108

2.16 Reflection coefficient P1S1......................109

2.17 Transmission coefficient P1P2....................110

2.18 Transmission coefficient P2P1....................111

2.19 Comparison of 3 ray methods for including absorption in synthetic seismograms..............121

2.20 Comparison of synthetic seismograms with and without absorption................................122

3.1 Traces used in testing spectral ratio method..129

3.2 Smoothed Fourier spectral ratio plot and dispersion curve for noise-free test example...131

3.3 Unsmoothed Fourier spectral ratio plot and dispersion curve for noise-free test example...133

3.4 Smoothed Fourier spectral ratio plot and dispersion curve for noise-added test example...134

3.5 Unsmoothed Fourier spectral ratio plot and dispersion curve for noise-added test example...135

3.6 Amplitude and phase smoothed Fourier spectral ratio plot and dispersion curve for noise-added test example.........................136

3.7 MEM spectral ratio plots for noise-free and noise-added test examples..........................141

3.8 MLM spectral ratio plots for noise-free and noise-added test examples..........................143

3.9 Simple model used in illustrating the correction for reflections and multiples.........150

3.10 Synthetic traces with and without absorption for model in the figure 3.9......................151

3.11 Uncorrected spectral ratio and dispersion curve for the synthetic traces at 285 and 615 meters...153

3.12 Corrected spectral ratio and dispersion curve for the synthetic traces at 285 and 615 meters...154

3.13 Uncorrected spectral ratio and dispersion curve for the synthetic traces at 585 and 615 meters....155

3.14 Corrected spectral ratio and dispersion curve for the synthetic traces at 585 and 615 meters....156

4.1 263 layer velocity model from a well in northern Canada....160

4.2 263 layer density model from a well in northern Canada....161

4.3 263 layer Q model for check shot model study....162

4.4 Synthetic check shot survey for model in figures 4.1 to 4.3....164

4.5 Synthetic check shot survey without including the effects of absorption and dispersion....165

4.6 Synthetic check shot data from figure 4.4 with 10% random noise added....166

4.7 Actual check shot data from a well in a sedimentary basin in northern Canada....182

4.8 Log spectral ratio plot for the depth interval 945 to 1311 meters....183

4.9 Measured dispersion curve for the depth interval 945 to 1311 meters....184

4.10 Log spectral ratio plot for the depth interval 549 to 1193 meters....186

4.11 Measured dispersion curve for the depth interval 549 to 1193 meters....187

1. INTRODUCTION

1.1 General Remarks

The attenuation model which will be used in this thesis is the familiar one of exponential decay as a function of distance which is described by the equation

$$A(r) = A(0)\exp(-ar) \qquad (1.1)$$

where A(r) is the amplitude at a distance r from the source and A(0) is the source amplitude. The spatial attenuation factor is exp(-ar) and "a" is the absorption coefficient which is written as

$$a = w/2cQ \qquad (1.2)$$

where w is the angular frequency, c is the phase velocity and Q is the specific attenuation factor or quality factor. This is sometimes defined as

$$\frac{2\pi}{Q} = \frac{\Delta E}{E} \qquad (1.3)$$

where ΔE is the amount of energy dissipated per cycle for a harmonic wave and E is the peak elastic energy in a cycle of the harmonic wave. Strictly speaking equations 1.2 and 1.3 are not exact but are expressions which are valid for large Q (Zener, 1948, pages 62-63). The quantity π/Q is referred to as the logarithmic decrement.

Until now the nature of the frequency dependence of the phase velocity c or of the quality factor Q has not been specified. A discussion of this topic will occur in later sections of this chapter; however, for the time being it is assumed that the absorption coefficient "a" will be treated as a linear function of frequency.

This thesis outlines a method for calculating synthetic seismograms which include the effects of absorption and dispersion. Synthetic seismograms will be used for the purpose of a model study on the measurement of absorption. The method which will be used to measure the absorption will be the spectral ratio method and in examining this method various methods of spectral estimation will be rewieved. An examination will be made of corrections which should be applied to the data with this method and a study will be made of the effect of random noise on the results. The model study will be concluded by outlining a procedure for measuring Q from real data and this will be applied to a limited amount of real data.

1.2 Experimental Measurements of Q

In this section a review is made of the literature on measurements of Q for rocks with particular attention being given to information on the frequency dependence of Q. This review will omit the Q measurements for the earth from earthquake records or normal mode data although the literature in this area is quite extensive. Those measurements are at low frequencies and often a linear frequency dependence of the absorption coefficient is assumed in order to infer the depth variation of Q. Most of the measurements have been made in the laboratory on rock samples although some field measurements have been made.

Birch and Bancroft (1938) measured the elastic coefficients and Q of a cylindrical block of Quincy granite 244 cm long and 23 cm in diameter at room temperature and pressure using a resonance technique. In this method the sample, usually rod-shaped, is caused to vibrate by an oscillatory force and the amplitude of vibration is measured. If the frequency of the oscillatory force is varied and its amplitude held constant, then the amplitude of vibration of the sample is found to trace out a resonance curve. If df is the width of the resonance curve when the amplitude of vibration equals .707 times the amplitude at the peak frequency f, then 1/Q = df/f. The Q measured in this manner is the Q associated with a particular type of vibration. In the case of longitudinal vibration the Q is that which is associated with Young's modulus while in the case of torsional resonance the Q is associated with the shear modulus. Details of this method are given by Zener (1937) or by White (1965). Birch and Bancroft used longitudinal, torsional and flexural resonances and concluded that Q of Quincy granite was approximately independent of frequency in the frequency range 140 to 1600 Hz.

Born (1941) used a longitudinal resonance technique to measure the logarithmic decrement on several rock types taken from quarry sites and from cores taken from wells. He found that the logarithmic decrement for the dry rock samples was independent of frequency. He also studied the effects of water saturation and concluded that for water saturated samples the total decrement was the sum of a frequency independent term and a term which was proportional to frequency. The latter term was attributed to viscous losses.

Ricker (1953) reported on field experiments made to test the validity of his "Wavelet Theory of Seismogram Structure". This theory uses a modified wave equation containing a term with a first derivative with respect to time to provide damping. Ricker attributed this equation to Stokes in 1845. This type of model is sometimes referred to as a Kelvin-Voigt solid. It is a model in which stress is a linear function of both strain and strain rate and leads to an absorption coefficient "a" which is proportional to the square of frequency or a Q which varies inversely as frequency. One of the predictions of Ricker's theory is that the wavelet breadth will increase as the square root of travel time. Ricker conducted experiments in which shots were fired at several offset distances from a hole containing geophones at depths of 422, 622 and 822 feet (129, 190 and 251 meters). These experiments were carried out in the Pierre shale near Limon, Colorado. This shale, which is of Cretaceous age, was chosen because it provided a thick section of very uniform material at or very near to the earth's surface. Ricker presented a graph of 46 points on a log-log plot of wavelet breadth versus travel time which shows a least squares slope of .508. This is in good agreement with his theoretical value of 1/2. He also presented a plot showing measured waveforms and a waveform computed from his theory. These show fair agreement; however, as pointed out by S Kaufman in comments at the end of Ricker's paper, the measured wavelets are at distances of 150 to over 1600 feet (46 to over 488 meters) and the theoretical wavelet is calculated for 3.5 feet (1.07 meters). Two spectra were presented and compared to theoretical spectra. The comparisons are fair for theoretical distances of from 3.5 feet (1.07 m) to infinity. Amplitude versus travel time plots were also presented and these tend to show some agreement with theory; however, amplitudes are fairly uncertain and the agreements aren't that striking.

Bruckshaw and Mahanta (1954) made laboratory measurements of the quality factor Q on 6 different rock types (granite, dolerite, diorite, sandstone, shelly limestone and oolitic limestone) in the frequency range 40 to 120 Hz. They used a flexural excitation technique in which a rod clamped at one end is set into forced vibrations at the other end by an alternating force. The motion on the opposite side of the bar at the driven end is detected and the phase difference with the driving force can be measured. This allows a calculation of energy loss per cycle. They found the energy loss per cycle to be practically independent of frequency.

Collins and Lee (1956) presented data measured by John L. Martin in 1947-48 but not published. These measurements made using longitudinal vibrations of a limestone core both dry and 100% water saturated indicate that Q is independent of frequency even for the 100% saturated case. This would not agree with the results of Born (1941). They also analysed strain measurements at distances of 10, 20 and 27.5 feet (3.05, 6.1 and 8.39 meters) from an explosion. Due to the scatter of the data they were not able to reach a definite conclusion on the frequency dependence of the absorption coefficient; however, they did state that it appeared that it varied more like the first power of frequency than the second power.

McDonal et al (1958) reported field measurements of attenuation made in the Pierre shale near Limon, Colorado. This is the area where Ricker did his work. Shots at depths of 250 to 300 feet (76.2 to 91.4 meters) were fired into 5 detectors at depths from 350 to 750 feet (107 to 229 meters). Using velocity log information corrections were made to the data for geometric spreading. Because of the uniformity of the shale it was felt that that there would be no problems with multiples. The absorption was measured by Fourier analysis of the corrected waveforms. For vertically travelling compressional waves the results indicated that the absorption coefficient was essentially a linear function of frequency with a least squares fit indicating a dependence on frequency to the power 1.1 from 100 to 600 Hz. For horizontally travelling shear waves the results were similar with the absorption coefficient having a linear dependence on frequency. They also found that the decay of wavelet amplitude with travel time and the wavelet broadening with travel time were less than Ricker had measured. The attenuation of shear waves in the near surface was found to be much greater than that of compressional waves.

Karus (1958) made in situ measurements on clays, lavas, gneiss and other metamorphic rocks using a pulse method in the frequency range 80 to 4500 Hz. He concluded that the aborption coefficient was almost directly proportional to frequency.

Knopoff and MacDonald (1958) reviewed the existing data on attenuation measurements and concluded that the experimental evidence indicated that the absorption coefficient was a linear function of frequency. They examined various theories and concluded that the absorption couldn't be accounted for by any linear theories.

Peselnick and Zietz (1959) used a pulse-echo technique to measure the absorption coefficient for shear and compressional waves from 3 to 10 MHz in three different limestone samples at atmospheric conditions. In this method a short pulse of compressional or shear waves is generated by a piezoelectric crystal transducer attached to one end of the specimen. The pulse duration and carrier frequency can be varied. The first arrival and multiply reflected signals are detected at the other end of the specimen by a second crystal. These arrivals are displayed on an oscilloscope and the decay in amplitude of the pulse can be measured for successive multiples and an absorption coefficient calculated. Explanation of this method is given by Roderick and Truell (1952) or White (1965). The absorption coefficient measured in this way includes the effects of apparent losses due to geometric spreading and reflections and transmissions at the specimen boundaries. By using 6 different lengths of sample Peselnick and Zietz found that these other losses were negligible in respect to the absorption. They found that the absorption coefficient was proportional to frequency for compressional and shear waves in the three samples.

Shumway (1960a, 1960b) used a longitudinal resonance technique to measure the attenuation of samples of unconsolidated marine sediments taken from the sea floor.

He tabulated many measurements on 111 samples at one, two or three frequencies in the range 20-30 kHz. He looked at the relation of absorption to porosity and also to frequency. His analysis of 65 samples gave a dependence of the absorption coefficient of frequency to the power 1.79 ± .98.

Auberger and Rhinehart (1961) used a pulse transmission technique in which a pulse was transmitted through samples of the same rock of three different lengths. The amplitudes of the transmitted pulses were compared and attenuation coefficients calculated. The piezoelectric transcuders which were used had frequencies in the range 250 to 1000 kHz. They carried out measurements of absorption versus frequency on 8 rock types (3 granites, andesite, 2 sandstones, limestone and marble). In all cases their absorption versus frequency curves showed irregular shapes consisting of peaks and troughs. In general there seemed to be an increase of attenuation with frequency, but this was not always seen. They attributed these peaks to resonance effects due to grains. It should be noted that their attenuation values are very high and this might indicate that they were not measuring just the effects of absorption. In fact Klima et al (1962) pointed out that the method of plotting peak amplitudes of a time domain pulse against distance without divergence corrections can lead to completely incorrect values of the absorption coefficient. In the case of a few observations at small distances this would cause the values to be too large.

Peselnick and Outerbridge (1961) measured the absorption coefficient of Solenhoffen limestone over the frequency range of 3.89 to 10^7 Hz. For frequencies of 3.89 and 6.52 Hz they measured the decay of free oscillations of a torsion pendulum. For frequencies of 8.2 to 28.5 kHz they used resonance methods and for frequencies around 10 MHz they used pulse-echo methods. The measurements were made at room conditions and indicated that the logarithmic decrement increased by 25% between 6.5 and 18,600 Hz and by about a factor of 4 between 6.5 Hz and 9 MHz. The increase observed in the MHz range may be too high because of Rayleigh scattering effects and the fact that a sample of lower density was used at these frequencies. This data would certainly suggest that over a very wide range of frequencies Q is essentially independent of frequency.

Usher (1962) measured Q for various rock types in the frequency range 2 to 40 Hz by using a forced oscillation technique and measuring the phase angle of the deformation in the rock relative to a steel bar. He calculated Q from this phase difference and found that Q was nearly constant as a function of frequency for dry rocks except at frequencies below 10 Hz. This could be due to experimental errors at low frequencies. For water saturated rocks he found a decrease in Q and an increase in its apparent dependence on frequency.

Wylie et al (1962) examined the absorption of waves in fluid saturated porous rocks as a function of fluid saturation using a resonant bar method. They suggested that the total logarithmic decrement was the sum of the frequency independent frame decrement (jostling losses) and a frequency dependent decrement associated with the fluid motion (sloshing losses). They indicated that the frame decrement might be the sum of a frequency independent term and a frequency dependent term resulting from chemical and physical effects of the fluid on the cementing material. They stated that the theory of Biot (1956) could be used to predict the sloshing decrement. No evidence was given showing the frequency dependence of the total decrement.

Nolle et al (1963) plotted amplitudes of the reflected signal against sand thickness for various thickness of sand and used this to calculate absorption coefficients. The reflected signal came from the bottom of a cylinder filled with sand overlain with water. The sand was a white quartz sand with all corners removed by erosion and was sieved to give particles of the same size. The signal frequency was 189 to 1000 kHz. They found the absorption coefficient to vary as the square root of frequency in this range.

Knopoff and Porter (1963) measured the absorption of Rayleigh waves on the surface of a sample of Westerly granite in the laboratory. They found that in the frequency range 50 kHz to 400 kHz Q was frequency independent. At higher frequencies they found a fourth power dependence of the absorption coefficient on frequency which they attributed to Rayleigh scattering. Knopoff (1959) has given a formula for relating the Q of Rayleigh waves to the Q for P waves and that for S waves.

Wood and Weston (1964) used a transmitted pulse technique to measure the attenuation of mud at the bottom of Emsworth harbor in the frequency range 4kHz to 50 kHz. They found that the absorption coefficient showed a linear dependence on frequency for the harbor mud.

Knopoff (1964) in an excellent review article discussed laboratory measurements of Q in metals, non-metals and rocks. The measurements in rocks have been discussed above; however, the measurements in metals and non-metals have not been discussed. He provides references to these measurements as well as tables. All of these data indicate that the absorption coefficient is dependent on the first power of frequency and hence that Q is independent of frequency for the small strains of interest in seismic wave propagation. He then discussed several models for the absorption process. This is a problem that will be examined later in this chapter. He also discussed measurements of attenuation using earthquake induced Rayleigh and Love surface waves of different periods and also measurements based on standing waves of the free modes of oscillation of the earth. Using the assumption of the frequency independence of Q and measurements of surface waves and free modes, he was able to infer a Q versus depth structure for the mantle. This is possible since surface waves of different periods sample different depths of the earth.

Wuenschel (1965) analyzed the data collected by McDonal et al (1958) for dispersion. He showed that dispersion was present along with the observed absorption and that both the absorption and dispersion of the data could be described by a theory given by Futterman (1962). He also performed model studies on plexiglass which showed the same good agreement with this theory.

Cole (1965) studied reflections from the Newfoundland abyssal plane and the Gulf of Alaska and showed that the energy loss on reflection was consistant with an absorption coefficient depending on the first power of frequency but not with one depending on frequency squared or on the square root of frequency. The frequency range of this study was 100 to 900 Hz.

Bradley and Fort (1966) concluded from a review of the literature that Q is essentially independent of frequency over a frequency range of about 10^6 Hz. They tabulated values of Q for several rock types and provide a very complete and extensive list of references to the literature from which these measurements were taken.

Atwell and Ramana (1966) analysed a great deal of the published data on absorption coefficients of rocks from laboratory measurements, field measurements and measurements from earthquake seismograms. They applied a least-squares analysis to all of the data and concluded that the absorption coefficient seemed to depend on the first power of frequency over the frequency range 10^{-3} Hz to 10^{8} Hz.

Hampton (1967) reported on laboratory measurements of attenuation in water saturated sediments. Measurements were made between 4 kHz and 30 kHz using a standing wave tube and between 50 kHz and 600 kHz by measuring pulse amplitudes. He concluded that that the absorption coefficient of clay and clay-sand mixtures (up to 15% sand by weight) depends on frequency raised to the power 1.37. As the sand proportion increases above 15% the exponent of the frequency decreases and becomes .5 for pure sand.

Sato (1967) reviewed results of Q measurements from recordings of body waves, surface waves and free oscillations associated with earthquakes. He also discussed inversion of this data to produce Q versus depth values for the entire earth. He presents theoretical relationships for the Q's associated with P and S waves to those associated with Love and Rayleigh waves.

Merkulova and Vasil'tsoy (1967) reported on Q measurements obtained from the decay of forced flexural vibrations of rod-like samples of coaly-clay shale and quartzite in the frequency range 50 to 1000 Hz. They concluded that Q is practically independent of frequency.

Merkulova (1968) used a resonance technique to calculate Q for rocks in the 10 kHz to 160 kHz range. Comparing these results to those of 1967 and to those obtained by a pulse method in the frequency range .6 MHz to 6 MHz reported by Merkulova (1966) he concluded that Q is essentially independent of frequency.

McLeroy and DeLoach (1968) measured the attenuation of samples of sea floor sediments collected in tanks 4 by 3 by 2 feet (120 by 90 by 60 cm) deep from Saint Andrew Bay, Florida. They used a transmitted pulse in the frequency range 15 kHz to 1 MHz and their conclusion was that the absorption coefficient depended on the first power of frequency.

Tullos and Reid (1969) conducted experiments in the sediments in the Gulf of Mexico in an attempt to measure attenuation. They used blasting caps as sources and geophones cemented to the earth at various depths in a borehole as receivers. The data was corrected for the angles between rays and the geophone axis and for geometric spreading. To remove the effects of constructive and destructive interference due to reflections the pulses were gated in the time domain. The spectra of the gated, corrected pulses were also smoothed in the frequency domain. The ratio of spectra at different depths was then calculated and from this spectral ratio it was possible to determine the nature of the frequency dependence of the absorption coefficient and also a value of Q. Either spectral ratios were averaged in a given region of depth or spectra were averaged over geophones that were close together or spectra were averaged over different shots recorded at the same location. They found that the absorption coefficient depended on the first power of frequency for depths of 1 to 1000 feet (.3 to 305 meters) and frequencies of 50 to 400 Hz. They calculated the absorption over the intervals 1 to 10 (.3 to 3 m), 7.5 to 100 (2.3 to 30), 100 to 500 (30 to 152 m) and 500 to 1000 feet (152 to 305 meters) with the measured Q values for P waves being 2, 180, 75 and 135 respectively.

Stoll and Bryan (1970) reviewed the theories of Biot (1956, 1962a, 1962b) in regard to predicting absorption. They calculated theoretical values of absorption for various fluid saturated sands, clays and muds and got fairly good agreement with the experimental results of Shumway (1960), Nolle et al (1963), Wood and Weston (1964), Cole (1965) and Hampton (1967). They concluded that the absorption is controlled by frame losses at low frequencies resulting in a linear dependence of the absorption coefficient on frequency. At higher frequencies viscous losses dominate and the dependence is on frequency raised to the n'th power where n increases in the range 1 to 2 and then decreases. At very high frequencies the frame losses again begin to be important. They pointed out that the terms high and low frequency are meaningful only with respect to the particular material being considered.

McCann and McCann (1969) concluded that the attenuation of compressional waves in sediments can be explained in terms of two mechanisms, namely viscous losses and solid friction losses. They also concluded that for real sediments in the frequency range 5kHz to 50kHz at a depth of burial of 2 meters or more solid friction losses dominate. They presented some experimental data.

Clowes and Kanasewich (1970) compared the autopower spectra of deep crustal seimic reflections from southern Alberta with theoretical spectra generated using a synthetic seismogram modelling program that included the effects of absorption. Assuming Q is a linear function of frequency they suggested that the average Q for P waves for the upper 2 kilometers of crust was 300 and that the average for the lower 40 kilometers was 1500.

Hamilton (1972) reported the results of in situ measurements of compressional velocity and absorption in the sea floor off San Diego in the frequency range 3.5 kHz to 100 kHz. He analysed this data as well as data from other sources in the literature and concluded that the absorption coefficient is approximately dependent on the first power of frequency. He also examined the relationship between the absorption coefficient and porosity and the mean grain size of sands. In a later paper Hamilton (1975) added more data from the literature to his 1972 data. This data further supports his conclusion about the frequency dependence of the absorption coefficient. He also studied the variation of absorption with depth.

Gladwin and Stacey (1974) have measured the rise time of pulses propogating through quarry walls, hard rock tunnel walls and concrete blocks as a function of distance. They found that the rise time varies directly as the travel time and not as the square root of travel time as Ricker (1953) predicted.

Hart et al (1977) have shown that if the dispersion associated with absorption is taken into account when comparing earth models deduced from normal mode data with those derived from body wave data then the resulting models will be in better agreement.

Toksoz et at (1979) used spectral ratios of ultrasonic pulses in the frequency range of .4 to 1.2 MHz to study the absorption as a function of frequency for P and S waves in dry and brine saturated rock samples at various pressures. In all cases the absorption coefficient was found to be a linear function of frequency.

In summing up all of the literature data which has just been discussed it is useful to consider laboratory data and field experiments separately.

In looking at the laboratory data we find that the works of Birch and Bancroft (1938), Born (1941), Bruckshaw and Mahanta (1954), Collins and Lee (1956), Peselnick and Zietz (1959), Peselnick and Outerbridge (1961), Usher (1962), Knopoff and Porter (1963), Merkulova (1968) and Toksoz et al (1979) all agree that in dry rocks the absorption coefficient depends on the first power of frequency and thus Q is independent of frequency. This agrees with results for metals and other solids as pointed by Knopoff (1964). The range of frequencies covered by these experiments is very wide (4 or 5 Hz to 10 MHz) and analysis of all of this collected data leads to the same conclusion about the frequency dependence as pointed by Atwell and Ramana (1966). The only laboratory experiments to suggest any other frequency dependence are those of Auberger and Rhinehart (1961) and as discussed earlier there may be problems with these measurements.

The laboratory data on the frequency dependence of Q for water saturated rocks is not as clear as that for dry rocks. At frequencies greater than 1000 Hz Born (1941), Shumway (1960a, 1960b), Nolle et al (1963) and Hampton (1967) all suggested some form of frequency dependence. This ranges from Q varying inversely as frequency to Q varying as directly as the square root of frequency. Hampton (1967) pointed out that the frequency dependence at these frequencies depends on the rock type. There is also evidence at these frequencies that Q does not depend on frequency for saturated rocks as pointed out by Collins and Lee (1956), McLeroy and DeLoach (1967) and Toksoz et al

(1979). Laboratory evidence on the frequency dependence of Q in water saturated rocks below 1000 Hz was given by Collins and Lee (1956) who reported that Q didn't seem to depend on frequency down to 100 Hz and by Usher (1962) who reported some frequency dependence for water saturated rocks between 2 and 40 Hz.

Field experiments have been done on land in the Pierre shale of Colorado by Ricker (1953) who concluded that the absorption coefficient is proportional to the square of frequency and hence that Q varies inversely as frequency and by McDonal et al (1958) who concluded that the absorption coefficient depends on the first power of frequency and hence that Q is constant. Karus (1958) also concluded that Q is constant. Wuenschel (1965) analysed the data of McDonal et al and fitted the observed dispersion to Futterman's model which requires a linear frequency dependence of the absorption coefficient.

In my opinion the conclusion that Ricker's Wavelet Theory agrees with his experimental data has not been proven in his paper. The wavelet breadth versus travel time plot doesn't prove that this is the only theory that could explain the results. The same criticism would apply to the amplitude versus travel time plots. As has been pointed in the previous discussion of this work there is a distance problem in the comparison of observed and theoretical wavelets. Also, I believe that one could argue that the theoretical and observed wavelet comparisons and spectral comparisons suggest that perhaps this theory might predict a basic wavelet shape near to the source but that it doesn't describe the wavelet propagation outside this region. A plot of the ratio of amplitude spectra versus frequency for the recorded waveforms from the same shot at different distances which was not made would have provided information about the frequency dependence of the process. McDonal et al (1958) in the same Pierre shale reported results which disagree with the amplitude decay and wavelet broadening reported by Ricker. They also do a Fourier analysis which shows that the absorption coefficient is proportional to the first power of frequency. Ricker's work has also been criticized by Van Melle (1954) on the basis of energy considerations. He calculated the actual energy in the travelling wave and then used Ricker's theory to extrapolate back towards the source. At a distance of 36 feet (11 meters) he calculated that the wavelet contains 7 times as much energy as the initial charge could possibly have had.

Other field experiments include those of Wood and Weston (1964) and Hamilton (1972) in the ocean bottom. These experiments showed that the absorption coefficient is a linear function of frequency in the range 4kHz to 100 kHz. Cole (1965) arrived at a similar conclusion from analyzing ocean bottom reflections in the frequency range 100 to 900 Hz.

Tullos and Reid (1969) measured absorption in the Gulf coast sediments down to a depth of 1000 feet (305 meters) in the frequency range 50 to 400 Hz and concluded that the absorption coefficient is a linear function of frequency and hence that Q is constant.

Based on all this data it is clear that the absorption coefficient is a linear function of frequency and hence that Q is a constant. This conclusion is made for frequencies of interest in seismic exploration (10 to 500 Hz) and for in situ rocks. All of the data support this conclusion except that of Ricker (1953) and some laboratory measurements on water saturated rocks. The discrepancy of the lab measurements can likely be explained in terms of Biot's theory with the losses made up of a viscous term due to the fluid motion plus a solid friction term due to the bulk rock material and the latter will likely dominate at the frequencies of interest as suggested by Stoll and Bryan (1969). McCann and McCann (1969) suggested that, while the viscous losses may dominate in the lab at zero overburden pressure, for real sediments at a depth of burial of two meters or more the solid friction method will dominate. The calculations of Johnston et al (1979) also indicate that the frictional losses will dominate.

Table 1.1 is a summary of the Q values measured for various rocks in the laboratory and the field along with the source of the measurement. The various Q's apply to

Rock Type	Frequency	Q Value	Reference
chalk	2-40	Qy=100-120	7
diorite	40-120	Qy=125	3
diorite	2-40	Qy=200-300	7
dolerite	40-120	Qy=90	3
granite	40-120	Qy=50	3
Quincy granite	140-1600	Qy=100-200	1
Quincy granite	140-1600	Qs=150-200	1
Westerly granite	50-400 kHz	Qr=79	8
limestone I-1	5-10 MHz	Qp=170	5
limestone I-1	3-15 MHz	Qs=400	5
limestone H-1	5-10 MHz	Qp=190	5
oolitic limestone	40-120	Qy=40	3
shelly limestone	40-120	Qy=60	3
Hunton limestone	2.8-10.6 kHz	Qy=59-71	2
Solenhoffen limestone	3-15 MHz	Qp=110	5
Solenhoffen limestone	3-9 MHz	Qs=190	5
Solenhoffen limestone	4 Hz-10 MHz	Qs=180-800	6
sandstone	4-120	Qy=20	3
Amherst sandstone	930-3830	Qy=51-55	2
Berea Sandstone			
15 psi dry	.6-1.1 MHz	Qp=22	11
15 psi wet	.6-1.1 MHz	Qp=16	11
5000 psi dry	.6-1.1 MHz	Qp=100	11
8000 psi wet	.6-1.1 MHz	Qp=78	11
15 psi dry	.4-1.2 MHz	Qs=20	11
15 psi wet	.4-1.2 MHz	Qs=8	11
5000 psi dry	.4-1.2 MHz	Qs=105	11
8000 psi wet	.4-1.2 MHz	Qs=36	11
Old Red sandstone	2-40	Qy=80-90	7
coaly-clay shale	50-1000	Qy=75	9
Pierre shale	100-600	Qp=32	4
Pierre shale	25-150	Qs=10	4
Sylvan shale	3.4-12.8 kHz	Qy=70-75	2
quartzite	50-1000	Qy=180	9
cap rock core	100-6600	Qy=35-62	2
Cockfield-Yegua core	3.6-10.9 kHz	QY=65-70	2
Gulf Coast Sediments			
.3 to 3 m	50-400	Qp=2	10
2.3 to 30 m	50-400	Qp=180	10
30 to 152 m	50-400	Qp=75	10
152 to 305 m	50-400	Qp=135	10

Table 1.1 Summary of Experimental Measurements of Q.

different elastic moduli and Qp is associated with P wave propagation, Qs with the the shear modulus or shear propagation, Qy with Young's Modulus and Qr with Rayleigh wave propagation. Table 1.2 lists the references for the measurements which are summarized in Table 1.1.

1.3 Absorption Models

In this section various models of the absorption mechanism will be discussed including the model which is used in this thesis. All of the models examined have a linear or nearly linear dependence of the absorption coefficient on frequency since the experimental data discussed in the previous section indicate that this is the case.

The first model to be examined is the one which will be used in this thesis. It was proposed by Futterman (1962). He defined the displacement of a one dimensional plane wave as

$$U(r,t) = U(0)\exp[i(Kr-wt)] \qquad (1.4)$$

where $U(r,t)$ is the displacement as a function of distance r and time t and $U(0)$ is the initial displacement at the source. The angular frequency is w and K is the complex propagation constant

$$K(w) = k(w) + i\,a(w) \qquad (1.5)$$

Number	Reference
1	Birch and Bancroft (1938)
2	Born (1941)
3	Bruckshaw and Mahanta (1954)
4	McDonal et al (1958)
5	Pesselnick and Zietz (1959)
6	Pesselnick and Outerbridge (1961)
7	Usher (1962)
8	Knopoff and Porter (1963)
9	Merkulova and Vasil'tsoy (1967)
10	Tullos and Reid (1969)
11	Toksoz et al (1979)

Table 1.2 References for Table 1.1.

where k is the wave number and a is the absorption coefficient. K obeys the symmetry relationship

$$K(w) = \text{CONJUGATE}\,[K(-w)] \qquad (1.6)$$

where CONJUGATE indicates the complex conjugate.

Futterman assumed two things in his derivations. The first was that the absorption coefficient would vary strictly linearly with frequency over the range of measurement. The second assumption was that the wave motion could be described by a linear theory. This meant that the superposition principle could be applied. It also meant that the presence of absorption was a necessary and sufficient condition for the presence of dispersion.

Futterman then introduced the notion of a complex index of refraction given by

$$N(w) = K(w)/k'(w) \qquad (1.7)$$

where $k'(w)$ defines the non-dispersive behaviour of the medium at the same frequency. It was then necessary to introduce into the theory a low frequency cutoff so that the phase velocity would be bounded as the frequency approached zero. If c^0 is the limit of the phase velocity below this cutoff frequency then this meant that the limits of $c^0/c(w)$ and $a(w)/w$ were finite as w approached zero. This implies that at very low frequencies "a" approaches zero faster than a linear function of frequency. Then

$$k'(w) = w/c^0 \qquad (1.8)$$

and

$$N(w) = c^0 K(w)/w \qquad (1.9)$$

and the limit of N(w) as w approaches 0 is 1.

There is also a high frequency cutoff limit in this theory. The high frequency cutoff was introduced so that the limit of a(w)/w would approach zero as w became infinite. This implies that at very high frequencies "a" behaves as if the frequency dependence is on a power less that one. This requirement is also required in order to satisfy the Paley-Wiener criterion (see Kanasewich (1975) page 146). Thus there is no absorption allowed at infinite frequency and the imaginary part of N(w) is zero.

By using the principle of causality Futterman applied a Kramers-Kronig type of relation (see Kittell (1976) page 324) or Hilbert transform to relate the real and imaginary parts of the complex index of refraction. This gave him a relationship between the dispersion which is described by the real part of the complex index and the absorption which is described by the imaginary part of the index. He then considered three forms of the absorption, all of which satisfied the assumption that the absorption coefficient was a linear function of frequency in the range of interest. The third absorption-dispersion pair which he described is the one which will be used as a model in this thesis. For this pair

$$\mathrm{Im}[N(x)] = [1-\exp(-x)]/2Q^0 \tag{1.10}$$

where $x=w/w^0$ and w^0 is the low frequency cutoff. Q^0 is the reduced quality factor given by

$$Q^0 = w / [2a(w)c^0]. \tag{1.11}$$

For $Q \gg 6.28$

$$2c(w)Q(w) = 2c^0Q^0 \tag{1.12}$$

and

$$a(w) = w/2c(w)Q(w) \tag{1.13}$$

where

$$Q(x) = Q^0 - \ln(\gamma x)/\pi \tag{1.14}$$

and

$$c(x) = c^0[1 - \ln(\gamma x)/\pi Q^0]^{-1}. \tag{1.15}$$

Euler's constant is $\ln(\gamma)=.5772157$. Equations 1.14 and 1.15 are valid only for $w \gg w^0$. Note that the group velocity associated with this absorption-dispersion pair is

$$u(x) = c^0[1 - \{1+\ln(\gamma x)\}/\pi Q^0]^{-1}. \tag{1.16}$$

Thus the group velocity will be slightly greater than the phase velocity.

Equations 1.13 to 1.15 describe the absorption model which will be used in this thesis. Note that the absorption coefficient given by equation 1.13 is a linear function of frequency in the frequency range of interest. In this model there is a low frequency cutoff below which no dispersion exists; however, the value of this low frequency cutoff can be made as close to zero as we want. Also note that in deriving these relations a high frequency limit was also introduced such that above this limit there is no absorption; however, this limit can be as high as we want so that the theory is valid over whatever frequency range we would be interested in for seismic exploration purposes. No attempt was made to describe a physical mechanism for the energy loss in this theory as the theory was just derived from the assumptions that a linear theory was valid and that the absorption coefficient varied as the first power of frequency.

It is interesting to compare Futterman's theory with one given by Lomnitz (1957) to explain the relationship between transient creep and internal friction in solid materials. Lomnitz started from Boltzman's "theory of elastic working" (Boltzman, 1876) which was later extended by Zener (1948). According to this theory the strain is related to the stress by an equation of the form

$$e(t) = [p(t) + \int_{-\infty}^{t} p(t) f(t-t') dt']/m \qquad (1.17)$$

where p(t) is the stress as a function of time, e(t) is the strain as a function of time, m is an elastic constant and f(t) is the creep function. Note that Zener (1948) refers to this function as the creep function but that Lomnitz (1957) refers to the function used above as the time derivative of what he calls the creep function. Also the stress is related to the strain by

$$p(t) = m[e(t) + \int_{-\infty}^{t} e(t) y(t-t')dt'] \qquad (1.18)$$

where y(t) is the relaxation function. Note that Zener refers to this function as the stress function and Lomnitz refers to it as the time derivative of the relaxation function.

Since the creep and relaxation functions are zero by definition for negative times in equations 1.17 and 1.18 then the integrals in these equations are convolution integrals. Lomnitz derived a relation between the creep function and the relaxation function by applying a Laplace transform to equations 1.17 and 1.18. He then introduced the idea that the relation between stress and strain should be described by a complex elastic modulus to account for the absorption. This idea is the same as Futterman's introduction of a complex wave number to describe the absorption. In fact a complex wave number, a complex elastic modulus, and a complex velocity will be used to modify the elastic theory of wave propagation to include absorption. This is discussed in the next chapter.

Fourier transforming equations 1.17 and 1.18 replaces the convolution integrals with multiplications and leads to

$$E(w) = P(w)[1+F(w)]/m \tag{1.19}$$

$$P(w) = mE(w)[1+Y(w)] \tag{1.20}$$

where the capital letters E, P, F and Y denote the Fourier transforms of e, p, f and y respectively and w is the angular frequency. If we write $P(w) = ME(w)$ where M is a complex elastic modulus then using equation 1.19 gives

$$M(w) = m/[1+F(w)]. \tag{1.21}$$

Now a complex wave number K will be defined as

$$K(w) = w/c - i\,a(w). \tag{1.22}$$

A wave travelling in the positive r direction is written as $\exp[i(wt-Kr)]$. This is the opposite sign convention to that used by Futterman (1962) and thus his complex wave number was the conjugate of this one. The complex velocity V is defined by

$$V = w/K = \sqrt{M/\rho} \tag{1.23}$$

where ρ is the density. Note that the elastic phase velocity v' is defined as

$$v' = \sqrt{m/\rho}. \tag{1.24}$$

Substituting for K and M in 1.23 and using m defined by 1.24 leads to

$$a^2 = \frac{w^2 G(w)}{2v'^2} \qquad (1.25)$$

and

$$c^2 = \frac{2v'^2 G(w)}{F''^2(w)} \qquad (1.26)$$

where

$$G(w) = [1+F'][\{1+F''^2/(1+F')^2\}^{1/2} - 1] \qquad (1.27)$$

with

$$F(w) = F'(w) + i\,F''(w). \qquad (1.28)$$

F' and F" are the cosine and sine transforms of f(t) respectively. Now the quality factor Q is defined such that

$$M = m(1+i/Q). \qquad (1.29)$$

Using 1.21 ;1.28 and 1.29 gives

$$F''(w) = Q/(Q^2+1) \qquad (1.30)$$

and

$$F'(w) = -1/(Q^2+1). \qquad (1.31)$$

If we consider that $Q \gg 1$ in order that we can neglect $1/4Q^2$ relative to 1 then 1.27 becomes

$$G(w) = \frac{F''^2(w)}{2[1+F'(w)]}. \qquad (1.32)$$

Also using 1.29 and 1.22 in equation 1.23 and again assuming that $Q >> 1$ gives

$$a = w/2cQ. \qquad (1.33)$$

Now, substituting 1.32 into 1.26 leads to

$$c/v' = [1+F'(w)]^{-1/2}. \qquad (1.34)$$

Also substituting 1.32 to 1.34 into 1.25 gives

$$1/Q = F''(w)/[1+F'(w)]. \qquad (1.35)$$

Note that Lomnitz's (1957) equation 27 and equation 1.35 are not the same. His equation 27 has a square root in the denominator which could be arrived at by assuming $c/v'=1$. However, this is not a necessary assumption in view of equation 1.34 which is Lomnitz's equation 28.

Lomnitz then showed how a creep function of the form

$$f(t) = qa/(1+at) \qquad (t>0) \qquad (1.36)$$

could be used to derive an expression for Q in terms of q and a parameter w/a where "a" plays the role of a high frequency cutoff. For $Q >> 1$ and $w/a << 1$

$$\frac{1}{Q} = \frac{q\pi/2}{1-q\ln(\gamma w/a)}. \qquad (1.37)$$

The frequency dependence of Q given by 1.37 is very similar to Futterman's frequency dependence. Savage and O'Neill (1975) have compared the two theories and concluded that they do not differ significantly. Pandit and Savage (1973) have compared values of Q measured with a resonance technique with values of Q calculated using equation 1.37 where "q" and "a" were measured from creep experiments on the same samples. They found that the values agreed reasonably well.

For a constant stress applied at t=o equation 1.36 leads to a time dependence of the strain given by

$$e(t) = p^0[1 + q \ln(1+at)]/m. \tag{1.38}$$

Kalinin et al (1967) considered four different forms of absorption laws as functions of frequency and using Kramers-Kronig relations derived expressions for the dispersion relations associated with the given absorption models. Their second model gives an absorption coefficient of the form

$$a(w) = bw/(1+dw) \tag{1.39}$$

where b and d are constants. This model has a linear dependence on frequency for dw << 1. The associated dispersion relations is

$$c(w) = \frac{c(\infty)}{1 - \dfrac{2bc(\infty)\ln(dw)}{\pi(1-d^2w^2)}} \tag{1.40}$$

where $c(\infty)$ is the limit of the phase velocity as the frequency becomes infinite.

Strick (1967) modeled the absorption coefficient as

$$a(f) = bf^{s} \tag{1.41}$$

where b is a constant and $0 < s < 1$. He derived a dispersion relation for this absorption model and also calculated a complex elastic modulus and a dynamic viscosity. He compared these curves to experimental data and got reasonable agreement. Strick went on to calculate a creep function from the complex elastic modulus. His comparison of the creep function to real data showed agreement in the basic shapes of the curves but not in the actual values.

In a later paper Strick (1970) considered the same model and developed an asymptotic expansion for the time domain shape of a travelling wave at large distance. He also developed an asymptotic expansion at large distances for a solid which obeys an absorption-dispersion pair similar to the first relation given by Futterman (1962). He used this expansion to calculate the pulse shape for the example Futterman used in his paper for his third pair. He compared the pulses and the shapes were similar but the time is very different. This is likely due to approximations that Strick made in calculating the dispersion relation (his equation 30). As a result of these approximations his expression applies only for frequencies much greater than the low frequency cutoff and yet, for the pulse in the example, the frequencies aren't in this range.

Gladwin and Stacey (1974) and Stacey et al (1975) examined the theories of Futterman (1962), Kalinin et al (1967), which they credited to Azimi et al (1968), and Strick (1967) in terms of pulse rise time as a function of travel time (or distance). They compared observed data to theoretical predictions and concluded that Strick's model does not satisfy the measured data. They then went on to reject Futterman's model as well on the grounds that the introduction of absorption had caused an increase in the phase and group velocities such that the attenuated pulses arrived earlier than expected on the basis of an elastic velocity calcualted from a purely elastic model (one in which there is no absorption). As has been pointed by Savage (1976) their conclusion appears to be based on a misunderstanding of Futterman's theory which arises from interpreting c^0 of equation 1.15 as the elastic velocity. In fact as Savage pointed out c^0 is the low frequency limit of the phase velocity and the elastic velocity should be taken as the high frequency limit. In accepting the theory of Kalinin et al they used the high frequency limit as the elastic velocity, and if this is also done in Futterman's theory there is no problem and the theory should not be rejected. Stacey et al (1975) also suggested that Futterman's behaviour of Q as the frequency approaches zero is incorrect as it is not consistent with creep under steady strain. Since the theory is not supposed to be valid below a low frequency cutoff this criticism seems unimportant. Lomnitz (1957) has shown that internal friction is part of the same phenomenum that produces creep. Thus the rejection of Futterman's theory in comparison to that of Kalinin et al seems to be based on incorrect reasons. In fact Kalinin et al used the same approach as Futterman in calcuating their dispersion.

Stacey et al (1975) went on to consider whether the absorption theory should be a linear (superposition principle is valid) or non-linear one. They pointed out that a linear theory suggests an elliptical stress-strain hysteresis loop while evidence reported by McKavanagh and Stacey (1974) indicates that the loop is cusped at the ends. They did conclude, however, that in the absence of more conclusive evidence a linear theory should be used. Brennan and Stacey (1977) report the measurement of elliptical hysteresis loops which supports the idea of a linear theory.

Another model which has been proposed for the absorption mechanism is that of the standard linear solid. This model is well described by Zener (1948). For this model the stress-strain relation is

$$p + t_1\dot{p} = m_1(e + t_2\dot{e}) \qquad (1.42)$$

where the dot indicates time differentiation, m_1 is a relaxed modulus and t_1 and t_2 are relaxation times. For a constant stress p^0 applied at $t=0$ the strain as a function of time is

$$e(t) = p^0[1 - (1-t_1/t_2)\exp(-t/t_2)]/m_1 \tag{1.43}$$

where

$$t_2/t_1 = m_2/m_1 \tag{1.44}$$

and m_2 is the unrelaxed modulus.

At $t=0$

$$e = p^0/m_2 \tag{1.45a}$$

and at infinite time

$$e = p^0/m_1. \tag{1.45b}$$

Fourier transforming equation 1.42 yields

$$P(w) = m_1 \frac{(1+iwt_2)}{(1+iwt_1)} E(w). \tag{1.46}$$

Defining a complex modulus M as in equation 1.29 yields

$$\frac{1}{Q} = \frac{w(t_2-t_1)}{1+w^2 t_1 t_2}. \tag{1.47}$$

Using 1.44 and defining

$$t' = (t_1 t_2)^{1/2} \tag{1.48}$$

leads to

$$\frac{1}{Q} = \frac{wt'}{1+w^2t'^2}\frac{(m_2-m_1)}{(m_1m_2)^{1/2}}. \tag{1.49}$$

This equation predicts that Q will not be nearly constant as a function of frequency but rather will have a a definite peak like a resonance curve.

Liu et al (1976) have shown that the concept of a relaxation spectrum can lead to a Q that is nearly constant over a band of frequencies. They give an example in which a spectrum of 12 different relaxation times leads to a Q value that is essentially constant over five decades of frequency and an absorption coefficient that is a linear function of frequency over the same range. They showed that the dispersion relation for such a model is the same as that arising from Futterman's theory. Thus the two theories are quite similar within the range where the absorption coefficient is proportional to the first power of frequency but are different outside this range.

1.4 Absorption Mechanisms

The models discussed in the previous section were all phenomenological which means that they dealt with a macroscopic description of the absorption mechanism but did not look at the microscopic causes of the absorption. In this section some of these possible causes will be examined.

Treitel (1959) considered the fact that all real materials have a finite thermal conductivity and as a result stress waves will suffer energy losses due to heat conduction. As the solid is compressed or expanded mechanical energy is converted to heat energy and the compressed parts are warmer than the rarified parts. Since there is no volume change associated with a shear wave this type of loss would only apply to a compressional wave. Heat flows because the conductivity is not zero and energy loss occurs. This type of loss is referred to as thermoelastic loss. Treitel showed that for this mechanism of energy loss the absorption coefficient was proportional to the square of frequency. He also calculated theoretical values of the absorption coefficient for rock and copper and showed that these values are much less than measured values at seismic frequencies. This led him to conclude that losses of this type were either absent or too small to be detected.

Knopoff and MacDonald (1960) reviewed three mechanisms of energy loss. These are thermoelastic losses, Rayleigh scattering losses and loss in ferro-magnetic materials. They concluded that it is unlikely that any of these losses are important in geophysical problems at seismic frequencies. They also suggested a solid friction model which can explain the linear frequency dependence of the absorption coefficient. This type of model has been described by Knopoff (1956). For plane waves propogating in one dimension this model has a differential equation of the form

$$c^2 \left[1 + \frac{1}{|w|Q} \frac{\partial}{\partial t} \right] \frac{\partial^2 u}{\partial x^2} = \frac{\partial^2 u}{\partial t^2} \qquad (1.50)$$

The second term on the left represents a frictional force where the friction varies as the gradient of the local stress. This sort of friction is justified by assuming that there is opportunity for relative motion between grains and that this motion is limited. As the relative displacements (and thus the stress gradients) increase the friction may be thought of as increasing also. In using this model Knopoff didn't allow for dispersion which must exist along with the absorption due to causality. Also note that this equation leads to a non-linear theory.

Savage (1965) has considered losses due to intergranular thermal currents. In a rock there will be regions of strain concentration such as contact points between grains or the volume surrounding cracks or pore spaces. Volume changes in these regions produce temperature fluctuations and absorption occurs due to thermoelastic loss. Note that this mechanism acts directly only on compressional waves but can also act on a shear wave indirectly due to the inhomogeneity caused by the strain concentrations. This mechanism can be described by a relaxation mechanism and a characteristic relaxation time. Savage showed that the relaxation time is related to the size of the strain concentration and that a spectrum of such sizes will lead to a constant Q.

Gordon and Nelson (1966) reviewed possible loss mechanisms. They mentioned nine possible mechanisms. Two of these were diffraction and scattering which are really geometrical effects and don't indicate the absorption of the medium. A third mechanism that they mentioned is magnetic damping. Since this is only present in magnetic materials it is not considered. Thermoelastic damping has alreading been discussed and it is not important at seismic frequencies for normal rocks.

A fifth mechanism which they mentioned and which is likely very important is frictional sliding at cracks or unbonded grain boundaries. When an alternating stress is applied to an unbonded boundary sliding is expected to occur. This sliding will cause the stress-strain curve to trace out an elliptical hysteresis loop. This mechanism leads to a value of Q which is independent of frequency and can be mathematically described by a complex elastic modulus. It is believed that this is the main source of internal friction in rocks at low pressures and temperatures.

A sixth type of loss is that due to viscous grain boundary damping. In this mechanism there is a relaxation of stress at grain boundaries. This mechanism has a Q given by

$$\frac{1}{Q} = D\,\frac{wt'}{1+w^2t'^2} \tag{1.51}$$

where D is the relaxation strength which is a ratio of the greatest non-elastic stress to the elastic strain. t' is a relaxation time which varies with temperature T according to an equation of the form

$$t' = t^0\exp(-G/kT) \tag{1.52}$$

where G is an activation energy and k is Boltzman's constant. Equation 1.51 is essentially the same as equation 1.49 where D is defined as $(m_2-m_1)/(m_1m_2)^{1/2}$ or $(m_2-m_1)/m_1$ or $(m_2-m_1)/m_2$ (see Zener, 1948 pp 56). Experiments on metals have shown well defined damping peaks as predicted by equation 1.51 which are absent in single crystals. These peaks may be smeared due to a spectrum of relaxation times.

A seventh type of loss is stress induced ordering. Under this mechanism there is a thermally activated redistribution of atoms or defects on the lattice sites of a crystal under the influence of an external stress. Equations 1.51 and 1.52 describe this mechanism.

An eighth type of loss is associated with dislocations. An applied stress may cause motion of dislocations in the crystal and relief of stress. Equations 1.51 and 1.52 describe this loss also. At high temperatures an applied stress can tear dislocations irreversibly away from impurity atoms. No specific frequency dependence is predicted in this latter case but this mechanism will be amplitude dependent.

The ninth type of absorption is that due to the presence of a fluid in a porous rock and is described by a theory by Biot (1956, 1962a, 1962b). This was discussed earlier.

Jackson and Anderson (1970) reviewed absorption mechanisms in an attempt to decide the most probable mechanisms of absorption in the mantle. In this thesis we are concerned with absorption in the sedimentary layers of the extreme upper crust so that their conclusions may not be valid for us but their descriptions of mechanisms are useful. They divided the absorption losses into four classes, namely, damped resonance losses, static hysteresis losses, relaxation losses and viscosity losses.

Damped resonance losses are associated with work done at a point in a solid against a restoring force which is proportional to relative velocity. This loss applies to forced resonance of dislocations in their potential wells. This is a high frequency loss mechanism that can be rejected.

The static hysteresis losses include sliding across cracks or at grain boundaries. This mechanism was discussed earlier and is likely the most important loss mechanism for sedimentary rocks, especially at low pressures. There is a hysteresis associated with tearing of dislocations from impurity atoms. This loss generally gives a frequency independent Q and is inoperative below a certain threshold strain. It will be neglected on the assumption that the strains are too small. Bhatia (1967) showed that there can also be an amplitude independent type of hysteresis loss associated with dislocations.

Relaxation mechanisms are generally described by equations 1.51 and 1.52. Thermoelastic losses are one form of relaxation loss. As has been pointed earlier these losses are negligible at seismic frequencies. Jackson and Anderson suggested that the same likely applies to intergranular thermal currents. The calculation of Savage (1966) might dispute this. Relaxations associated with dislocations can also likely be neglected at our frequencies and temperatures. There are several mechanisms caused by rearrangement of atoms into a position of lower Gibbs free energy in a stressed state but these are likely not important at seismic frequencies. Relaxations associated with phase changes will likely not occur in the sediments. Grain boundary relaxations were discussed earlier and these may account for some absorption in our range of interest.

The viscous mechanism which Jackson and Anderson discussed is associated with the mechanism of melting and would therefore not concern us.

Johnston et al (1979) have discussed absorption of a dry rock matrix and also the effect of a saturating fluid in the matrix on the absorption. They suggest that Q of the dry matrix is composed of two factors. The first is an intrinsic elasticity which is large (little absorption) and can usually be neglected in minerals. The second factor is frictional dissipation due to relative motions at grain boundaries and at crack surfaces and is very important. One of the effects of saturating a dry rock is to lubricate the cracks which leads to more sliding and greater frictional loss. Fluid flow is also present in a saturated rock and leads to absorption as described by the theories of Biot (1956, 1962a, 1962b). In addition to Biot fluid flow they include a loss due to "squirt flow" which is induced between adjacent cracks due to the relative volume change caused by a stress wave. They present a formulation for calculating this loss. They also discuss the effects of partial saturation from a qualitive point of view. The last loss mechanism they include in their model is the geometrical effect of scattering. They fit a model incorporating all of these loss mechanisms to real data measured as a function of pressure for dry and saturated Berea sandstone at ultrasonic frequencies and then extrapolate to other frequencies. They present extrapolated curves of the absorption coefficient as a function of frequency for P waves in Berea sandstone at surface pressure and at a depth of ten thousand feet (3.05 kilometers). These curves show that the main source of absorption at seismic frequencies for both depths will be frictional sliding. This means that at seismic frequencies the absorption coefficient will be essentially a linear function of frequency.

In conclusion it seems that the most important absorption mechanism for sedimentary rocks at seismic frequencies would be sliding at cracks or grain boundaries. This mechanism can be described in terms of a phase angle between stress and strain which leads to a hysteresis loop. We can mathematically model this with a complex elastic modulus. This type of loss is not well understood. There have been theories by White (1966) and Walsh (1966) to attempt to explain it; however, they are not entirely satisfactory. Winkler et al (1979) suggest that this type of loss is not important at low strains such as those associated with seismic waves. Their reasoning is based on the assumption that a crack must slide a certain minimum distance (of the order of atomic spacing). There is no reason given as to why they feel that this is the case. They also show that at higher strains (above 10^{-6}) the absorption and velocity depend on strain amplitude. Johnston et al (1979) in an excellent paper rate sliding as the most important cause of absorption.

A second source of absorption could be in a relaxation mechanism such as grain boundary damping, intergranular thermal currents, or possibly stress-induced ordering. If these mechanisms are present then it would seem that there must be a spectrum of relaxation times in order to account for the experimental evidence that Q is essentially independent of frequency. As was mentioned earlier, Liu et al (1976) have shown that in the case of nearly constant Q due to a spectrum of relaxation times the dispersion relation in the frequency range where Q is nearly constant is the same as that of Futterman (1962).

A third possible source of absorption is the presence of a fluid in a porous medium. Stoll (1977) outlined in good detail a mathematical model for this situation based on the works of Biot (1956, 1962a, 1962b). This model allows for two methods of energy loss. The first is due to intergranular skeletal losses and is described by a complex elastic modulus. The second comes from viscous losses associated with motion of the fluid in the pores. The experimental data which was reviewed earlier would suggest that the frame losses generally dominate.

2. SYNTHETIC SEISMOGRAMS

2.1 Plane Waves at Vertical Incidence Including Absorption

In this section a method for the calculation of synthetic seismograms which include the effects of absorption and dispersion will be outlined. This method, which can be used to produce normal incidence synthetic seismograms for plane waves propogating in a flat layered model, is a modification of the communication theory approach to synthetic seismograms. Details of this method can be found in papers by Baranov and Kunetz (1960), Wuenschel (1960), Goupillaud (1961), Kunetz and D'Erceville (1962), Trorey (1962), Kunetz (1964), Sherwood and Trorey (1965), Darby and Neidell (1966), Treitel and Robinson (1966), Robinson (1967, 1968), Claerbout (1968) and Robinson and Treitel (1977).

Consider a plane compressional wave propogating in the positive z direction. The elastic wave equation can be written as

$$\frac{\partial^2 u}{\partial t^2} = \frac{m\partial^2 u}{\rho\partial z^2} = c^2\frac{\partial^2 u}{\partial z^2} \qquad (2.1)$$

where m is an elastic constant, ρ is the density, c is the phase velocity and u is the displacement in the z direction. In this case the solution to equation 2.1 has the form

$$u = A\exp[i(wt-kz)] + B\exp[i(wt+kz)] \qquad (2.2)$$

where the A term represents a wave propogating in the positive z direction, and the B term represents a wave propogating in the negative z direction. k is the wave number and is equal to the angular frequency w divided by the phase velocity c.

Now, in the case of exponential attenuation with distance, a solution to the wave equation will be written as

$$u = A\exp[-az+i(wt-kz)] + B\exp[az+i(wt+kz)] \qquad (2.3)$$

where "a" is the absorption coefficient. It must be pointed out that equation 2.3 has been arbitrarily selected as a solution in the presence of absorption. A simple mathematical modification can be made to equation 2.1 in order that equation 2.3 will be a solution. This modification is to let the elastic constant, velocity and wave number be complex as given by equations 1.29, 1.23 and 1.22 respectively. Equation 2.1 is now written as

$$\frac{\partial^2 \underline{U}}{\partial t^2} = \frac{\underline{M}\partial^2 \underline{U}}{\rho\partial z^2} = \underline{V}^2\frac{\partial^2 \underline{U}}{\partial z^2} \qquad (2.4)$$

where M is a complex elastic constant, V is the complex velocity and U is the displacement as a function of frequency. The fact that M is complex implies that there is a phase difference between stress and strain. This phase difference leads to an elliptical stress-strain curve where the area of the ellipse will be proportional to the energy loss per cycle (White, 1965, pp. 96). M will be a complex function of frequency and will have the requirement that $M(w)$ equals $M^*(w)$ where * denotes the complex conjugate. This will ensure that the time domain expression of M is real.

Now, let

$$V = v' + i\, v'' \qquad (2.5)$$

where v' and v" are the real and imaginary components of the complex velocity. Substituting equations 1.22 and 2.5 into equation 1.23 and equating real and imaginary parts gives

$$\frac{v''}{v'} = \frac{a}{k} \qquad (2.6)$$

and

$$c = v'(1+a^2/k^2). \qquad (2.7)$$

Substituting equation 1.29 into 1.23 and eliminating m leads to

$$a/k = (Q^2+1)^{1/2} - Q. \qquad (2.8)$$

Now taking $Q \gg 1$ so that $1/4Q^2$ is negligible with respect to 1 reduces this equation to

$$a/k \doteq 1/2Q \qquad (2.9)$$

or

$$a \doteq w/2cQ. \qquad (2.10)$$

Thus equation 2.6 becomes

$$v'' \doteq v'/2Q. \qquad (2.11)$$

Substituting equation 2.8 into equation 2.7 gives

$$v' = c[1 + (1+1/Q^2)^{-1/2}]/2. \qquad (2.12)$$

For $Q \gg 1$ (neglecting $1/4Q^2$ relative to 1) equation 2.12 becomes

$$v' \doteq c. \qquad (2.13)$$

Having introduced the mathematical representation which will be used for the absorption model, it is now necessary to consider the reflection and transmission of normal incidence plane waves at a boundary. Consider a plane boundary as shown in figure 2.1. Let a wave of unit displacement amplitude given by $\exp[i(wt-K'z]$ be incident from medium 1. The reflected wave in medium 1 will be $R\exp[i(wt+K'z)]$ and the transmitted wave in medium 2 will be $T\exp[i(wt-K''z)]$.

In order to satisfy the boundary conditions the displacement and the normal stress must be continuous across the boundary. The normal stress is given by

$$p = M\frac{\partial u}{\partial z}. \qquad (2.14)$$

If we let the boundary be at $z=0$, then the continuity of displacement gives

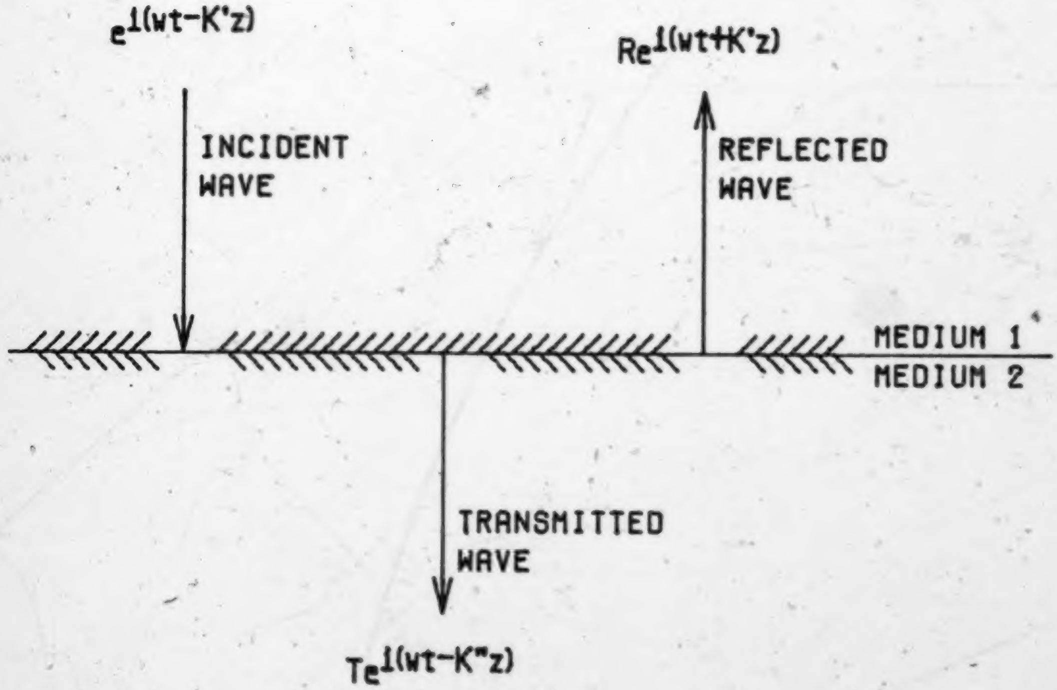

$e^{i(wt-K'z)}$
INCIDENT WAVE
$Re^{i(wt+K'z)}$
REFLECTED WAVE
MEDIUM 1
MEDIUM 2
TRANSMITTED WAVE
$Te^{i(wt-K''z)}$

Figure 2.1 The reflection and transmission at a boundary.

$$1 + R = T \tag{2.15}$$

and the continuity of normal stress gives

$$M'K'(1-R) = TM''K'' \tag{2.16}$$

where the prime refers to the medium 1 and the double prime to medium 2. Equations 2.15 and 2.16 can be solved for R and T giving

$$R = \frac{M'K'-M''K''}{M'K'+M''K''}$$

and

$$T = \frac{2M'K'}{M'K'+M''K''}.$$

Substituting into the above two equations from equation 1.23 gives

$$R = \frac{\rho'V'-\rho''V''}{\rho'V'+\rho''V''} \tag{2.17}$$

and

$$T = \frac{2\rho'V'}{\rho'V'+\rho''V''}. \tag{2.18}$$

Thus the formulas for the reflection and transmission coefficients are the same as in the elastic case, except that the phase velocity is replaced by the complex velocity. Note that R and T are now complex functions of frequency. Equation 2.17 can be shown to be the same equation for the reflection coefficient as that given by Averbukh and

Trapeznikova (1972) or by Crowe and Alhilali (1975). Their formulas are in terms of the phase velocity.

It is interesting to observe what happens to the reflection coefficient if Q is constant at a boundary. By equations 2.5, 2.6, 2.8, 2.12 and 2.17 it can easily be shown that in this case

$$R = \frac{\rho' c' - \rho'' c''}{\rho' c' + \rho'' c''}.$$

Similarly,

$$T = \frac{2\rho' c'}{\rho' c' + \rho'' c''}.$$

Thus for a constant Q interface, the reflection and transmission coefficients are real constants and the formulas are the same as in the elastic case. In general, however, if Q is not constant at a boundary R and T will be complex functions of frequency. The fact that they are complex indicates a phase change on reflection or transmission.

The synthetic seismogram equations for a flat layered model will now be considered. If D(i) is the spectrum of the downgoing wave at the top of layer i, then the downgoing wave at the bottom of layer i is given by

$$D'(i) = D(i)\exp[-ad]\exp[-iwd/c] \qquad (2.19)$$

where d is the thickness of the i'th layer and c is the phase velocity in the i'th layer. The first exponential term represents the energy loss due to the absorption as the wave propogates from the top to the bottom of the layer. The complex exponential term represents the time delay in traveling through this layer. Since the presence of absorption requires the presence of dispersion, then the phase velocity will be a function of frequency. In a similar manner U'(i) (the upgoing wave spectrum at the bottom of layer i) is related to U(i) (the upgoing wave spectrum at the top of layer i) by

$$U'(i) = U(i)\exp[ad]\exp[iwd/c]. \quad (2.20)$$

Figure 2.2 shows the relationship between the waves at the top and bottom of layer i.

The exponential loss in the medium is the major form of frequency dependent loss. However, there is also the frequency dependence of the reflection and transmission coefficients to account for. Now consider an interface as shown in figure 2.3. The upgoing wave in layer i is made up of two parts, that due to the transmission of the upgoing wave from layer i+1 and that due to the reflection of the downgoing wave in layer i. Likewise the downgoing wave in layer i+1 is made of the reflected part of the upgoing wave in layer i+1 and the transmitted part of the downgoing wave in layer i. If R and T are the reflection and transmission coefficients for incidence from above an interface and R' and T' are the reflection and transmission coefficients for

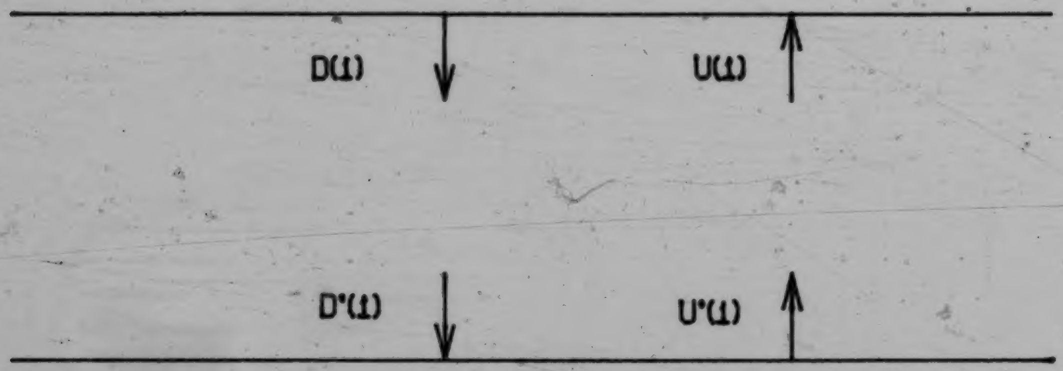

$$D'(i) = D(i)e^{-ad}e^{-iwd/c}$$

$$U'(i) = U(i)e^{ad}e^{iwd/c}$$

Figure 2.2 The relationship of waves at the top and bottom of a layer.

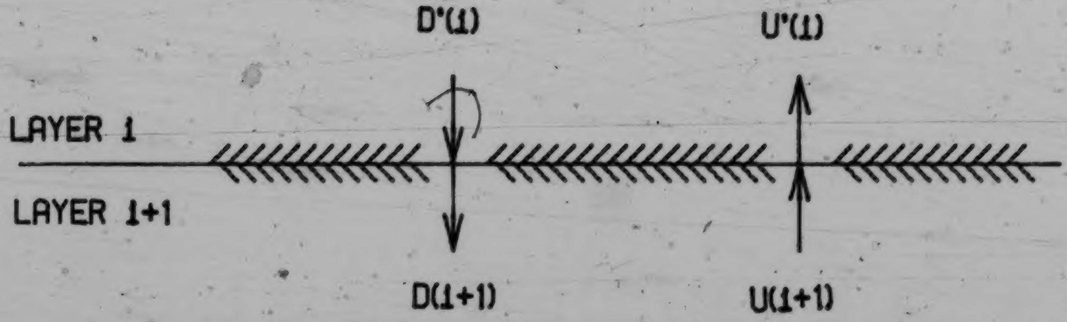
D'(i)
U'(i)
LAYER i
LAYER i+1
D(i+1)
U(i+1)

$$D(i+1) = TD'(i) + R'U(i+1)$$

$$U'(i) = RD'(i) + T'U(i+1)$$

Figure 2.3 The relationship of upgoing and downgoing waves at an interface.

incidence from below an interface then

$$U'(i) = RD'(i) + T'U(i+1) \tag{2.21}$$

and

$$D(i+1) = TD'(i) + R'U(i+1). \tag{2.22}$$

From equation 2.17 it is apparent that

$$R' = -R. \tag{2.23}$$

Also, from equations 2.15 and 2.23

$$TT'-RR' = 1. \tag{2.24}$$

Using equations 2.21 tc 2.24 it follows that

$$D'(i) = [D(i+1)+RU(i+1)]/T \tag{2.25}$$

and

$$U'(i) = [RD(i+1)+U(i+1)]/T. \tag{2.26}$$

Combining equations 2.25 and 2.26 with equations 2.19 and 2.20 gives

$$D(i) = \exp[iKd][D(i+1)+RU(i+1)]/T \tag{2.27}$$

and

$$U(i) = \exp[-iKd][RD(i+1)+U(i+1)]/T \tag{2.28}$$

where K is the complex propagation constant for layer i and is given by equation 1.22. Rewriting the above two equations in matrix form gives

$$\begin{bmatrix} D(i) \\ U(i) \end{bmatrix} = A(i) \begin{bmatrix} D(i+1) \\ U(i+1) \end{bmatrix} \qquad (2.29)$$

where

$$A(i) = \frac{1}{T} \begin{bmatrix} \exp[iKd] & R\exp[iKd] \\ R\exp[-iKd] & \exp[-iKd] \end{bmatrix}. \qquad (2.30)$$

For a model of n layers the waves in the first layer are related to those in the n+1'th layer by successive applications of equation 2.29 to yield

$$\begin{bmatrix} D(1) \\ U(1) \end{bmatrix} = A(1)A(2)\ldots A(n) \begin{bmatrix} D(n+1) \\ U(n+1) \end{bmatrix}. \qquad (2.31)$$

If the input is a downgoing spike at time zero at the surface, then the total downgoing wave in the first layer will be made up of this spike plus the reflection of the upgoing wave from the surface. If r is the reflection coefficient of the surface as seen from above, then -r is the reflection coefficient of the surface for upgoing waves in the first layer. Thus

$$D(1) = 1-rU(1). \qquad (2.32)$$

Equation 2.32 gives the total downgoing wave in the top layer since no energy is input from above the model. If the bottom or n+1'th layer is a half space, then there can be no upgoing wave in this layer. Thus

$$U(n+1) = 0. \tag{2.33}$$

Substituting equations 2.32 and 2.33 into equation 2.31 gives

$$\begin{bmatrix} 1-rU(1) \\ U(1) \end{bmatrix} = A(1)\,A(2)\ldots A(n) \begin{bmatrix} D(n+1) \\ 0 \end{bmatrix}. \tag{2.34}$$

Equation 2.34 is two equations in two unknowns. One unknown is $\tilde{U}(1)$ which is the Fourier transform of the upgoing wave in layer 1 and the other unknown is $D(n+1)$ which is the Fourier transform of the downgoing wave in the half space. The Fourier transform of the surface synthetic seismogram, $X(w)$, is given by the sum of the upgoing and downgoing waves at the surface. Thus

$$X(w) = (1-r)U(1)+1. \tag{2.35}$$

Therefore, given an n layer model, it is possible to calculate the Fourier transform of the surface synthetic seismogram for an initial downgoing spike at the surface. This Fourier transform can be multiplied by the Fourier transform of the wavelet if a wavelet different from a spike is desired as the input wavelet.

It must be remembered that equation 2.34 is a continuous frequency function. If a discrete Fourier transform is going to be used, it is necessary to sample this function at some frequency spacing df. This spacing must be small enough that for times greater than $T=1/df$ the amplitude of the synthetic seismogram is negligibly small. If such is not the case, the amplitudes at times greater than T will be aliased back into the principle time band from 0 to T. This is the analogous case to sampling in the time domain where the requirement is that the amplitude be negligible beyond the Nyquist frequency. The spacing of points in the time domain will be controlled by the maximum frequency that is used in the frequency domain before the discrete Fourier transform is applied. If this maximum frequency is F then the sample interval , dt, is dt= 1/2F.

The matrix formulation of equation 2.31 has the advantage that it can be used to generate the response in any layer. If we are interested in a surface synthetic seismogram only, a different approach can be used. Dividing equation 2.28 by equation 2.27 gives

$$Y(i) = \exp[-2iKd]\,\frac{R+Y(i+1)}{1+RY(i+1)} \qquad (2.36)$$

where

$$Y(i) = U(i)/D(i). \qquad (2.37)$$

Y(i) is the ratio of the spectrum of the upgoing wave in layer i to the spectrum of the downgoing wave in layer i. For an n layer model over a half-space Y(n+1)=0. Equation 2.36 can be successively applied from the bottom layer to the surface until Y(1) is solved for. Then using equations 2.32 and 2.37 the upgoing wave in layer 1 can be solved for, and the surface synthetic seismogram can be calculated from equation 2.35. Equation 2.36 is a continuous function of frequency and the previous comments about sampling still apply.

It is important to note that equations 2.31 and 2.36 have not been written as z transforms, but rather they have been left as functions of frequency for layers of specified thickness. The reason for this is that the presence of absorption also requires the presence of dispersion, and hence, the travel time through each layer will not be a constant at all frequencies. It is also important to note that even in the case where there is no absorption the formulation of these equations could be used to calculate synthetic seismograms for models where all layer thicknesses are not integral multiples of the sample interval.

In the limit as zero frequency is approached there is no dispersion and the phase velocity approaches c^0. The reflection and transmission coefficients are real and at zero frequency will be defined by

$$R = \frac{\rho' c^{0\prime} - \rho'' c^{0\prime\prime}}{\rho' c^{0\prime} + \rho'' c^{0\prime\prime}} \tag{2.38}$$

and

$$T = \frac{2\rho' c^{0\prime}}{\rho' c^{0\prime} + \rho'' c^{0\prime\prime}}. \tag{2.39}$$

The absorption model being used in this thesis is given approximately by equations 1.1 and 1.13 to 1.15. Equation 1.13 is an approximation which is valid for large Q while the exact express is given by equation 2.8 which can be written as

$$a = [(Q^2+1)^{1/2}-Q]w/c. \qquad (2.40)$$

If Q' is defined as

$$1/2Q' = (Q^2+1)^{1/2}-Q \qquad (2.41)$$

then

$$a = w/2cQ' = w/2c^0Q^0. \qquad (2.42)$$

Equation 1.14 will actually describe the variation of Q' and not Q with frequency for $w \gg w^0$. For large Q, Q' is approximately equal to Q. The absorption model which is used in this thesis is given by equations 1.1 and 2.42 with the dispersion relation given by 1.15 and is valid for $w \gg W^0$.

Equations 2.42 and 1.15 allow the calculation of "a", c, and Q as functions of frequency. At zero frequency, equations 2.38 and 2.39 are used for R and T and at higher frequencies equations 2.17 and 2.18 are used with the complex velocity as a function of frequency given by equations 2.5 to 2.8, or by equations 2.5 to 2.7 and 2.9 where Q in 2.9 is replaced by Q' given by 2.41. With these equations and equations 2.30, 2.34 and 2.35 or 2.32, and

2.35 to 2.37, it is possible to calculate a synthetic seismogram in the frequency domain. This can be Fourier transformed into the time domain, but consideration must be given to selecting df appropriately so as to avoid aliasing in the time domain.

Another point to consider is that in order to perform the discrete Fourier transform it is necessary to cut the data off at some high frequency. This is equivalent to multiplication of the spectrum by a boxcar in the frequency domain which is the same as convolution with a sinc function in the time domain. This can have undesirable effects since we have, in effect, ignored the contributions of frequencies beyond some maximum frequency. These undesirable effects can be minimized by multiplying the frequency domain synthetic seismogram by the transfer function of an appropriate anti-alias filter, as suggested by Kaiser (1963), so that the amplitudes beyond this maximum frequency are negligible. The time domain seismogram can then be used to approximate the synthetic seismogram that would have been recorded through this anti-alias filter.

The important point to emphasize is that the equations for the calculation of the synthetic seismogram in the frequency domain including the effects of an anti-alias filter can be written using the frequency f as a continuous variable. However, in order to calculate a synthetic seismogram on a digital computer, it is necessary to discretize these equations. This can be done by evaluating the frequency domain expressions at discrete frequencies separated by df. It is necessary to choose df sufficiently small in order to minimize the effects of time domain aliasing. This approach leads to satisfactory results on a digital computer.

Equations 2.31 or 2.36 and 2.37, along with equations 2.32 and 2.35, can be used to generate a synthetic seismogram for a downgoing spike as a source at the top of the first layer. It is often desirable to be able to simulate a buried source. This can be done by first solving equation 2.34 or 2.36 for the upgoing wave in layer one when the source is at the surface. It is then necessary to subtract the reflections off the layers above the source from U(1) since these reflections would not appear for a buried source. Let Rs be the Fourier transform of these reflections. The next step is to replace the spike source at the surface by a source which will simulate a spike at time zero at the requested depth. This is done by multiplying U(1)-Rs by (1-Rs')/Ts where Ts is the Fourier transform of the wave transmitted from the surface to the source and Rs' is the Fourier transform of the wave reflected off the layers between the source and the surface as seen from the source. This calculation will simulate a downgoing pulse equal to 1-Rs' at the source. The 1 in the preceding expression represents the input spike and the Rs' term represents the ghost reflections off the layers above the source. The reason for the negative sign on this term is that the upgoing spike which is reflected is a -1 in our coordinate system and Rs' will be solved for as if a spike of +1 is reflected. The final step is to include the direct wave from the source to the surface. This is done by adding -Ts' which is the negative of the Fourier transform of the wave transmitted from the source to the surface. Again, the minus sign appears because the upgoing spike is -1 in our coordinate system. If U" is the Fourier transform of the upgoing wave in layer one for a buried spike source, then

$$U'' = [U(1)-Rs]D'' - Ts' \qquad (2.43)$$

where

$$D'' = (1-Rs')/Ts. \qquad (2.44)$$

The quantities Rs, Ts, Rs' and Ts' can be defined in terms of the model parameters as follows. Let the buried source be at the top of layer L as shown in figures 2.4 and 2.5. Equation 2.31 then becomes

$$\begin{bmatrix} D(1) \\ U(1) \end{bmatrix} = B \begin{bmatrix} D(L) \\ U(L) \end{bmatrix} \qquad (2.45)$$

where B is a 2 x 2 matrix given by

$$B = A(1)A(2)\ldots A(L-1). \qquad (2.46)$$

For a spike at the surface D(1)=1-rU(1), and if layer L is treated as a halfspace, then U(1)=Rs and D(L)=Ts. The

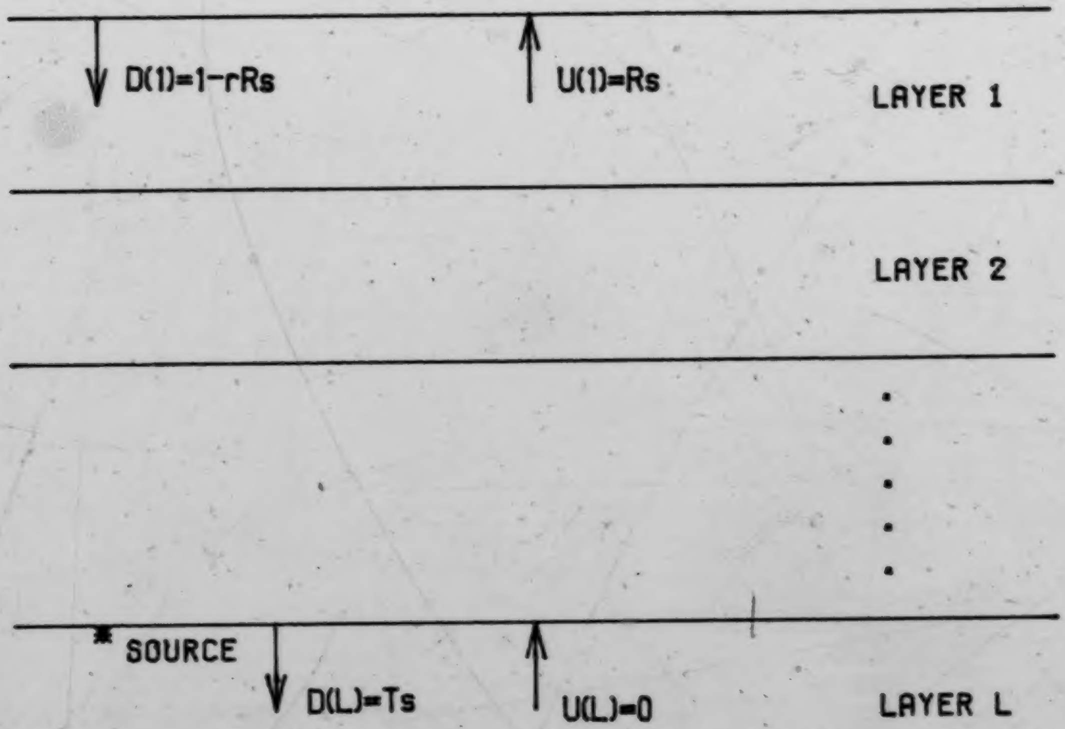
D(1)=1-rRs
U(1)=Rs
LAYER 1
LAYER 2
SOURCE
D(L)=Ts
U(L)=0
LAYER L

Figure 2.4 The reflection and transmission of layers between the source and surface as viewed from the surface.

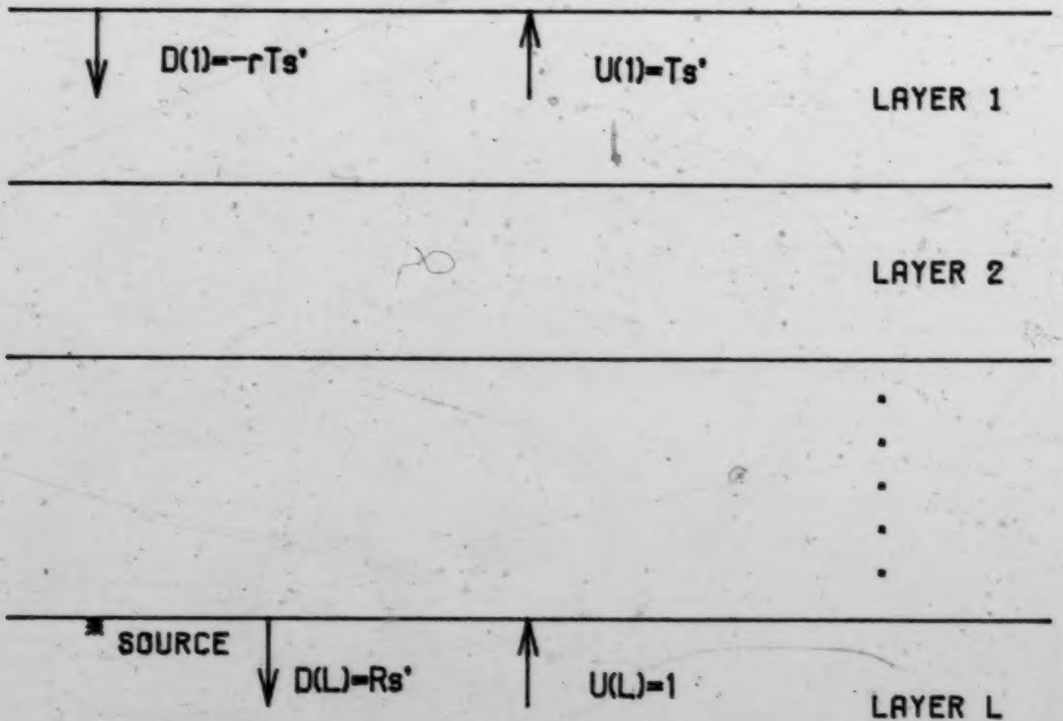
D(1)=-rTs'
U(1)=Ts'
LAYER 1
LAYER 2
SOURCE
D(L)=Rs'
U(L)=1
LAYER L

Figure 2.5 The reflection and transmission of layers between the source and surface as viewed from the source.

upgoing wave in layer L will be zero. This is the case shown by figure 2.4 and we have

$$\begin{bmatrix} 1-rRs \\ Rs \end{bmatrix} = B \begin{bmatrix} Ts \\ 0 \end{bmatrix} \qquad (2.47)$$

or

$$Ts(w) = \frac{1}{B_{11}(w)+rB_{21}(w)} \qquad (2.48)$$

and

$$Rs(w) = B_{21}(w)Ts(w). \qquad (2.49)$$

Likewise the situation shown in figure 2.5 can be solved to give

$$\begin{bmatrix} -rTs' \\ Ts' \end{bmatrix} = B \begin{bmatrix} Rs' \\ 1 \end{bmatrix} \qquad (2.50)$$

or

$$Rs'(w) = \frac{-B_{12}(w)-rB_{22}(w)}{B_{11}(w)+rB_{21}(w)} \qquad (2.51)$$

and

$$Ts'(w) = B_{21}(w)Rs'(w) + B_{22}(w). \qquad (2.52)$$

Equations 2.47 to 2.52 define the quantities needed to simulate a buried source in terms of the model parameters. The result is

$$D''(w) = B_{11}(w) + B_{12}(w) + r[B_{21}(w) + B_{22}(w)] \qquad (2.53)$$

and

$$U''(w) = U(1)D''(w) - B_{21}(w) - B_{22}(w). \qquad (2.54)$$

It should be pointed that in the case of the surface source, the total source is a single downgoing spike and there is no upgoing energy originating at the source. For the buried source this is not the case and both downgoing and upgoing energy originate from the source. The downgoing wave is a unit spike of positive amplitude. Since we are dealing with displacement which is a vector quantity, the upgoing wave originating from the source will be a unit spike of negative amplitude.

It was mentioned earlier that it was possible to use the matrix formulation of equation 2.31 to solve for the upgoing and downgoing waves in any layer. This is still true for the case of a buried source. In order to solve for the upgoing and downgoing waves in a layer K below the source (K > L), the 2 x 2 matrix C is defined as

$$C = A(1)A(2)...A(K-1) \qquad (2.55)$$

and

$$D''\begin{bmatrix} 1-rU(1) \\ U(1) \end{bmatrix} = C\begin{bmatrix} D(K) \\ U(K) \end{bmatrix}. \qquad (2.56)$$

Since U(1) has been solved for and D" is given by equation 2.53, then the equation 2.56 consists of two equations in two unknowns and is easily solved. The Fourier transform of the synthetic seismogram in layer K is D(K)+U(K).

In order to solve for the upgoing and downgoing waves in a layer K above the source (K < L), the matrix C is given by equation 2.55 and

$$\begin{bmatrix} -rU'' \\ U'' \end{bmatrix} = C \begin{bmatrix} D(K) \\ U(K) \end{bmatrix}. \qquad (2.57)$$

With U" defined by equation 2.54, equation 2.57 is two equations in two unknowns.

In solving for the upgoing and downgoing waves right at the source (K=L), it is best to average the results of equations 2.56 and 2.57. This insures that the direct upgoing wave and the direct downgoing wave at the source will cancel each other to give a zero displacement right at the source at time zero.

2.2 Synthetic Seismograms Without Absorption by Ray Methods

The ray theory approach has become a well established method of constructing synthetic seismograms. The basic idea behind this method is that the displacement field is divided into contributions which are attributed to individual rays. Each ray represents a particular travel path form the source to the receiver and the final synthetic seismogram is the resulting sum of the amplitudes of all these rays with their appropriate arrival times. Since there are an infinite number of rays the first basic problem in the generation of synthetic seismograms by ray methods is that of choosing which rays to include in the calculation. This choice must be made in such a way that the synthetic seismogram will be a good approximation to the true seismogram that would result from the given model without allowing the number of rays included to be so large as to make the calculation time prohibitive. Of course if we are trying to match the synthetic seismogram to the real earth then there is also the second problem of how well the chosen model approximates the real earth. In this section one solution to the first problem will be described and the second problem will be examined briefly.

The first step in generating synthetic seismograms by the ray method is the selection of which rays to include in the synthetic seismogram. Once these rays have been selected the next step is to calculate the amplitude and arrival time of each ray. In order to do this it is necessary to specify a ray code which describes each particular ray. The ray code used in this thesis is that based on groups of kinematic and dynamic analogs as suggested by Hron (1971).

A group of rays are said to be kinematic analogs if they have the same travel time from the source to the receiver. All kinematic analogs do not have the same amplitude. Groups of rays which arrive at the receiver at identical times and with identical amplitudes are referred to as dynamic analogs. For a model that consists of N layers, a string of 2N-1 integers is used to represent the ray code. The first N integers, n(i) for i=1 to N, represent half the number of segments of the ray in the i'th layer. These integers form the kinematic code. The next N-1 integers, m(i) for i=1 to N-1, represent the number of upward reflections of the ray from the interface at the bottom of layer i. These integers form the dynamic code. Thus the total ray code is of the form [n(1), n(2), ... n(N); m(1), m(2), ... m(N-1)]. There is no m(N) since this number must always be equal to n(N). Figure 2.6 illustrates 3 rays in a 2 layer model. All of these rays are kinematic analogs and the rays in B and C are dynamic analogs. The ray code for ray A has n(1)=2, n(2)=2 and m(1)=0 so that the code is (2, 2; 0). The ray codes for rays B and C are (2, 2; 1).

Following the suggestion of Vered and Ben-Menahem (1974) the technique used for ray code generation is based on the concept of permuted partitions. A partition of an integer N is defined to be a set of 1 to N integers whose sum is N, taken without regard to order. The integers which form the partition are called its parts. Table 2.1 shows the partitions of the number N which ranges from 1 to 8

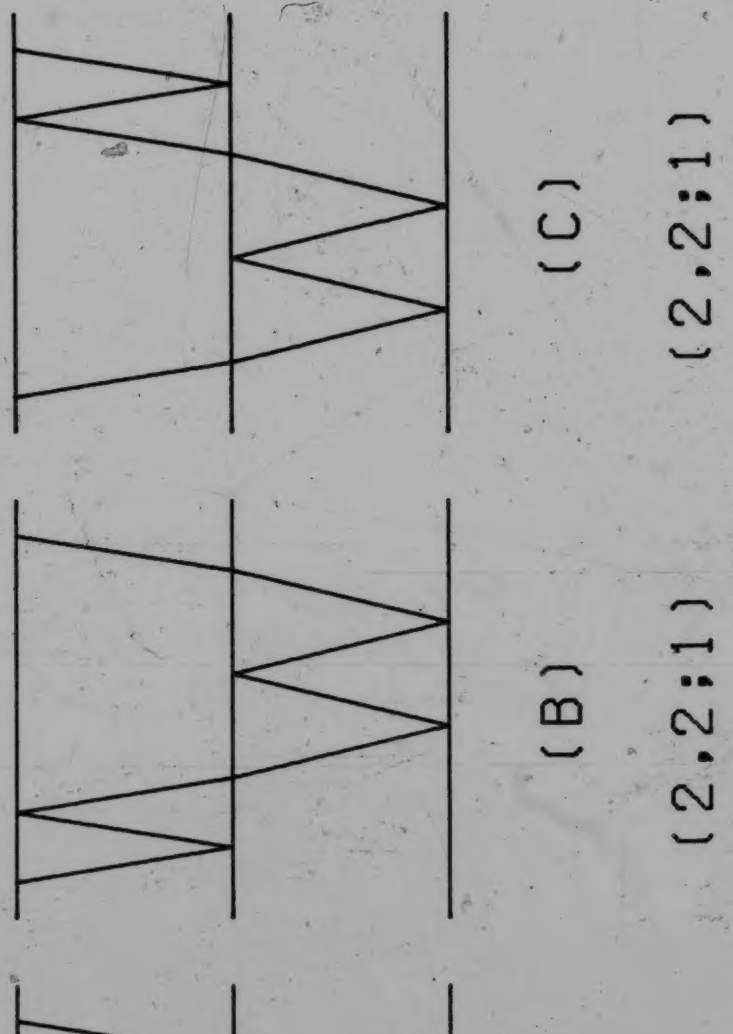
(A)
(2,2:0)
(B)
(2,2:1)
(C)
(2,2:1)

Figure 2.6 Illustration of ray codes.

	Number of Parts							
N	1	2	3	4	5	6	7	8
1	1							
2	2	1^2						
3	3	12	1^3					
4	4	13 2^2	1^22	1^4				
5	5	14 23	1^23 12^2	1^32	1^5			
6	6	15 24 3^2	1^24 123 2^3	1^33 1^22^2	1^42	1^6		
7	7	16 25 34	1^25 124 13^2 2^23	1^34 1^223 12^3	1^43 1^32^2	1^52	1^7	
8	8	17 26 35 4^2	1^26 125 134 2^24 23^2	1^35 1^224 1^23^3 12^23 2^4	1^44 1^323 1^22^3	1^53 1^42^2	1^62	1^8

Table 2.1 Partitions of N for N= 1 to 8.

grouped by the number of parts in each partition. For simplicity repeated parts such as 1111 are abbreviated 1^4.

The concept of partitions can be used to generate ray codes in the following manner. If the maximum number of half segments to be used in any ray code is M and the number of layers in the model is N, then all of the partitions of the integers from 1 to M which have N or less parts are generated. These partitions are permuted in all possible ways. This set of permuted partitions represents all of the possible kinematic ray codes for our model which contain from 1 to M half segments. For each kinematic code it is possible to generate the set of all possible dynamic codes which satisfy this kinematic code by using the criteria defined by Hron (1971).

Using the algorithm given by Lehmer (1964) it is possible to generate all of the partitions in a systematic way so that it is not necessary to store any of them. A routine to permute these partitions based on the fact that not all of the parts in the partition are different has been given by Churney (1977). The storage space required by this method is proportional to the square of the number of layers in the model plus 3 times the number of layers. This presents a very considerable saving in storage over the ray generation method of Hron (1972), wherein the storage is proportional to the largest number in the last row of a Pascal's triangle containing as many rows as there are layers in the model. Table 2.2 illustrates a comparison of the number of storage locations required using Churney's method and using Hron's method.

Figure 2.7 is a flow chart of the algorithm for ray code generation using the permuted partition concept. IHS is the number of half segments in the code and MNHS will be the maximum number of half segments.

The simplest restriction that can be applied to selecting rays is a time criterion. With this restriction the amplitudes of rays whose arrival time is outside some time window of interest are rejected. This method of restriction is almost always used with the most common window being one from time to zero to some maximum time.

Hron and Kanasewich (1971) suggest using the maximum number of half segments in a ray as a restriction criterion; however, this has the disadvantage that the number of rays increases very rapidly with the number of layers even when the number of half segments is just equal to the maximum number of layers. This places a rather severe restriction on the number of layers that a model may contain.

Churney (1977) suggests using a permuted partition approach and restricting the number of parts in the partition. This greatly reduces the number of rays but has the disadvantage that some rays which are left out of calculation contribute significant amplitudes, while some

Number of Layers	Hron Algorithm	Churney Algorithm
2	2	10
4	6	28
6	20	54
8	70	88
10	252	130
12	924	180
14	3432	238
16	12870	304
18	48620	378
20	184756	460
22	705432	550
24	2704156	648

Table 2.2 Comparison of required storage locations for the methods of Hron (1972) and Churney (1977).

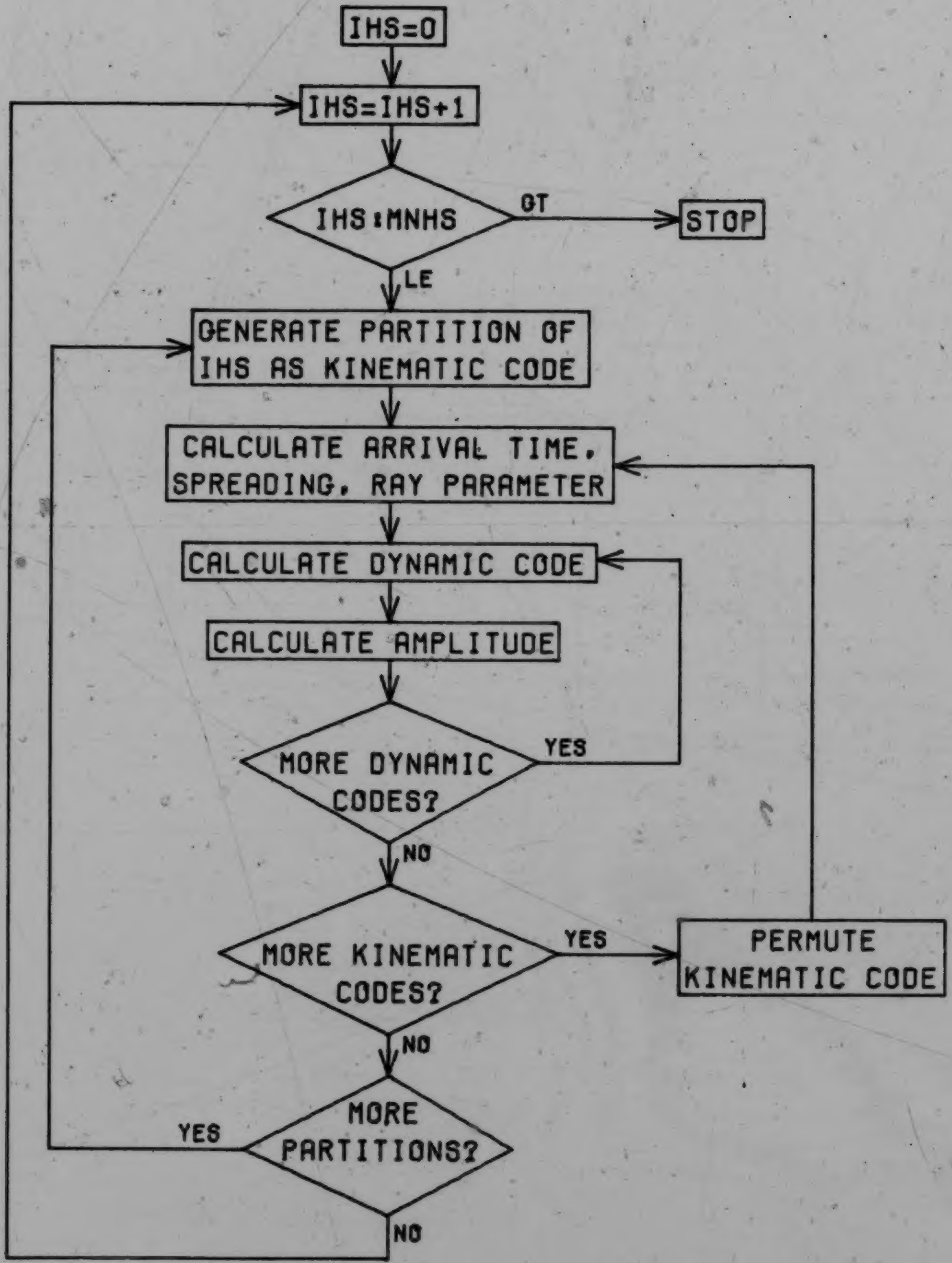
IHS=0
IHS=IHS+1
IHS:MNHS
GT
STOP
LE
GENERATE PARTITION OF IHS AS KINEMATIC CODE
CALCULATE ARRIVAL TIME, SPREADING, RAY PARAMETER
CALCULATE DYNAMIC CODE
CALCULATE AMPLITUDE
MORE DYNAMIC CODES?
YES
NO
MORE KINEMATIC CODES?
YES
PERMUTE KINEMATIC CODE
NO
MORE PARTITIONS?
YES
NO

Figure 2.7 Flow chart of ray code generation scheme using permuted partitions.

rays which are included contribute quite insignificantly.

The criterion for restricting rays being suggested here is based on a multiples-order approach. The synthetic seismogram will be restricted to include primary reflections plus all multiple reflections up to and including a specified order of multiple. Since amplitude decreases as the number of reflections increases one would intuitively expect this to be a logical way to eliminate rays of low amplitude from the calculation while retaining the more significant phases.

This multiples-order approach is applied to the permuted partitions method in two steps. The first step restricts the partitions by using only those partitions whose largest part is less than one plus the highest order of allowed multiple. Thus, if only multiples up to and including the second order are desired, all partitions whose largest part is greater than 3 would not be used. This is because any reflected ray with a larger number of half-segments than 3 in any layer is a multiple of greater than second order. If "O" is the maximum order to be considered and N is the integer being partitioned, no partitions will be generated with less than (N-1)/(O+1) parts. All partitions with more than this number of parts and less than N-O parts will be generated, but only some of them will be used. All partitions containing N-O or more parts will be generated and used. For example, if the integer being partitioned is 8 and only multiples up to and including second order are desired, then no partitions containing 1 or 2 parts would be generated. All partitions containing 3 to 5 parts would be generated, but only some of them would be used, and all partitions consisting of 6, 7 or 8 parts would be used.

The second step of the restriction process is applied in the generation of the dynamic codes. The sum of the numbers m(i) in the dynamic code plus the last number, n(N), from the kinematic code is the total number of upward reflections of the given ray. If this is greater than one plus the maximum order of allowable multiple, then this ray is not included in the calculation.

Figure 2.8 is a plot of a 20 layer velocity-depth model made from a sonic log from a well near Edmonton, Alberta. The method used for blocking sonic or density logs in this thesis is as follows. First, the log is manually edited to attempt to correct cycle skips etc. In the case of a velocity log an adjustment is made by simple linear scaling so that integrated travel times over various depth intervals will agree with check shot times if they are available. The log is then spatially filtered with a low pass, zero phase Butterworth filter to attempt to remove layers less than a specified thickness. After filtering, the log is again scaled so that integrated log values over 15 meter depth intervals are the same as before filtering. Finally, layers

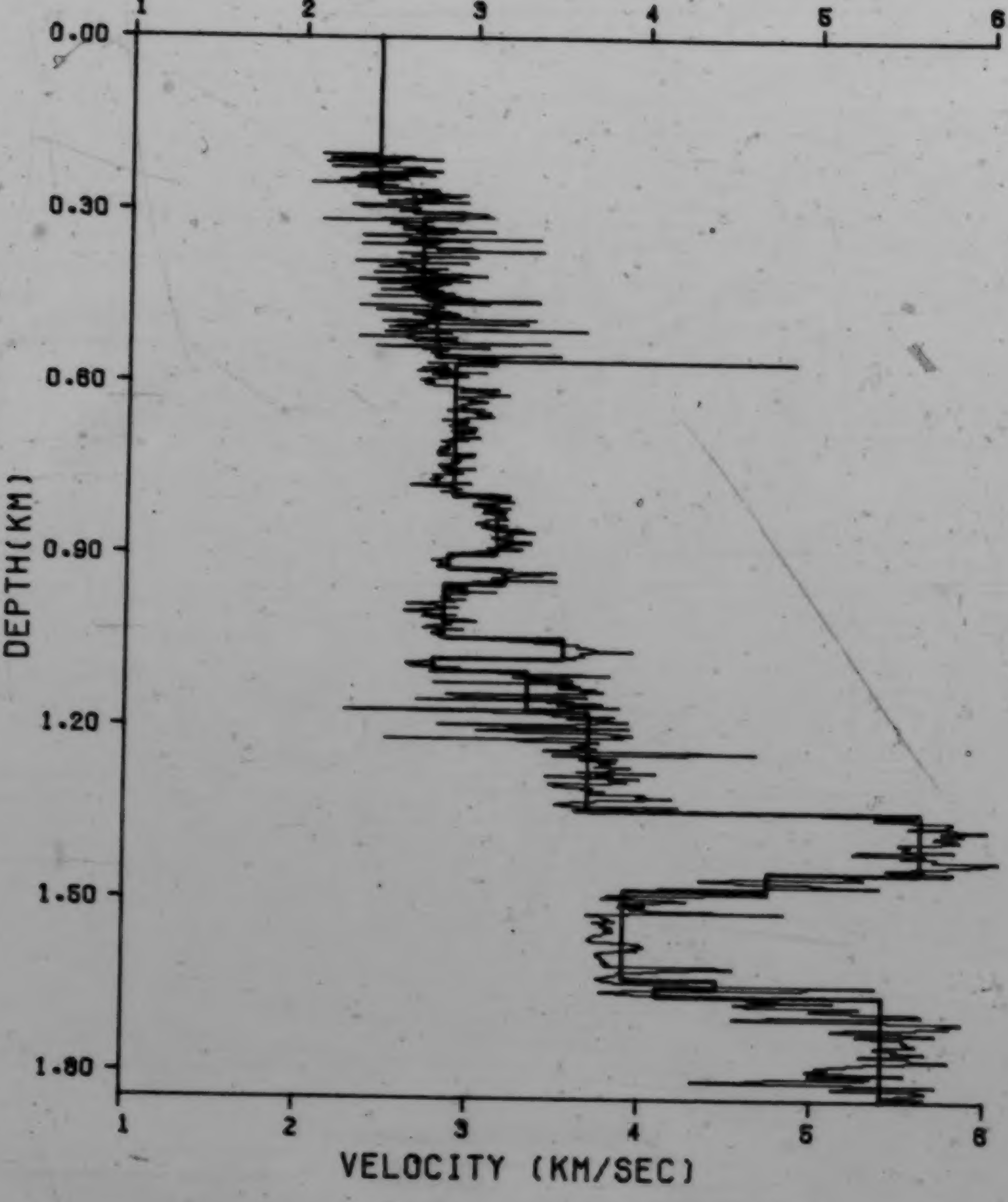

Figure 2.8 20 layer velocity-depth model near Edmonton, Alberta. Alsc shown is the 974 layer model.

are constructed by averaging log values (density or transit times) over the entire layer thickness subject to the restriction that a new layer will be recognized if the change in log value between the layers is greater than a specified percentage of the value in the previous layer. In all cases the appropriate physical quantities (transit time or mass) are conserved. Also shown is figure 2.8 is a 974 layer velocity-depth model which was produced by creating layers whose thickness was one millisecond in terms of two way transit time.

Figure 2.9 shows the primaries only, primaries plus first order multiples, and primaries plus first and second order multiples synthetic seismograms for the model in figure 2.8. In making these seismograms the density was assumed to be constant. These synthetics are calculated for vertical incidence. Also shown in this figure is the exact solution for the 20 layer model calculated using the method outlined in the previous section with no absorption. These synthetic traces don't include the effects of geometric spreading. The fifth trace in the figure shows the exact solution for the 974 layer model. It is apparent that there is little difference between the primaries only, the primaries plus first order multiples, and the primaries plus first and second order multiples synthetic seismograms. There is also little difference between these traces and the exact solution for the 20 layer model. It is interesting to note the difference between the exact solutions for the 20